Magnetospheric Atmospheric X-ray Imaging Experiment (MAXIE)

W. L. Imhof
H. D. Voss
J. Mobilia
D. W. Datlowe
V.L. Chinn
M. Hilsenrath
R. R. Vondrak

Space Sciences Laboratory, 091-20, B252
Lockheed Martin Advanced Technology Center
3251 Hanover Street
Palo Alto, Ca. 94304

June 6, 1996

Final Report
Period Covered March 1993-April 1996

Prepared for :

The Office of Naval Research
800 North Quincy Street
Arlington, Virginia 22217

DISCLAIMER NOTICE

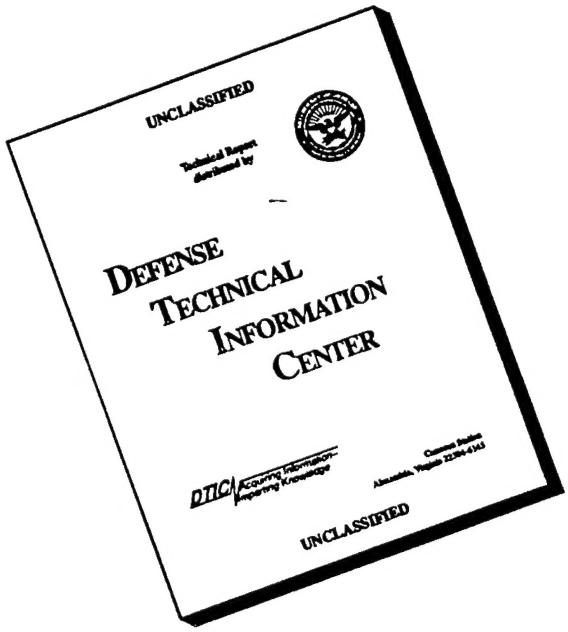

THIS DOCUMENT IS BEST QUALITY AVAILABLE. THE COPY FURNISHED TO DTIC CONTAINED A SIGNIFICANT NUMBER OF PAGES WHICH DO NOT REPRODUCE LEGIBLY.

Magnetospheric Atmospheric X-ray Imaging Experiment (MAXIE)

W. L. Imhof
H. D. Voss
J. Mobilia
D. W. Datlowe
V.L. Chinn
M. Hilsenrath
R. R. Vondrak

Space Sciences Laboratory, 091-20, B252
Lockheed Martin Advanced Technology Center
3251 Hanover Street
Palo Alto, Ca. 94304

June 6, 1996

Final Report
Period Covered March 1993-April 1996

Approved for public release, distribution unlimited

Prepared for :

The Office of Naval Research
800 North Quincy Street
Arlington, Virginia 22217

REPORT DOCUMENTATION PAGE

Form Approved
OMB No. 0704-0188

1. AGENCY USE ONLY (Leave blank)	2. REPORT DATE	3. REPORT TYPE AND DATES COVERED
	6 June 1996	Final Report March 1993 to April 1996

4. TITLE AND SUBTITLE

Magnetospheric Atmospheric X-ray Imaging Experiment (MAXIE)

5. FUNDING NUMBERS

Contract
N00014-93-C-0049

6. AUTHOR(S)

W.L. Imhof, D.W. Datlowe, R.R. Vondrak+, H.D. Voss*, V.L. Chinn, J. Mobilia, M. Hilsenrath

7. PERFORMING ORGANIZATION NAME(S) AND ADDRESS(ES)

Lockheed Martin Advanced Technology Center
Space Sciences Laboratory (O91-20 B252)
3251 Hanover Street
Palo Alto, Ca. 94304-1191

8. PERFORMING ORGANIZATION REPORT NUMBER

9. SPONSORING/MONITORING AGENCY NAME(S) AND ADDRESS(ES)

Office of Naval Research
Dept. of the Navy
800 North Quincy Street
Arlington, Virginia 22217-5000 Contract Manager Dr. R. McCoy

10. SPONSORING/MONITORING AGENCY REPORT NUMBER

11. SUPPLEMENTARY NOTES

* Taylor University, Physics Dept., 500 W. Reade Ave., Upland, In. 46989-1001
+ NASA GSFC, Code 690, Greenbelt, Md. 20771

12a. DISTRIBUTION/AVAILABILITY STATEMENT

Approved for public release; distribution unlimited

12b. DISTRIBUTION CODE

13. ABSTRACT *(Maximum 200 words)*

This report summarizes the activities sponsored by the Office of Naval Research for the Magnetospheric Atmospheric X-ray Imaging Experiment (MAXIE). The MAXIE instrument was developed as a joint activity of Lockheed, The Aerospace Corporation, and the University of Bergen, Norway. Lockheed was responsible for the overall management of the program, interfacing with the appropriate government agencies, the overall electrical and mechanical design, flight software, environmental testing, spacecraft integration activities, on-orbit checkout, and data processing activities. The Magnetospheric Atmospheric X-ray Imaging Experiment (MAXIE), the ONR 401 experiment, is the first in a new class of satellite-borne remote sensing instruments. The primary innovation is the ability to obtain rapid, sequential, images with high sensitivity of the earth's X-ray aurora from a low altitude polar orbiting satellite. These images can be used to identify dynamic temporal variations in the three-dimensional (energy and position) distribution of electron precipitation into the atmosphere. MAXIE was launched on the TIROS NOAA-13 satellite on 9 August 1993. The experiment performed well during its turn-on sequence; however, the spacecraft bus failed on 21 August 1993. New spacebased technologies successfully used in MAXIE were mixed-mode ASIC microcircuits, a zero torque scanning system with associated viscoelastic damping, a paraffin stow release mechanism, a parallel integrating PHA processor, a low noise Si(Li) sensor telescope, and an advanced thermal cooling system. MAXIE's on-orbit operation, control of penetrating particle backgrounds, and scientific data indicated good overall performance.

14. SUBJECT TERMS

Bremsstrahlung, X-rays, magnetospheric imaging, Atmospheric remote sensing, radiation belt, precipitating electrons, auroral x-ray spectrum, aurora

15. NUMBER OF PAGES

16. PRICE CODE

17. SECURITY CLASSIFICATION OF REPORT	18. SECURITY CLASSIFICATION OF THIS PAGE	19. SECURITY CLASSIFICATION OF ABSTRACT	20. LIMITATION OF ABSTRACT
Unclassified	Unclassified	Unclassified	SAR

Contents

SUMMARY

This report summarizes the activities sponsored by the Office of Naval Research for the Magnetospheric Atmospheric X-ray Imaging Experiment (MAXIE). The MAXIE instrument was developed as a joint activity of Lockheed, The Aerospace Corporation, and the University of Bergen. Lockheed was responsible for the overall management of the program, interfacing with the appropriate government agencies, the overall electrical and mechanical design, flight software, environmental testing, spacecraft integration activities, on-orbit checkout, and data processing activities. All activities at The Aerospace Corporation and the University of Bergen were funded by separate sources. Aerospace was responsible for procuring and testing the sensor, for the design and fabrication of part of the mechanical configuration, and for the development of the GSE equipment. The prime responsibilities of the University of Bergen centered around the electronically controlled motion systems. The Aerospace Corporation and the University of Bergen both participated in the instrument and spacecraft level testing and the on-orbit checkout.

The Magnetospheric Atmospheric X-ray Imaging Experiment (MAXIE), the ONR 401 experiment , is the first in a new class of satellite-borne remote sensing instruments. The primary innovation is the ability to obtain rapid, sequential, images with high sensitivity of the earth's X-ray aurora from a low altitude polar orbiting satellite. These images can be used to identify dynamic temporal variations in the three-dimensional (energy and position) distribution of electron precipitation into the atmosphere. MAXIE mechanically scans using an array of 16 cooled silicon telescopes to acquire a 256 pixel image of the earth's atmosphere, at selected periods such as once every five seconds, over the X-ray energy range of 6 to 120 keV. Each image covers a cross-track horizon-to-horizon distance of 6100 km (area of 20 million km^2) with a spatial resolution of 125 km in the nadir pixels. Up to 150 successive images are made during each auroral oval pass. MAXIE was launched on the TIROS-I, NOAA-13, satellite on 9 August 1993. The experiment performed well during its turn-on sequence; however, the spacecraft bus failed on 21 August 1993. New spacebased technologies successfully used in MAXIE were mixed-mode ASIC microcircuits, a zero torque scanning system with associated viscoelastic damping, a paraffin stow release mechanism, a parallel integrating PHA processor, a low noise Si(Li) sensor telescope, and an advanced thermal cooling system. MAXIE's on-orbit operation, control of penetrating particle backgrounds, and scientific data indicated good overall performance.

INTRODUCTION

The MAXIE instrument was developed as a joint activity of Lockheed, The Aerospace Corporation, and the University of Bergen. Lockheed was responsible for the overall electrical and mechanical design. All activities at The Aerospace Corporation and the University of Bergen were funded by separate sources. Aerospace was responsible for procuring and testing the sensor, for the design and fabrication of part of the mechanical configuration, and for the development of the GSE equipment. The prime responsibilities of the University of Bergen centered around the electronically controlled motion systems.

Additional instrument development items in the MAXIE for ONR 401 flight experiment, such as the incorporation of two silicon sensors in each pixel, had been funded by NASA headquarters to Lockheed. Many concepts in MAXIE were developed since 1984 under a Lockheed continuing Independent Research Program. The detailed design and fabrication of the instrument were completed under the continuing Independent Research and Development Program.

The satellite flight of MAXIE as the ONR-401 experiment was implemented under the present contract with ONR. Lockheed had the overall responsibility for the activities required to test the MAXIE instrument in orbit. Under ONR sponsorship, Lockheed also was responsible for conducting tests needed for flight and meeting the spacecraft interface requirements.

The following activities were pursued under the present contract:

1) Management of the program with responsibility for interfacing with the appropriate government agencies
2) Provide interface electronics for on-board conditioning of sensor signals
3) Development of the software for test and calibration of the flight units
4) Perform environment and system tests for the ONR 401 experiment
5) On orbit checkout of the instrument
6) Data processing software

MAXIE (Magnetospheric Atmospheric X-ray Imaging Experiment) was designed to overcome limitations of previous magnetospheric X-ray imaging experiments. MAXIE was launched on the NOAA-13 spacecraft into an 800 km sun-synchronous polar orbit on 9 August 1993. After a brief period of operation the satellite failed due to an electrical power short on 21 August 1993. Several orbits of data were obtained during the MAXIE turn-on process.

Following is a brief description of the instrument and scientific justifications for the experiment. A more detailed description of the instrument is included in Appendix A which

includes the MAXIE instrument paper (Voss et al., 1996). This paper is under review by IEEE Geoscience and Remote Sensing. Several other papers and abstracts pertaining to MAXIE are also included in Appendix A. This report also briefly summarizes the spacecraft integration activities and on-orbit checkout of the instrument.

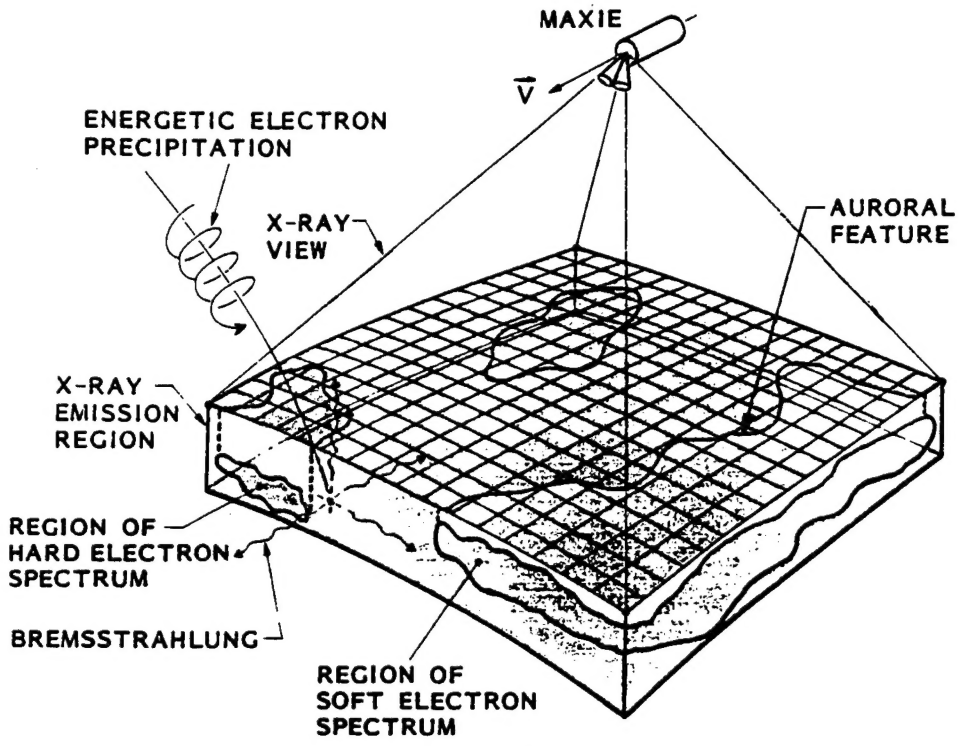

Figure 1 MAXIE X-ray imaging concept using 2-dimensional imaging and energy analysis for understanding the (3 dimensional) morphology of electron precipitation

METHODS, ASSUMPTIONS & PROCEDURES

The Magnetospheric Atmospheric X-ray Imaging Experiment (MAXIE), the ONR 401 experiment, is the first in a new class of satellite-borne remote sensing instruments. A conceptual drawing of the experiment is shown in figure 1. The primary innovation is the ability to obtain rapid, sequential, images with high sensitivity of the earth's X-ray aurora from a low altitude polar orbiting satellite. These images can be used to identify dynamic temporal variations in the three-dimensional (energy and position) distribution of electron precipitation into the atmosphere. MAXIE mechanically scans using an array of 16 cooled silicon telescopes to acquire a 256 pixel image of the earth's atmosphere, at selected periods such as once every five seconds, over the X-ray energy range of 6 to 120 keV. Each image covers a cross-track horizon-to-horizon distance of 6100 km (area of 20 million km^2) with a spatial resolution of 125 km in the nadir pixels. Up to 150 successive images are made during each auroral oval pass. MAXIE was launched on the TIROS-I, NOAA-13, satellite on 9 August 1993. The experiment performed well during its turn-on sequence; however, the spacecraft bus failed on 21 August 1993.

The primary external sources of energy input into the upper atmosphere are solar ultraviolet (UV) radiation, joule heating by ionospheric electrical currents, and energetic particle precipitation. At high latitudes energetic electrons are observed to provide a significant energy input into the upper atmosphere that is quite variable in both time and position. For investigations of atmospheric effects, as well as studies of magnetospheric phenomena, it is important to provide adequate measurements of these inputs. *In situ* particle spectrometers provide detailed spatial, temporal, and energy information, but only at the point of observation. To obtain measurements of large scale events, remote sensing techniques must be employed. Optical, UV, and Bremsstrahlung X-rays photons are all produced by energetic particles hitting the atmosphere. Bremsstrahlung X-rays are generated by more energetic electrons (E > 5 keV), whereas optical and UV emissions are associated primarily with lower energy electrons. A unique advantage of X-ray remote sensing is that both day and night coverage is obtained. The Bremsstrahlung interaction process and the corrections for albedo, absorption, and background are all well understood. Using mathematical techniques, the characteristics of the electron population can be calculated from the X-ray measurements using multiparameter fits . Satellite X-imaging techniques have been summarized by Imhof et al., 1994, and McKenzie et al., 1994. Both are included in the attached appendix.

The instrument maps intensities and energy spectra of X-rays from 6 keV to 120 keV produced by electrons that precipitate into the atmosphere. From the X-ray energy distribution, information can be derived concerning the precipitating electron spectrum and the atmospheric energy deposition, ionization, and conductivity. Previous X-ray imaging experiments produced an image by using an array of sensor elements and building up a 2-D image by using a push broom effect. A snapshot would be taken and then, allowing for the satellite motion, the next snapshot would be acquired further along the path. The accumulation of these snapshots allows an image to be obtained. A disadvantage is that a region is only observed for a small period of time. MAXIE overcomes this limitation by scanning forward and backwards allowing one region to be observed for up to ten minutes.

Design of the MAXIE instrument was guided by several important considerations. In order to measure the spatial and temporal characteristics of electron precipitation it was desirable to perform X-ray measurements with a multisensor instrument on a low-altitude satellite. Because the electron-induced X-ray flux is relatively weak (about 10^{-5} of the typical precipitating auroral electron flux), the instrument must feature high sensitivity with good background rejection. The spatial, spectral, and temporal characteristics of the X-ray emissions are obtained by repeated observations of a given region in space as illustrated in Figure 1; a mechanical scanning spectrometer accomplished this feature. Mechanical scanning of a one-dimensional sensor array was a compromise based on the limiting requirement of having a 16 by 16 pixel image (256 pixels), instrument cost, and mass requirements allowing for a limited number of sensors (sixteen 5.0-cm^2 telescopes). With such a device, the atmosphere was observed continuously, in contrast with the lower duty cycle (typically <25%) achievable from a spinning satellite.

Limb to limb scans in a direction parallel to the satellite's orbit plane were obtained as fast as once every 5 seconds. Adequate spatial resolution (~100 km at nadir) was obtained with collimation that was sufficiently wide to provide a reasonable sensitivity for detection of Bremsstrahlung X-rays from the atmosphere and yet was adequately narrow for mapping purposes. A suitable energy range of detection (6 to 120 keV) was achieved with cooled silicon detectors.

As the polar orbiting satellite moves across the auroral oval, MAXIE observes approximately one half of the auroral oval with multiple images per pass. Previous X-ray imagers have acquired only one image per satellite pass. MAXIE was designed to obtain up to 60 images of an individual auroral form at a specific geographic location during 5

minutes of satellite overpass. By acquiring repeated sequential images (movies) of the atmosphere, the experiment provides the opportunity to study auroral dynamics on a fast time scale.

The spacecraft resources available for the instrument were a power of 38 W inclusive of thermoelectric cooling, and a mass of 47 kg. The telemetry rate of 11.2 kbits/s required on-board data compression. Furthermore, the instrument requirements for the NOAA-13 spacecraft demanded a net uncompensated angular momentum of $< 2.9 \times 10^{-6}$ kg m^2/s and EMI requirements below those called out in MIL-STD-461.

Design overview and measurement capabilities

MAXIE is comprised of two counter-rotating heads (figure 2) that have 16 fields-of-views scanning parallel to the spacecraft orbit plane. The f-o-v of the instrument is ~2800 km crosstrack. Each of the heads contains eight cooled (-60°C) solid-state detector modules consisting of two silicon sensors each. Passive radiation to space and a thermoelectric cooler are employed. The instrument is microprocessor controlled with a dedicated microprocessor for the motion system. Pulse height and anticoincident analysis from each of the silicon sensors is obtained with custom built microcircuits and will provide the X-ray energy spectra through a telemetry bandwidth of 11.2 kilobits per second. With mechanical scanning, the instrument will obtain new high resolution X-ray imaging data on auroral and substorm processes with a spatial resolution as fine as 80 km, temporal resolution of 0.25 seconds, and selectable scan rate (≥5 sec per image) that have not been available before.

The eight telescopes in each head view through a common aperture, a large "pinhole". The camera approach has several advantages over eight individual telescopes with collimators: lower weight and size, greater local radiation shielding, ease of cooling the sensor array, a single sweeping magnet, and a single collimator and aperture window. The housing and external collimators were made of aluminum to provide structure with a low atomic-number (Z) material. The low Z is required to minimize the production of local Bremsstrahlung X-rays by penetrating electrons. The broom magnet has a maximum internal field of 0.1 tesla (1.0 kG) in the center of the gap to bend potentially contaminating electrons away from the aperture. The two internal collimators are made of a high Z material (lead) to absorb local Bremsstrahlung and help define the field of view edges.

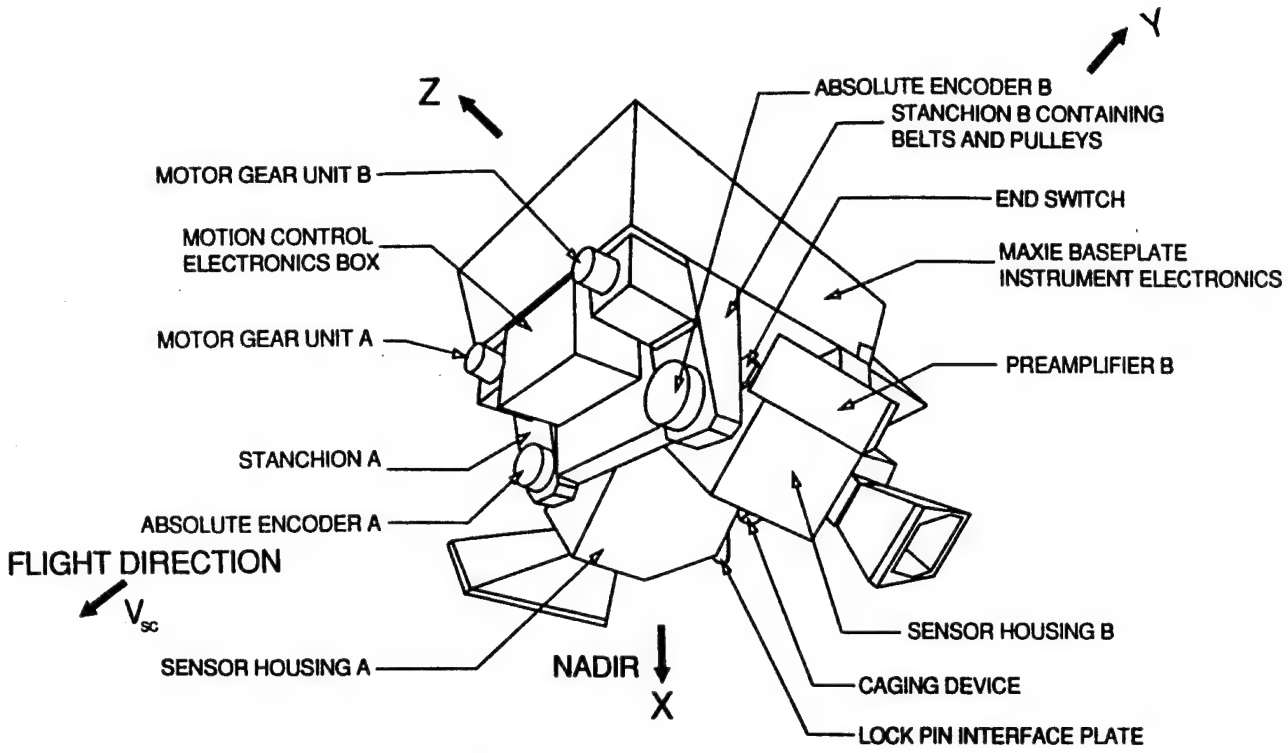

Figure 2 View of the MAXIE instrument showing the mechanical design

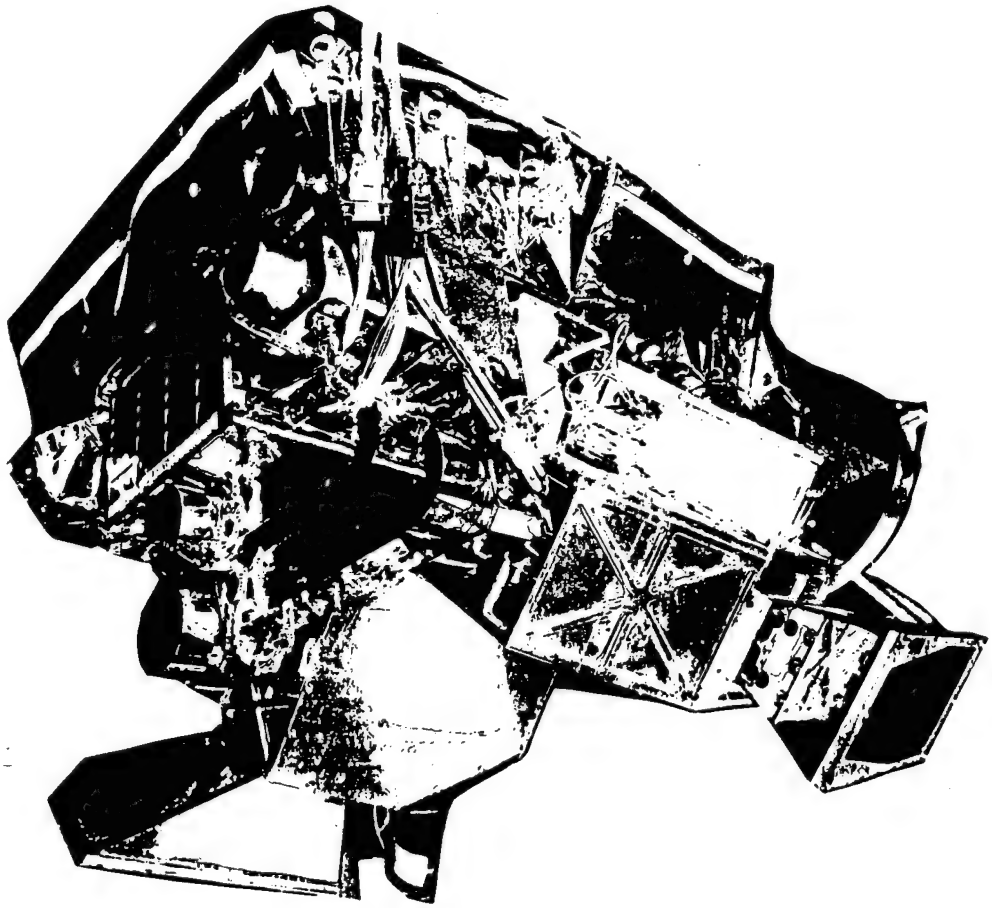

Figure 3 Photograph of the MAXIE instrument including the thermal blankets

Figure 3 shows the MAXIE instrument, which is mounted on the earthward side of the NOAA-13 vehicle. The two large heads, shown at the outward extremes of their angular ranges, scan through a range of 87 degrees along the satellite track, but with opposite rotation senses to minimize the uncompensated angular momentum imparted to the vehicle. The low noise preamplifier electronics are located in the rectangular box on the housing. Vertical stanchions support the sensor heads at bearings and are made of stainless steel to add the necessary structural strength while maintaining thermal isolation from the baseplate and electronics boxes. The baseplate is cooled with a nadir viewing radiator shelf and is thermally isolated from the spacecraft with fiberglass standoffs. The main digital electronics box, high voltage bias supply box, and motion control box are mounted to the baseplate.

High reliability was accomplished by using two independent instrument halves: two sensor heads, two high voltage power supplies, two microprocessors, and two low voltage power supplies. Half of the instrument could be operated while the other half was shut down. This design philosophy provided fault tolerance and the ability to diagnose and reconfigure the instrument. The instrument is microprocessor controlled with a dedicated microprocessor for the motion control system. Pulse height and anticoincidence analysis from each of the silicon sensors is obtained with custom built application specific integrated circuits (ASICs).

Spacecraft Integration, Testing, and On-orbit Activities

The NOAA-13 spacecraft was built by Lockheed Martin AstroSpace (at the time of launch Martin Marietta AstroSpace) in East Windsor, New Jersey. Activities related to spacecraft integration and testing under the present contract included several performance tests. The final such test at the New Jersey facility occurred in May 1993. Following this testing the Spacecraft was shipped to Vandenberg Air Force base where the instrument underwent a series of performance tests prior to launch on 9 August 1993.

To prepare for on-orbit checkout a PC-based GSE was set up at the NOAA spacecraft operations center (SOCC) in Suitland, Maryland. This system was interfaced into the NOAA system and tested prior to launch. Software was developed to display both science and engineering data. Software was also developed to process the data tapes generated by NOAA and quick look data received over the internet for data analysis.

On orbit power was first applied to the MAXIE instrument on 16 August 1993. The initial checkout sequence was scheduled to take place over a two week period. All subsystems were verified to be working including all of the electronic subsystems, the thermoelectric coolers, and the scanning motors.

The motion control system was performing as designed. Bias was applied to the silicon detectors with appropriate detector response. This was clearly demonstrated when the satellite traveled through the radiation belts. On 20 August one orbit of data was acquired when the instrument was scanning and bias was applied to the sensors. This data is described in the next section. Due to reduced operations over the weekend MAXIE was put into a safe state with the checkout to continue on the following Monday (23 August). On the night of 21 August the spacecraft suffered a failure in its power system and as a result began to tumble. All attempts at communication with the satellite failed and the vehicle was lost.

RESULTS and DISCUSSION

Only one orbit of data was obtained with the MAXIE instrument scanning just before the spacecraft demise. The data for one of the pixels (Housing B pixel 5) during this orbit are shown in Figure 4. The pass starts over the northern polar cap, proceeds to the low cosmic ray backgrounds at the magnetic equator, then to the southern polar cap with the two conspicuous auroral oval horns, then to the high background environment of the South Atlantic Magnetic Anomaly (SAMA), back over the northern polar cap with its auroral oval horns, and finally ending in the low background near the magnetic equator. The superimposed count rate spikes, particularly over the SAMA region, are due to the scan motion permitting locally trapped energetic particles to penetrate into the sensor enclosure. The penetrating background count rate, without anticoincidence, is about ten counts/s over the polar cap and about two counts/s near the equator for the 800 km orbit. For a weak auroral event the count rate without integration and anticoincidence rejection would be well above the noise over the polar cap. Unfortunately, at this time the magnetic and auroral activity was low, and no strong X-ray auroral forms were observed. The scan motion is particularly useful at identifying auroral forms over the polar cap where the background is relatively constant so that the scanning modulation can be readily subtracted from the slowly varying background.

CONCLUSION

The development of the MAXIE satellite X-ray imager is a great advance in the evolution of satellite remote sensors of atmospheric X-rays. The MAXIE instrument

design provides the sensitivity, time resolution, spectral resolution, and background rejection needed for the imaging of the dynamic aurora. The spatial resolution is greatly superior to previous designs and is adequate for detailed images. New satellite instrument technologies in MAXIE were proven, such as ASIC microcircuits, a "zero" torque scanning system, a paraffin stow release mechanism, a parallel integrating PHA processor microcircuit, a low-noise sensor telescope, a mechanical scanning system that effectively suppresses microphonics with viscoelastic damping, and an advanced thermal cooling system. Instrument on-orbit operation, penetrating particle backgrounds and science data validate satisfactory overall performance.

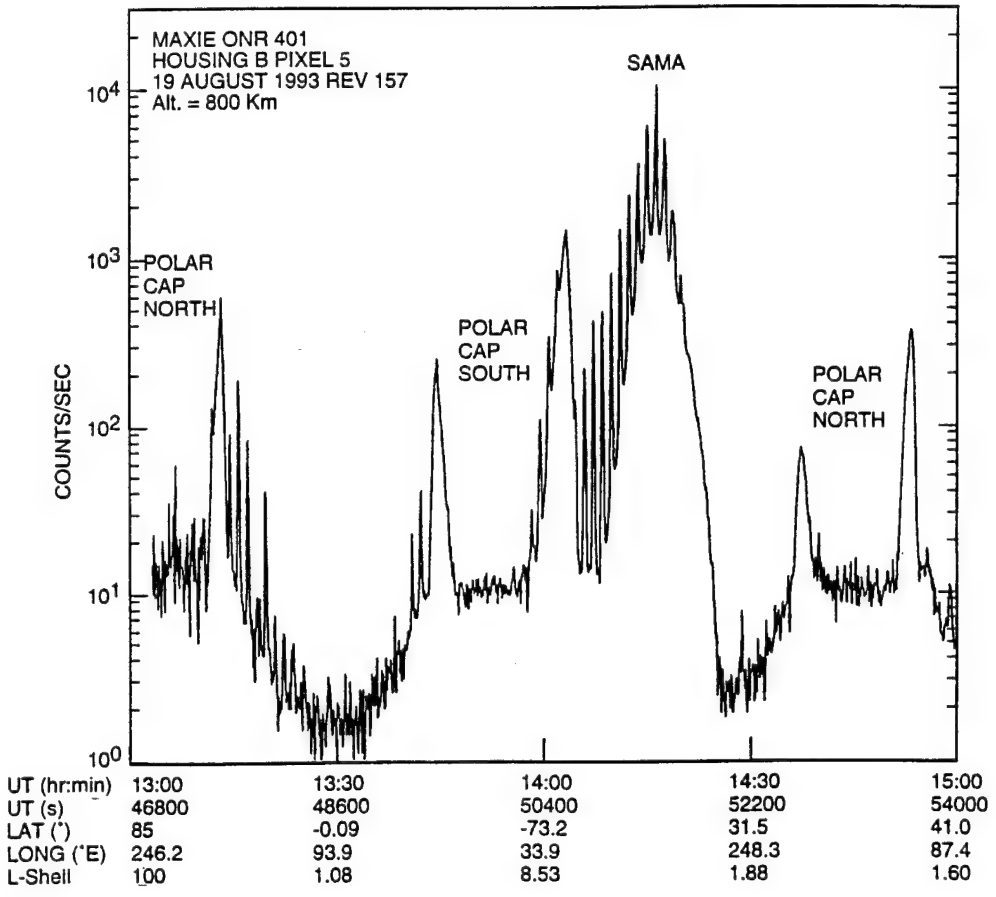

Figure 4 Scaler count rate plots for MAXIE covering a complete NOAA-13 orbit

REFERENCES

Imhof, W.L., H.D. Voss, and D.W. Datlowe, 'Imaging of X rays for Magnetospheric Investigations', Optical Engineering ,1994.

McKenzie, D.L., D.J. Gorney, and W.L. Imhof, 'Auroral X-ray Imaging from High- and Low-Earth Orbit', Optical Engineering, 1994.

Voss et al., 'MAXIE : A Remote Sensing Satellite Experiment for Rapid Imaging of Auroral X-rays', IEEE Geoscience and Remote Sensing, under review 1996.

APPENDIX A : Papers and Abstracts

Papers and Abstracts

A Mechanically Scanning Auroral X-ray Imager for Flight on a TIROS Satellite

H D Voss, W L Imhof, V L Chinn, M Hilsenrath, R R Vondrak
Lockheed Palo Alto Research Laboratory

D L McKenzie, C J Rice, D Roux, R Young
The Aerospace Corporation

K Broenstad, J Stadsnes, A O Solberg, A Myskja
University of Bergen, Norway

The satellite borne x-ray imager MAXIE (Magnetospheric Atmospheric X-ray Imaging Experiment) is planned for flight as the ONR-401 experiment on the NOAA-I/TIROS spacecraft to be launched into an 800 km polar orbit in 1991. The instrument maps the intensities and energy spectra of x-rays from 4 keV to 100 keV produced by electrons that precipitate into the atmosphere. From the x-ray energy distribution, information can be derived concerning the precipitating electron spectrum and the atmospheric energy deposition, ionization, and conductivity. MAXIE is comprised of two counter-rotating heads that have 16 fields-of-view that scan parallel to the spacecraft orbit plane. Each of the heads contains eight cooled (-60° C) solid-state detector modules consisting of two silicon sensors each. Pulse height and anticoincidence analysis from each of the silicon sensors will be obtained with custom built microchips and will provide the x-ray energy spectra through a telemetry bandwidth of 11 kilobits per second. With mechanical scanning the instrument will obtain new high-resolution x-ray imaging data on auroral and substorm processes with a spatial resolution (as fine as 80 km), temporal resolution (0.25 second) and scan rate (≥5 seconds per image) that have not been available before. Previous X-ray imagers have acquired only one image per satellite pass. MAXIE will obtain approximately 60 images of an auroral form during the 10 minutes that it is visible. By repeated scans of the atmosphere, the experiment will provide the opportunity to study auroral dynamics on a fast time scale.

1. 1990 Fall Meeting
2. AGU Member
3. Dr. H.D. Voss
   Dept. 91-20, Bldg. 255
   Lockheed
   3251 Hanover St.
   Palo Alto, CA 94304
   (415) 424-3299
4. New Instrumentation (SA-01)
5. New instruments, instrumentation concepts and techniques with application to research in aeronomy.
6. Oral
7. 0%
8. Invoice $60.00
   P.O.
   Inquiries to:
   Technical Information
   Dept. 90-11, Bldg. 201
   Lockheed
   3251 Hanover St.
   Palo Alto, CA 94304
   Attn: Jan Thomas
   (415) 424-2810
9. Invited
10. No special request
11. Not student paper

MAXIE : A Mechanically Scanning Auroral X-ray Imaging Experiment for Flight on a TIROS Satellite

H.D. Voss, W.L. Imhof, V.L. Chinn, M. Hilsenrath, J. Mobilia,
R.R. Vondrak, Lockheed Palo Alto Research Laboratory
D.L. McKenzie, C.J. Rice, D. Roux, R. Young,
The Aerospace Corporation
K. Broenstad, J. Stadsnes, A.O. Solberg, A. Myskja,
Unversity of Bergen, Norway

The satellite borne x-ray imager MAXIE (Magnetospheric Atmospheric X-ray Imaging Experiment) is planned for flight as the ONR-401 experiment on the NOAA-I/TIROS spacecraft to be launched into an 800 km polar orbit in late 1992/early 1993. The instrument maps intensities and energy spectra of x-rays from 4 keV to 100 keV produced by electrons that precipitate into the atmosphere. MAXIE is comprised of two counter-rotating heads that have 16 fields-of-views scanning parallel to the spacecraft orbit plane. Each of the heads contains 8 cooled solid-state detector modules consisting of two SiLi sensors each. With mechanical scanning, the instrument will obtain high resolution x-ray imaging data on auroral and substorm processes with a spatial resolution as fine as 80 km, temporal resolution of 0.25 seconds, and selectable scan rate (>5 sec per image).

For submission to Astronmy and Space Instrumentation
IEEE 1992
Nuclear Science Symposium
For oral presentation and publication in IEEE Trans. on Nuclear Science

Dr. H.D. Voss
Lockheed Palo Alto Research Laboratory
3251 Hanover St.
Palo Alto, Calif. 94304-1191
415-424-3299 Fax 415-424-3333

Alternate contact Mr. J. Mobilia
415-424-3292 Fax 415-424-3333

The Imaging of X-rays for Magnetospheric Investigations

W. L. Imhof, H. D. Voss, and D. W. Datlowe
Space Sciences Laboratory, O/91-20 B/255
Lockheed Palo Alto Research Laboratory
3251 Hanover Street Palo Alto, CA 94304
(415) 424-3252 / (415) 424-3333 (Fax)

We wish to submit this abstract to the conference on "Instrumentation for Magnetospheric Imagery" (S. Chakrabarti, chair) at San Diego '92.

Precipitation of energetic electrons from the magnetosphere into the auroral zone produces x-ray bremmstrahlung. Although in-situ electron spectrometers can provide detailed information at the point of observation, only x-ray imagers can provide large scale maps of the 1 to 300 keV energy electron precipitation. X-ray imaging provides complete day and night coverage of the electron energy spectra at each position. Early x-ray images, such as those obtained by the P78-1 CdTe instrument and the SEEP proportional counter system, served to demonstrate the importance of narrow elongated arcs of energetic electron precipitation in the auroral zone. They also characterized the spectral parameters and precipitation rates required for understanding source and loss mechanisms in the magnetosphere, but they were limited in field of view and to one map for each pass over the emitting regions. The Magnetospheric Atmospheric X-ray Imaging Experiment (MAXIE), soon to be launched on a TIROS satellite, will make time-space mappings by scanning a 16 pixel pinhole camera. These data will distinguish intensity variations of a fixed auroral feature from motion of a steadily radiating feature. However, the spatial deconvolution is complex and features stay in the field of view for only ~10 minutes. These problems will be resolved by a high altitude (~9 Re) imaging spectrometer PIXIE on the ISTP/GGS Polar Satellite to be launched in 1994. PIXIE's position sensitive proportional counter will continuously image the entire auroral zone for periods of hours. The resulting images will be important for understanding how the electrons are accelerated in the magnetosphere and why and where they precipitate into the atmosphere. Future needs and plans for next generation imagers will be discussed.

W. L. Imhof received the B.A., M.A. and Ph.D. degrees in Physics from the University of California, Berkeley in 1951, 1953, and 1956. Since 1956 he has been at the Lockheed Palo Alto Research Laboratory and is the leader of the Energetic Particles and Fields Group. He has participated in many space science investigations and is the author or co-author of over 100 scientific papers in Space Physics. He has been the principal investigator in several satellite programs and holds this role on both the MAXIE and PIXIE programs .

Imaging of x rays for magnetospheric investigations

William L. Imhof
Henry D. Voss
Dayton W. Datlowe
Lockheed Palo Alto Research Laboratory
Space Sciences Laboratory
3251 Hanover Street
Palo Alto, California 94304
E-mail: SPAN=LOCKHD::IMHOF

Abstract. X-ray imagers can provide large-scale maps of bremsstrahlung x rays produced by electron precipitation into the atmosphere. Complete day and night coverage is obtained and the electron energy spectra at each position in space can be derived from the measured x-ray energy spectra. Early x-ray imagers were limited in field of view and to one map for each pass over the emitting regions. The Magnetospheric Atmospheric X-ray Imaging Experiment, launched on a TIROS satellite, makes time-space mappings by scanning a 16-pixel pinhole camera. The data distinguish intensity variations of a fixed auroral feature from motion of a steadily radiating feature. However, the spatial deconvolution is complex and features stay in the field of view for only ~10 min. These problems will be resolved by a high-altitude (~9 R_e) imaging spectrometer PIXIE on the ISTP/GGS Polar Satellite to be launched in 1994. PIXIE's position-sensitive proportional counter will continuously image the entire auroral zone for periods of hours.

Subject terms: magnetospheric imagery; atmospheric remote sensing; x-ray imaging; radiation belt; precipitating electron imaging.

Optical Engineering 33(2), 383–390 (February 1994).

1 Introduction

To obtain worldwide precipitation patterns, a clear need exists for remote sensing techniques such as the observation of electromagnetic emissions in the optical, UV, or x-ray range that are generated by electrons striking the atmosphere. By means of optical techniques with ground-based and satellite instruments, patterns of auroral electron precipitation have been obtained. However, such observations are dominated by <100-eV electrons, by proton precipitation, and are generally not applicable to the study of energetic electron precipitation. Widespread electron precipitation phenomena have also been studied by correlating measurements of cosmic noise absorption between riometers at widely separated stations, but it is difficult to derive detailed electron energy spectra from such data. Bremsstrahlung x-ray detectors on balloons have provided a wealth of information on temporal/spatial variations in electron precipitation, but the fields of view are limited to radii of the order of 100 km, and coordinated measurements between sensors placed at different latitudes and longitudes have been few in number. Also, interpretations of the x-ray spectra are complicated by atmospheric effects. Bremsstrahlung x rays have been measured from parachutes launched by rockets, but the technique is not well suited for long-term studies on a global basis. For investigating energetic electron precipitation patterns many of the foregoing limitations are overcome by measuring bremsstrahlung x rays from a satellite, where a large field of view (FOV) can be covered and the geometry is such that the atmosphere provides little distortion in either the energy spectrum or the direction of arrival of the x rays.

Paper MI-038 received July 3, 1993; revised manuscript received Aug. 18, 1993; accepted for publication Aug. 30, 1993. This paper is a revision of a paper presented at the SPIE conference on Instrumentation for Magnetospheric Imagery, July 1992, San Diego, Calif. The paper presented there appears (unrefereed) in SPIE Proceedings Vol. 1744.

2 Previous Satellite X-Ray Imaging

In 1972–73 for the first time local time distributions in electron precipitation at a given instant in time were obtained by Imhof et al. from x rays.[1] The distributions were derived from the x-ray counting rates recorded in a single collimated detector on the spinning P72-1 satellite by least-squares fitting techniques. Although the spatial resolutions were rather broad, the data did indicate that the precipitation levels near local noon were generally greater than in the early morning hours. This noon time preference for individual intense large-scale events compares favorably with time-averaged profiles obtained from localized measurements of precipitation, but it is not evident that the average local time profiles should necessarily resemble the instantaneous profiles. More systematic measurements of instantaneous electron profiles are clearly needed for a better understanding of worldwide electron loss processes.

The P78-1 spacecraft was launched into a sun synchronous noon-midnight polar orbit at 600-km altitude on February 24, 1979. The satellite spun with a period of approximately 5.5 s about an axis perpendicular to the orbit plane. Mounted at selected orientation angles with respect to the P78-1 spacecraft spin axis was an array of gamma-ray environment mapping spectrometers,[2] GEMS 002. The sensors consisted of cadmium telluride, in which x-ray counts were accumulated

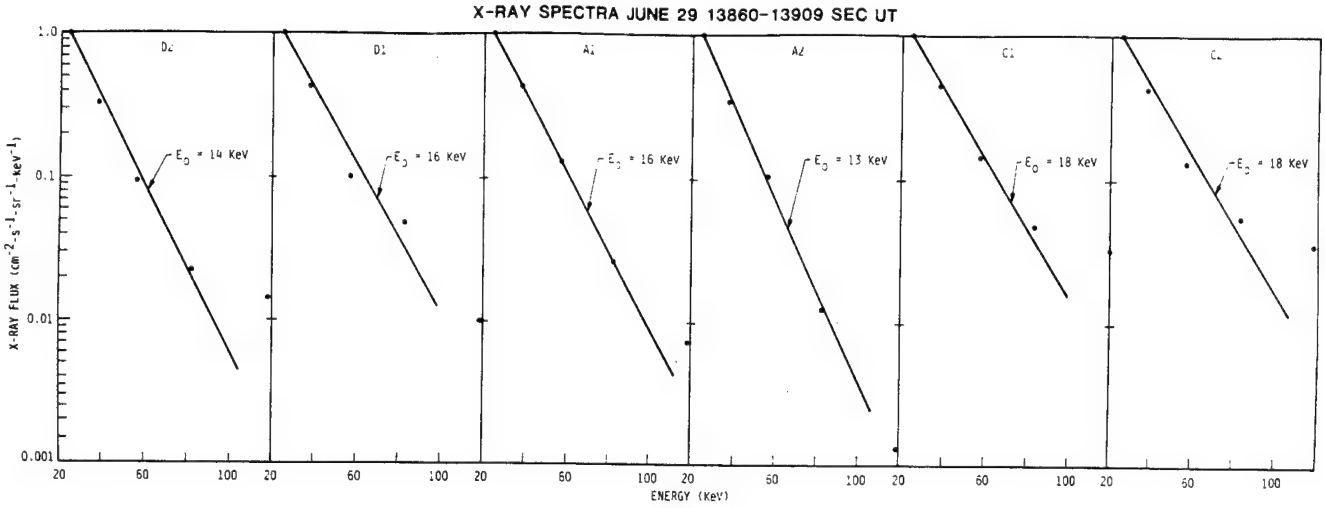

Fig. 1 Examples of x-ray energy spectra emitted simultaneously from different local time sectors.

and telemetered in successive 0.032-s intervals, during which period the satellite rotated approximately 2 deg about the spin axis. Each of the cadmium telluride sensors had an active area of 0.98 to 1.22 cm^2 and a viewing aperture of ± 40 deg along the spin direction. Four spectrometers viewed to the right of the satellite path. Two of them, Aa and Ab, had central view angles of 10 and 30 deg with collimation of ± 10 deg perpendicular to the spin direction, while the other two sensors, Ca and Cb, had central view angles of 44 and 56 deg with collimation of ± 6 deg. A similar arrangement occurred on the left side of the plane normal to the spin axis. The spectrometers that viewed to the left at 10 and 30 deg failed to operate soon after launch. The other two spectrometers were named Da and Db. The spectrometers were designed to provide horizon-to-horizon mappings that are contiguous at the 50% efficiency points with some overlap. Due to the satellite spin motion, the central view direction of each detector traced out the surface of a cone in space, the projection on the top of the atmosphere being the intersection of this cone and the spherical earth. For the data considered here, the threshold levels for signal analysis were set by command at 21 keV, and the channels covered the following x-ray energy ranges: 21 to 30, 30 to 46, 46 to 68, 68 to 98, 98 to 139, and >139 keV. To be detected by the cadmium telluride sensors, the x rays had to pass through a 1 g/cm^2 polyethylene absorber. This absorber ensured that electrons below about 2.1 MeV or protons below approximately 34 MeV could not reach the cadmium telluride.

Since the brēmsstrahlung x-ray spectra are produced by precipitating electrons and since the bremsstrahlung process is understood, we can calculate a well-defined relationship between the two typēs of energy spectra. From a satellite the energy spectra of x rays emitted from different regions of the atmosphere can be measured simultaneously and indications obtained on the variations with local time and/or longitude in the energy spectra of the precipitating electrons. Examples of x-ray energy spectra observed to be emitted simultaneously from different local time sectors are shown in Fig. 1.

From maps of the measured x-ray counting rates one can infer the distributions of electron precipitation intensities on the basis of the known bremsstrahlung emission as a function of direction. In Fig. 2, examples from the P78-1 data are shown in which the x-ray fluxes were emitted at comparable zenith angles and therefore the relative x-ray counting rates should provide a good measure of the relative fluxes of precipitating electrons.

Bremsstrahlung x-ray mappings from the P78-1 satellite were performed at critical times and locations near the onset of a magnetospheric substorm.[3] The x-ray intensities emitted from the atmosphere were over a wide range of longitudes and L shells were negligible just before the substorm onset, then rose to a maximum within about 1 min or less and remained at an enhanced level for the next 9 min. Figure 3 shows the net counts from detectors Ab and Ca in the forward-downward direction minus those in the backward-downward direction, each from five spins of the satellite.

The x-ray imager on the S81-1 satellite consisted of a single large-area proportional counter, with Xe/CH_4 gas and a 0.030-in. beryllium window. Position sensitivity and energy discrimination were provided by collecting charge at both ends of resistive anodes; the ratio of the charges gives the position, and the sum of the charges gives the energy. The image plane consisted of 16 pixels arranged perpendicular to the motion of the satellite. Imaging in the direction of motion was obtained from the time variation of the flux as the FOV scanned over the Earth. The angular resolution was 7×7 deg at the center of the field of view and varied to 7×4 deg at the outer pixels. At the position below the satellite the size of 1 pixel was ~40 km assuming a 100-km x-ray production altitude. The time resolution of the data was 64 ms for the center 2 pixels. However, to improve counting statistics, most spectral fits were done with a 4-s accumulation, approximately the time it took the satellite to move a distance equal to the FOV of 1 pixel.

Examples of x-ray patches recorded with the S81-1 instrument are shown in Fig. 4 (see p. 388). Each section represents the mapping observed during a different pass of the spacecraft. The upgoing x rays were always observed from an area ahead of the satellite, and one of the remote sensing pixels viewed the x-ray emitting region 17 to 43 s earlier than the *in situ* particle measurements; the exact time difference depends on the magnetic field geometry and the al-

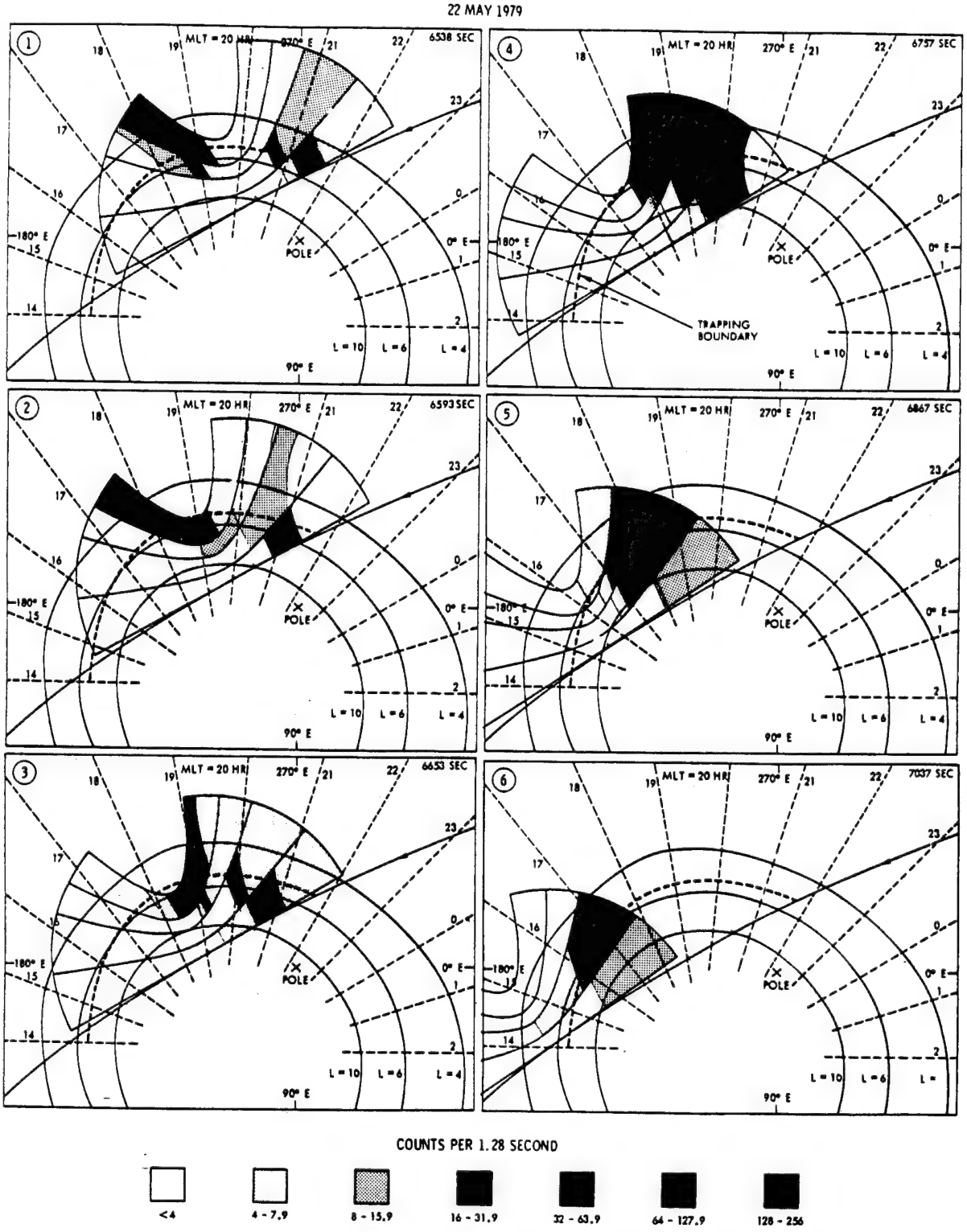

Fig. 2 Spatial distributions in electron precipitation obtained from P78-1 data (from Ref. 2).

titude difference between the satellite and the x-ray production region. The maps represent total x-ray counting rates for energies >4 keV except during June 18 to 23, 1982, when the gain was set lower and the energies were >6 keV.

Figure 5 (see p. 389) shows an intense discrete auroral arc imaged by the S81-1 X-ray instrument. The arc was observed at 18:08 on June 22, 1982, during a geomagnetic disturbance (Kp = 4 +). The figure maps the total x-ray counting rate in each of 16 pixels. The satellite moves from left to right in the illustration, viewing 240 km on each side of the ground track. The polar cap, a region of low x-ray emission, is in the FOV at the start of the observations. The prominent fea-

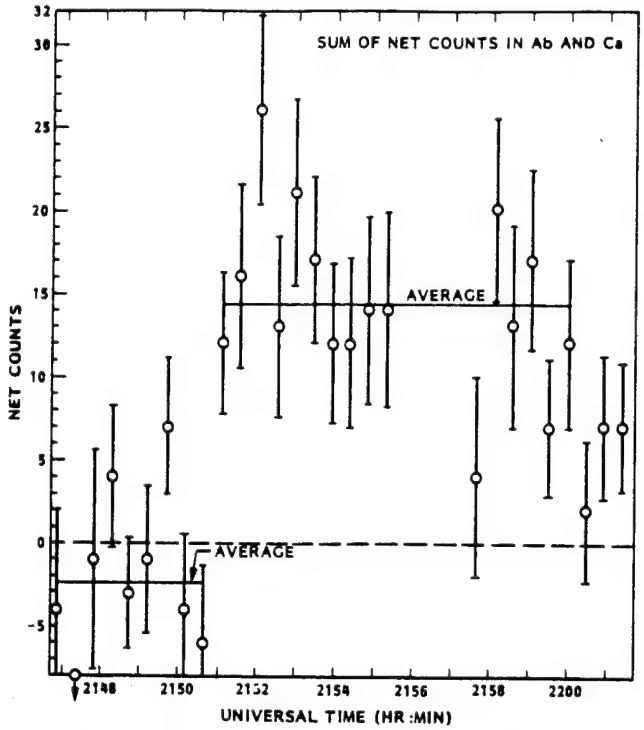

Fig. 3 Total counts of x rays within each spin of the P78-1 satellite (from Ref. 3).

ture in the center of the illustration is a discrete auroral arc, caused by the precipitation of electrons with energies of tens of keV into the Earth's atmosphere. In this particular arc the precipitation rate exceeded 100 erg/cm^2 s, making it one of the most intense measured by S81-1. At the extreme right of the map, 800 km from the first arc, there is evidence of a second very weak arc. In a study of 50 discrete auroral arcs, Datlowe, Imhof, and Voss[4] found that the median precipitation rate was 8 erg/cm^2 s.

3 MAXIE X-Ray Imager

The satellite-borne x-ray imager MAXIE (Magnetospheric Atmospheric X-ray Imaging Experiment) is the ONR-401 experiment on the NOAA-13/TIROS spacecraft launched on August 9, 1993. The MAXIE-1 instrument was developed as a joint activity of Lockheed, The Aerospace Corporation, and the University of Bergen, Norway. The instrument maps the intensities and energy spectra of x rays from 4 to 100 keV produced by electrons that precipitate into the atmosphere. The x rays are detected in solid-state silicon sensors. Pulse height analyses from each of the silicon sensors are obtained with custom-built chips and provide the x-ray energy spectra through a telemetry bandwidth of 11 kbits/s.

MAXIE is comprised of two counterrotating heads that have FOVs that scan parallel to the spacecraft orbit plane. Each of the heads contains eight solid-state silicon detector modules consisting of two silicon sensors each. With mechanical scanning the instrument obtains new high-resolution x-ray imaging data on auroral and substorm processes with a spatial resolution as fine as 80 km, and a temporal resolution (0.25 s) and repetition rate (once every 5 to 10 s) that have not been available before. Previous x-ray imagers have acquired only one image per satellite pass. MAXIE obtains approximately 60 images of an auroral form during the 10 min that it is visible. The viewing geometry at several positions within one scan of the imager is shown in Fig. 6.

Since the TIROS spacecraft is at an altitude of 870 km, the MAXIE spectrometer will measure x rays over a much wider FOV than was true for the S81-1 spectrometer. These viewing differences are illustrated in Fig. 7 (see p. 389) where the MAXIE field of view is superposed on an S81-1 image acquired during a pass of the satellite over the southern polar region.*

4 PIXIE X-Ray Spectrometer

The Polar Ionospheric X-ray Imaging Experiment (PIXIE) is to be flown in 1994 on the POLAR satellite. Examples of the expected images are shown in Fig. 8 (see p. 390). The PIXIE instrument is a multiple-pinhole x-ray camera that uses a multiwire position-sensing gas proportional counter for the focal plane detector. The instrument is designed to cover an energy range from 3 to 60 keV with a $\pm$21-deg FOV. The instrument uses multiple pinholes to project nonoverlapping auroral images onto the focal plane. The number and size of the pinholes are selectable via movable aperture plates, enabling the FOV and sensitivity to change as the POLAR satellite moves from perigee to apogee in its highly eccentric orbit. PIXIE will be located on the POLAR satellite's despun platform. The PIXIE data provide spatial, spectral, and temporal characteristics of the auroral x-ray image. The weight, volume, power, and telemetry format are optimized within satellite resources. The PIXIE instrument mass is 24.5 kg, the power consumption is 11.0 W (with an additional 8 W used on an infrequent basis to move the aperture plates), and the telemetry rate is 3.5 kbit/s.

5 Future Improvements

The recommendations for further improvements in bremsstrahlung x-ray measurements can be summarized as follows. Finer spatial resolution down to distances of ~100 km or less should be achieved because balloon data have indicated that some phenomena may be localized to such distances. The FOV coverage should be wide so that the entire precipitation region observable from a satellite can be mapped; in some cases a flexible FOV may be desirable. Higher sensitivities extending up to several hundred kilo-electron-volts are needed. This improvement entails the use of larger area sensors combined with good rejection of background even when the satellite is in the radiation belts. Improvements in energy resolution are probably not as critical to achieve since adequate resolutions are obtainable with any of the sensor techniques commonly used (proportional counters, scintillators, solid-state detectors). Minimum impact on the spacecraft interface requirements is important. To some extent this desire is contradictory to the need for a large sensor area, but to optimize future flight opportunities the total weight, volume, telemetry bandwidth, and cryogenic requirements should obviously be minimized.

*On-orbit the MAXIE instrument performed as designed and expected, but communication with the satellite was lost a few days after launch.

Fig. 6 The viewing geometry of MAXIE at several positions within one scan.

Acknowledgments

The work at Lockheed was supported by the Lockheed Independent Research Program. We thank all of the people at Lockheed Palo Alto Research Laboratory, The Aerospace Corporation, the University of Bergen, and the University of Maryland who have contributed to various phases of the different programs.

References

1. W. L. Imhof, G. H. Nakano, R. G. Johnson, and J. B. Reagan, "Satellite observations of bremsstrahlung from widespread energetic electron precipitation events," *J. Geophys. Res.* **79,** 565–574 (1974).
2. W. L. Imhof, J. R. Kilner, G. H. Nakano, and J. B. Reagan, "Satellite x ray mappings of sporadic auroral zone electron precipitation events in the local dusk sector," *J. Geophys. Res.* **85,** 3347–3359 (1980).
3. W. L. Imhof, J. Stadsnes, J. B. Reagan, J. R. Kilner, E. E. Gaines, D. W. Datlowe, J. Mobilia, and G. H. Nakano, "Satellite bremsstrahlung x-ray measurements at the onset of a magnetospheric substorm," *J. Geophys. Res.* **87,** 8149–8156 (1982).
4. D. W. Datlowe, W. L. Imhof, and H. D. Voss, "X ray spectral images of energetic electrons precipitating in the auroral zone," *J. Geophys. Res.* **93,** 8662–8680 (Aug. 1988).

William L. Imhof: Biography appears with the paper "Auroral x-ray imaging from high- to low-Earth orbit" in this issue.

Henry D. Voss received the BS degree in 1972 from the Illinois Institute of Technology in electrical engineering. He received the MS and PhD degrees in 1974 and 1977, respectively, from the University of Illinois in electrical engineering. Since 1979, Dr. Voss has been with the Lockheed Space Sciences Laboratory in Palo Alto, California. He has been co-investigator on eight instrument payloads that have studied the charged-particle environment. Dr. Voss is currently the principal investigator for the Source/Loss-cone Energetic Particle Spectrometer of the CEPPAD experiment for flight on the NASA/ISTP POLAR satellite mission. His current areas of scientific interest are the study of energetic electrons and ions in the magnetosphere plasma, the use of bremsstrahlung x rays to image electron precipitation remotely in the Earth's atmosphere, advanced instrumentation for space flight, and the use of semicustom microcircuits for space flight.

Dayton W. Datlowe received his SB from the Massachusetts Institute of Technology in 1964 and his PhD in physics from the University of Chicago. He held a postdoctoral appointment at the University of California, San Diego, from 1970 to 1976, working in the area of solar flare x rays. He joined Lockheed Palo Alto Research Laboratories in 1976. He has authored papers on solar x-ray emission, auroral x-ray emission, and electrons in the geomagnetic environment.

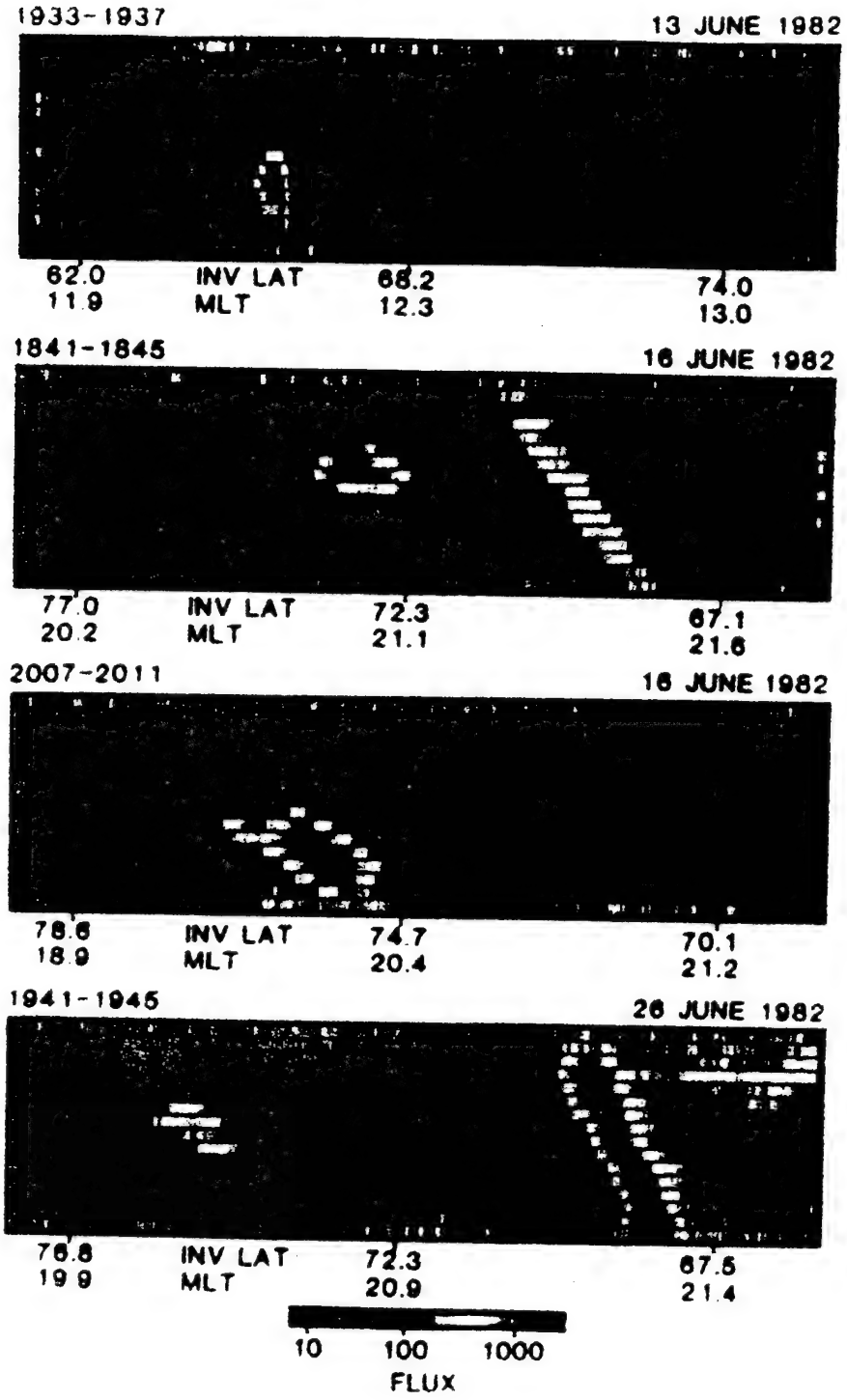

Fig. 4 Examples of x-ray patches recorded with the S81-1 imager (from Imhof et al., *J. Geophys. Res.* **90,** 6515, 1985).

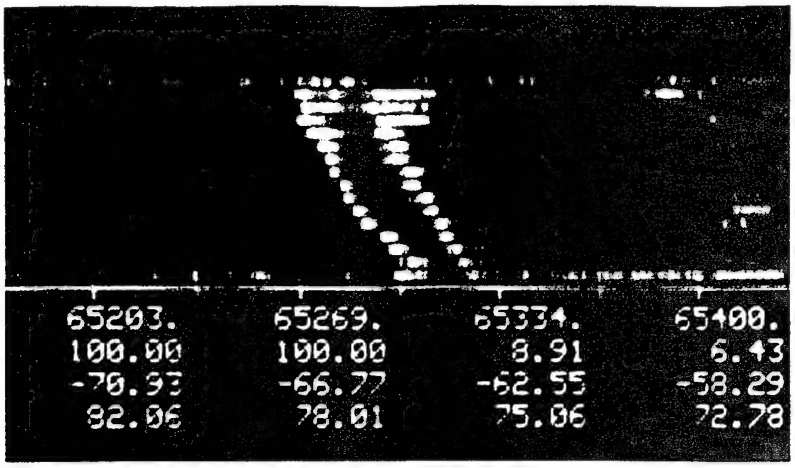

Fig. 5 An intense discrete auroral arc imaged by the S81-1 x-ray spectrometer.

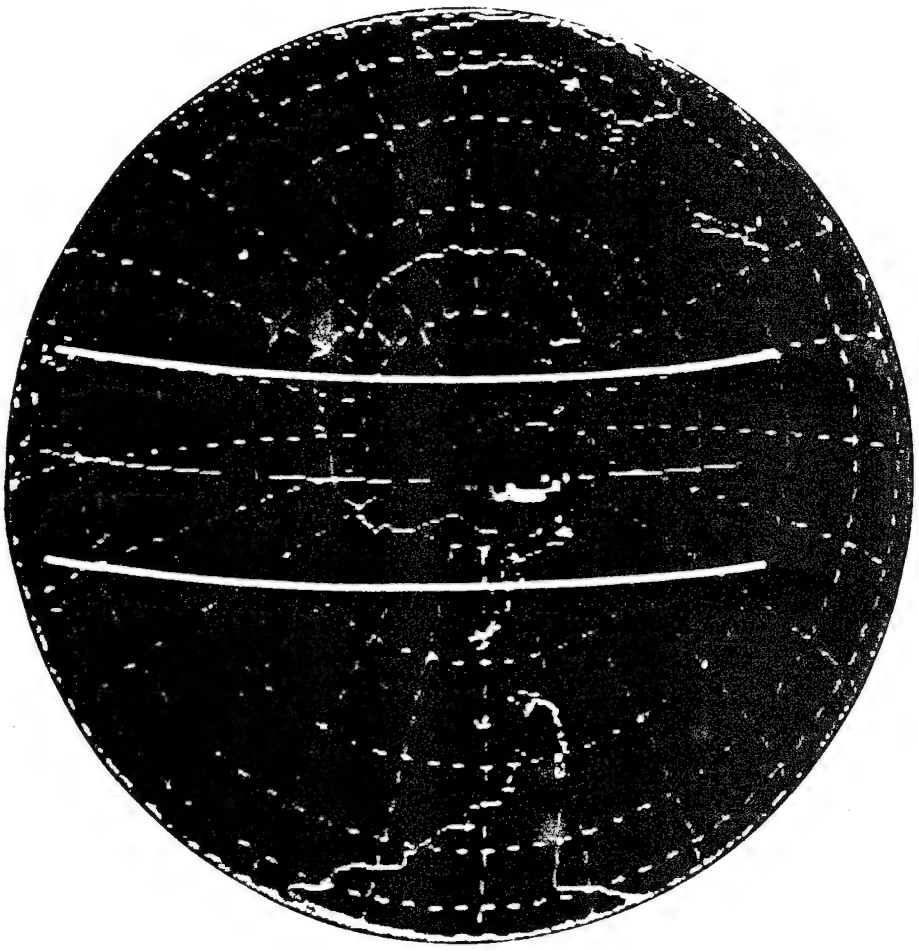

Fig. 7 An x-ray image of the auroral zone during a pass of the S81-1 satellite. Also shown is the much wider field of view of the MAXIE instrument.

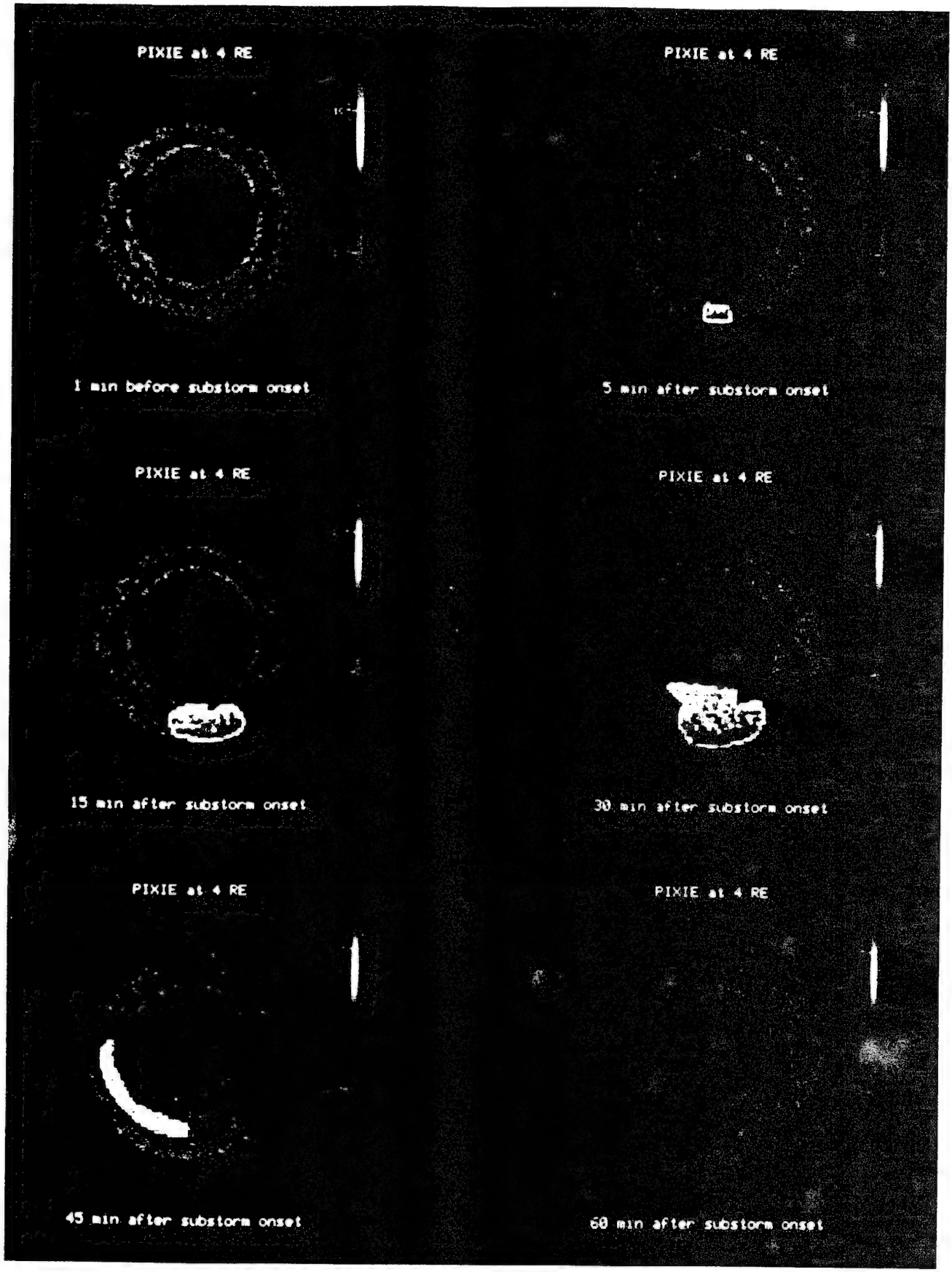

Fig. 8 Examples of the expected images to be obtained with the PIXIE x-ray imaging spectrometer.

Auroral x-ray imaging from high- and low-Earth orbit

David L. McKenzie
The Aerospace Corporation, M2-266
Space and Environment Technology Center
P.O. Box 92957
Los Angeles, California 90009
E-mail: mckenzie@dirac2.nsi.gov

David J. Gorney
The Aerospace Corporation, M2-264
Technology Operations
P.O. Box 92957
Los Angeles, California 90009

William L. Imhof
Lockheed Palo Alto Research Laboratory
Organization 91-20, Building 255
3251 Hanover Street
Palo Alto, California 94304-1191

Abstract. Observations of bremsstrahlung x rays emitted by energetic electrons impacting the Earth's atmosphere can be used for remotely sensing the morphology, intensity, and energy spectra of electron precipitation from the magnetosphere. The utility of the technique is derived from the broad energy range of observable x rays (2 to >100 keV), the simple emission process, the large x-ray mean free path in the atmosphere, and negligible background. Two auroral x-ray imagers, developed for future spaceflights, are discussed. The Polar Ionospheric X-Ray Imaging Experiment is scheduled for launch on the NASA International Solar-Terrestrial Physics/Global Geospace Science program POLAR satellite in 1994. The POLAR orbit, with an apogee and perigee of 9 and 1.8 R_e (Earth radii), respectively, affords the opportunity to image the aurora from a high altitude above the north pole continuously for several hours. The Magnetospheric Atmospheric X-Ray Imaging Experiment (MAXIE) was launched aboard the NOAA-I satellite on August 8, 1993. The 800-km polar orbit passes over both the northern and southern auroral zones every 101 min. MAXIE will be capable of obtaining multiple images of the same auroral region during a single satellite orbit. The experimental approaches used to exploit these very different orbits for remote sensing of the Earth's auroral zones are emphasized.

Subject terms: magnetospheric imagery; atmospheric remote sensing; aurora; auroral x rays; x-ray imaging; auroral remote sensing; auroral x-ray spectrum.

Optical Engineering 33(2), 414–422 (February 1994).

1 Introduction

During the past two decades, scientists at The Aerospace Corporation and Lockheed Palo Alto Research Laboratory have been carrying out a space-based program for measuring the fluxes and spectra of auroral x rays in the Earth's polar regions. The bremsstrahlung x-ray continuum that dominates the spectrum in the kilo-electron-volt energy range is produced when precipitating electrons collide with atmospheric species. Energetic electrons play an important role in the transfer of energy within the magnetosphere. Auroral electrons, constrained to spiral around magnetic field lines, impact the atmosphere in the polar regions and are a major source of ionization in the upper atmosphere. Therefore, they play a controlling role in ionospheric conductivity and, thus, in the global electrical circuit. By measuring the x-ray spectrum, it is a relatively straightforward problem to reconstruct the auroral electron spectrum for energies above approximately 2 keV.

Paper MI-031 received June 29, 1993; revised manuscript received Aug. 24, 1993; accepted for publication Aug. 30, 1993. This paper is a revision of a paper presented at the SPIE conference on Instrumentation for Magnetospheric Imagery, July 1992, San Diego, Calif. The paper presented there appears (unrefereed) in SPIE Proceedings Vol. 1744.

The use of the x-ray spectrum to investigate energetic electron processes in the polar upper atmosphere has several advantages. The bremsstrahlung process is well understood, and its dependence on unknown factors such as the atmospheric composition is negligible. While it is impossible to make a unique determination of the incident electron spectrum, physical insight allows the determination of key parameters, such as the total atmospheric energy deposition due to electrons and the nature of the spectrum. With the imaging capabilities of the latest generation of detectors, these parameters can be measured as a function of position expressed in terms of magnetic latitude and magnetic local time. Since the detectors simultaneously respond to x rays over a broad energy range (typically 1 to 2 decades), spectra that are free from distortion due to temporal variations in the incident flux can be obtained.

A second advantage is that x rays produced in the upper atmosphere can propagate freely to an exo-atmospheric (satellite-borne) detector so that spectral distortion is negligible. This is because x rays have a much larger mean free path than electrons of the same or even substantially higher energy. An electron of a given energy that is incident from above the atmosphere will lose its energy over a small range of altitudes in the upper atmosphere. The electron loses its energy primarily by undergoing ionizing collisions with am-

bient atoms; these same collisions give rise to bremsstrahlung x rays. For this reason, it is possible to determine the height profile of atmospheric ionization from the x-ray spectrum, and this, in turn, allows upper-atmospheric conductivities to be calculated.

The third advantage of the use of the bremsstrahlung x-ray spectrum is that the x-ray background is low. In Fig. 1 we have plotted x-ray background spectra along with spectra from auroral features derived from analysis of DMSP-F2 spacecraft data.[1] The auroral spectra are numbered: Spectrum 1 is believed to be typical of widespread auroral emission during relatively quiet times; spectrum 2 is more typical of diffuse emission during active times; spectrum 3 is that of a westward-traveling surge (a very active auroral feature) observed on November 17, 1977 (the "bump" in the spectrum is due to argon K x rays, produced by fluorescence in the atmosphere); and spectrum 4 is that of a bright auroral arc. Background spectrum C is the cosmic x-ray background spectrum[2]; spectrum A is an extrapolation of the diffuse atmospheric x-ray spectrum reported by Imhof, Nakano, and Reagan[3]; and spectrum S is the Earth-albedo solar x-ray spectrum for a time of high solar activity but in the absence of flaring.[4] At energies above 2 keV, each of the background spectra is much less intense than the weakest auroral spectrum shown. The major contribution to the background counting rate arises from cosmic-ray interactions in the detector that elude background-limiting electronic veto schemes. The figure illustrates another advantage of x-ray measurements: Both the sunlit and nighttime polar regions can be imaged.

In addition to these advantages, auroral x-ray imaging has a major disadvantage: weak signal fluxes. Although the auroral x-ray intensities shown in Fig. 1 are seemingly large, the area-solid angle products for detectors aboard high-altitude (several Earth radii) satellites are such that even the brightest sources are expected to yield counting rates on the order of 1/pixel s^{-1} or less. It is therefore necessary, in the case of the Polar Ionospheric X-Ray Imaging Experiment (PIXIE) instrument to be discussed later, to trade off spatial and/or temporal resolution against sensitivity. Instruments in low-Earth orbit, such as the Magnetospheric Atmospheric X-Ray Imaging Experiment (MAXIE), can obtain images in a few seconds time with spatial resolution on the order of 100 km. This is larger than the narrow-direction dimensions of many active auroral features such as bright arcs.

2 Overview of Auroral X-Ray Imaging

Precipitating energetic charged particles play an important role in the transfer of energy within the Earth's magnetosphere/ionosphere/upper-atmosphere system. Many poorly understood large-scale and small-scale plasma-physical processes are associated with this particle precipitation, particularly in the high-latitude auroral regions. The complexity of the system can be studied most effectively by observing the auroral displays directly. To understand the mechanisms involved in determining the spatial configurations and structures of the auroral phenomenon, it is necessary to observe the spatial structure of the auroral features as well as the temporal variations of the global system.

Satellite-based auroral imagers have become widely recognized as essential tools for the study of global (macroscale) magnetospheric activity, but to date only ground-based optical measurements have been able to provide true 2-D imaging of the aurora with high temporal and spatial resolution. The ground-based measurements have limited fields of view compared to the typical dimensions of the features of interest and are limited to observing in wavelength ranges where the radiation can propagate all the way to the ground. Balloon- and rocket-borne detectors are severely limited in both spatial and temporal coverage. Satellite-borne energetic charged-particle spectrometers have been used extensively to study precipitating auroral electrons, but these *in situ* measurements only provide information on the particle fluxes in the immediate vicinity of the spacecraft. Auroral imagers flown on both low-altitude polar platforms and high-altitude platforms are needed to provide complete images of the large-scale scene and also the details of the small-scale embedded features of the aurora.

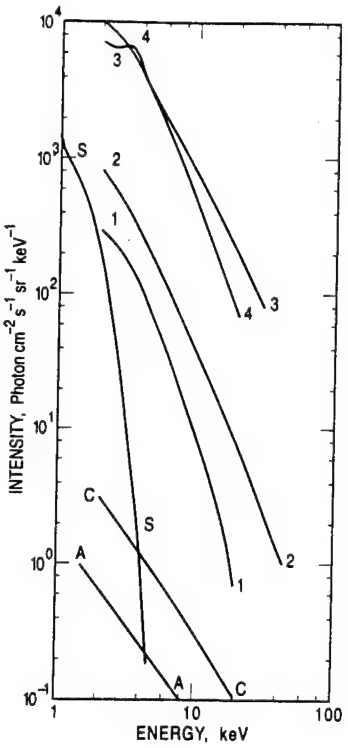

Fig. 1 X-ray spectra of auroral features and of major background components for a satellite-borne auroral x-ray detector.

Bremsstrahlung x-ray imagery provides a means for obtaining a spatial map of energetic electron precipitation while retaining information on the precipitation intensity and energy spectra. X-ray measurements from satellites, or from high-altitude rockets, are not seriously hampered by atmospheric absorption and scattering. Therefore, x-ray measurements from space can be extended down to energies of 1 keV or less, depending on the detector technology that is used. The lack of scattering and absorption for upward-directed bremsstrahlung emission also allows for easier interpretation of the x-ray spectrum in terms of derived quantities such as the incident primary electron spectrum, the atmospheric energy input, ionization density altitude profiles, and ionospheric conductance.[5,6] X-ray spectral measurements can be acquired in full daylight without contamination by solar flux.[6]

A variety of imaging x-ray detectors have been flown on satellites. Most satellite x-ray instruments have used single detectors or arrays of collimated detectors that scan over the x-ray production layer in the atmosphere. Figure 2 depicts various imaging techniques that have been applied and Fig. 3 shows their resulting viewing geometries. The earliest satellite-based x-ray measurements did not image at all, but rather used single collimated down-looking detectors to produce a sequence of linearly arranged pixels along the satellite track [see Figs. 2(a) and 3(a)]. Later satellite-based detectors incorporated increasingly capable imaging techniques involving either scanning or 2-D imaging detectors. The detector scan motion has been accomplished either mechanically[7] or by means of the satellite's spin motion.[8] Images formed by cross-track mechanical scanning of a single detector [Figs. 2(b) and 3(b)] provide relatively good spatial resolution, but very poor temporal resolution (since only one complete image is produced for each satellite polar pass) and very low duty cycle (since a single detector is scanned over the entire scene). The duty cycle problem can be overcome by using an array of collimated detectors that are swept over the atmosphere by the satellite motion. The disadvantage of poor temporal resolution remains, since only a single image can be acquired on each polar pass. Recently, this technique was implemented by Imhof et al.,[9] who used a multiwire proportional counter detector as part of the Simulated Emission of Energetic Particles payload on the low-altitude S81-1 satellite. A further refinement is to scan a linear array of detectors either across the satellite track or along the track [Figs. 2(c) and 3(c)] as in the MAXIE instrument to be discussed later. Sufficiently rapid scans can be used so as to allow multiple images of the same auroral region on a single polar-cap pass. The PIXIE instrument, also to be discussed later, is designed to produce global images of auroral x rays and to provide an instantaneous 2-D view of the atmosphere [Figs. 2(d) and 3(d)].

The scientific goals of auroral imagery investigations place demands not only on the geometric imaging parameters of the x-ray instrument but also on its ability to provide spectral data of sufficient quality to allow the determination of the large- and small-scale distribution of the electron energy precipitated into the atmosphere. Although visible imaging measurements can be used to determine the energy deposition in the nighttime regions, the spatial distribution of the precipitation, and some information on the electron energy distribution over a limited energy range, only x-ray bremsstrahlung measurements offer the possibility of providing spectral information over a broad (2- to 100-keV) energy range at all local times. The energy range of greatest interest for studies of atmospheric effects is between a few and several tens of kilo-electron-volts. Except during solar flares, the solar x-ray spectrum falls rapidly with energy so that atmospherically backscattered fluxes above 2 keV are negligible.[4] The decrease in precipitating particle intensity with increasing energy limits the application of the bremsstrahlung technique at energies above about 100 keV.

Atmospheric bremsstrahlung x rays result from collisions between precipitating energetic electrons and (primarily neutral) atmospheric constituents. At low energies, the bremsstrahlung is emitted fairly isotropically, and the x rays undergo little attenuation before exiting the top of the atmosphere. These emission and transport properties allow the bremsstrahlung x-ray flux observed in space to be used for remote sensing of the electron precipitation and of the atmospheric effects of the precipitation. The flux of x rays F_X of energy E_X is related to the incident flux of electrons F_e at energy E_e through an integral relationship involving a known convolution kernel $\Phi(E_X,E_e)$:

$$F_X(E_X) = \int_{Ex}^{\infty} \Phi(E_X,E_e) F_e(E_e)\, dE_e \ . \qquad (1)$$

In practice, the discrete form of this integral equation is used, and the upper limit is set to an energy of about 100 keV, where the flux of electrons is so low that it can be neglected. The form of the x-ray production kernel Φ is such that large errors can arise in the numerical spectral inversion procedure, particularly at low energies. Recently, however, optimization schemes that reduce the propagation of errors at low energies and provide stable results have been developed.[10] A clear result of these analysis efforts is that as the level of mea-

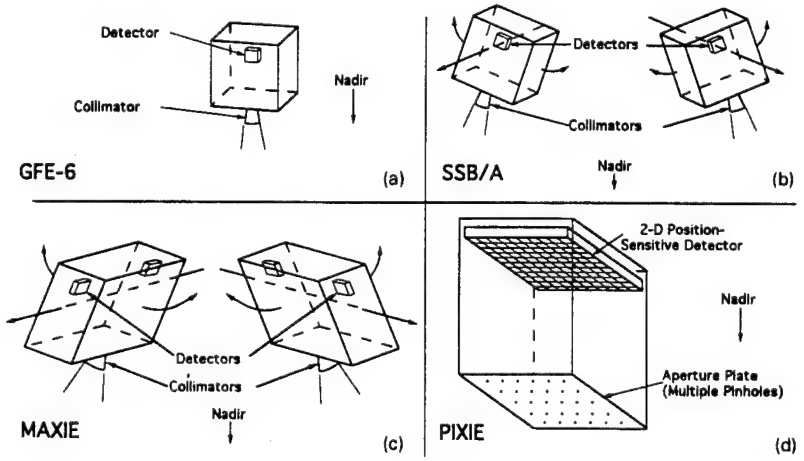

Fig. 2 Some detector arrangements for satellite-borne auroral x-ray instruments.

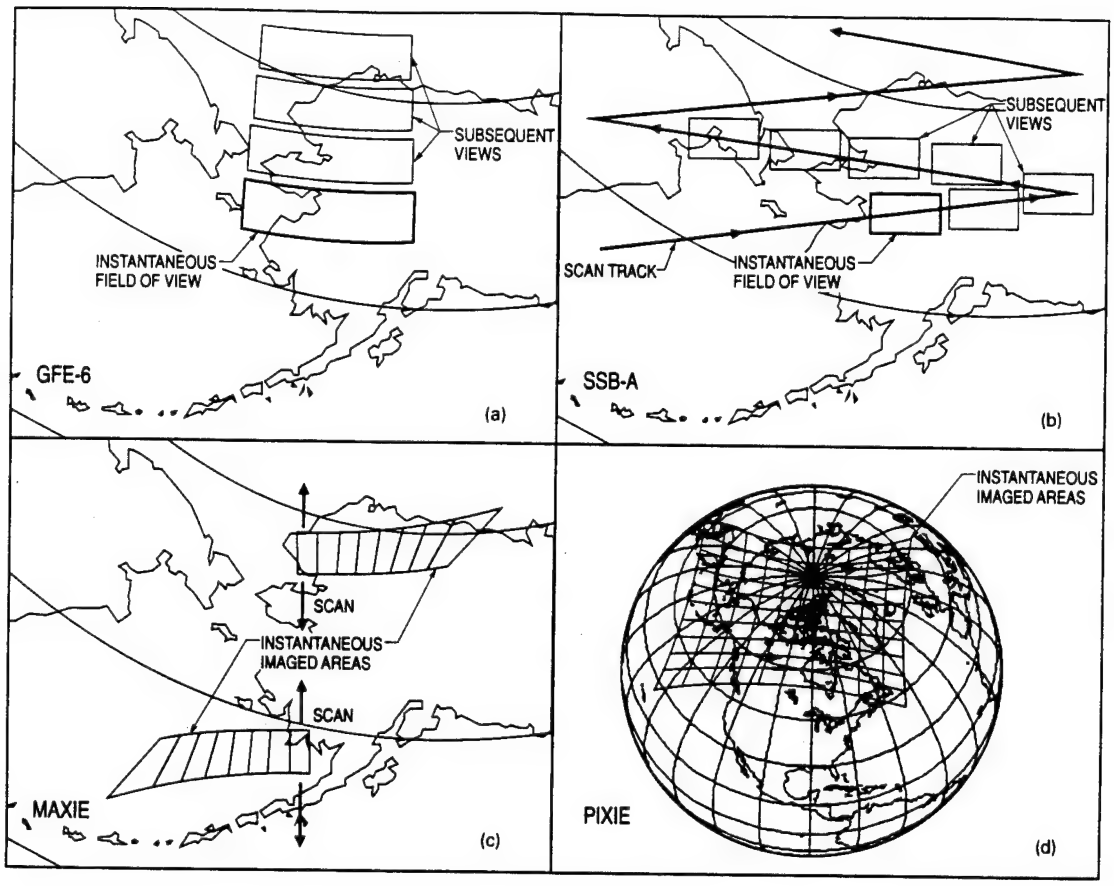

Fig. 3 Imaging techniques for the detector arrangements shown in Fig. 2.

surement noise increases, the quality of the solution decreases dramatically, especially at the lower energies. This characteristic of the analysis procedures places stringent requirements on the quality of the x-ray observations and, in particular, on the counting statistics.

The SSB/A scanning x-ray imager flown on the DMSP-F6 spacecraft[7] [Figs. 2(b) and 3(b)] has been especially useful in testing these numerical deconvolution procedures, since the electron fluxes inferred from the observed x-ray fluxes can be compared with those measured directly by onboard particle detectors. Furthermore, onboard instruments provide visible-range imagery. Figure 4 shows the observed and inferred electron precipitation from an active auroral event. The optical imagery indicated that the satellite passed over a bright narrow arc at high latitude before encountering the broad core of an auroral surge. The precipitating electron data (solid line) indicate an energy deposition rate of about 20 erg cm^{-2} s^{-1} in the poleward arc and 10 to 15 erg cm^{-2} s^{-1} within the core, with little precipitation between the two regions. The quantities inferred from the x-ray observations are plotted as crosses, with the horizontal error bar indicating the effective spatial resolution of the measurement and the vertical bars depicting uncertainties attributable to counting statistics in the x-ray data.

Besides comparisons with direct measurements of the precipitating electron flux, such as that shown in Fig. 4, other comparisons have been carried out with ground-based ionospheric measurements such as incoherent-scatter radar[6] and multiple-frequency riometers.[5] In all cases, the comparisons produced positive results within the limitations of the various measurement techniques. These ground-truth experiments have been vital in evaluating the feasibility of the bremsstrahlung remote-sensing technique, in optimizing numerical procedures for maximizing the scientific return, and in providing a benchmark by which future instrument performance can be evaluated in terms of meaningful geophysical parameters.

3 The PIXIE Instrument

The Polar Ionospheric X-ray Imaging Experiment (PIXIE) is being developed by Lockheed Palo Alto Research Laboratory, The Aerospace Corporation, the Universities of Maryland and Bergen, Norway, and UCLA for flight aboard the POLAR satellite as part of NASA's Global Geospace Science segment of the International Solar-Terrestrial Physics Program. One of the principal mission objectives of the POLAR spacecraft, currently scheduled for launch in May 1994, is

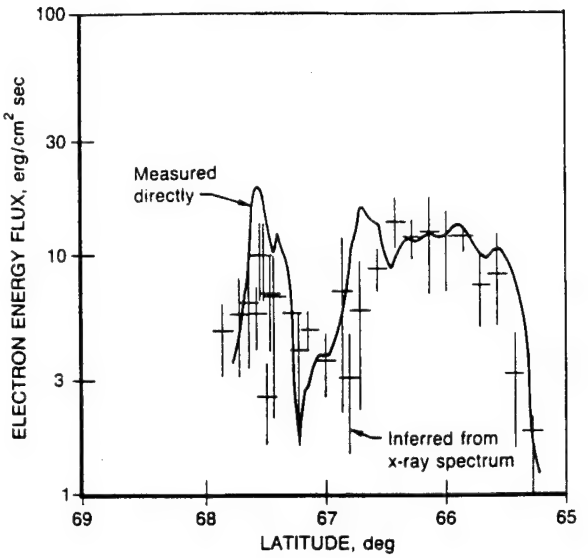

Fig. 4 The precipitating electron spectrum measured by particle detectors aboard a DMSP satellite is compared with that obtained by analyzing the auroral x-ray spectrum in the subsatellite region.

to characterize the energy input to the ionosphere. Three instruments, PIXIE and imagers in the UV and visible bands, will provide global multispectral auroral images of the footprints of magnetospheric energy deposition into the ionosphere. In this context, *global* means simultaneous imaging of the entire northern polar cap. In addition to the imagers, POLAR carries several instruments designed to measure the properties of polar magnetospheric plasmas, waves, fields, and energetic particles under all conditions of geomagnetic activity.

A global auroral x-ray imager should be designed to make use of the advantages discussed in Secs. 1 and 2 while coping with the major limitation of low signal fluxes. A number of imaging techniques were considered for the PIXIE instrument, but only the multiple-pinhole camera and the coded aperture, both of which use a large-area position-sensitive proportional counter for the detector, were found to be capable of simultaneously imaging an entire polar cap over a broad energy range while conforming to strict limits on satellite resources, in particular, size and weight. The choice between these two imaging techniques hinges on the nature of the x-ray source region, which is imperfectly known. A coded aperture[11–14] consists of a plate divided into a large number of individual cells, some fraction (usually one-half) of which is open to transmit x rays. Each point of the source scene creates a shadow image of the plate on the position-sensitive detector. Many source points produce overlapping shadow images, and it is necessary to reconstruct the image of the source region mathematically from the detector count matrix. The great strength of the coded aperture lies in imaging bright objects against a dark field. It is greatly superior to the pinhole camera for this application. However, the noise in every pixel in a coded-aperture image is proportional to the square root of the total number of events registered by the detector. Thus, the system's sensitivity is degraded for bright-field imaging, and its ability to image fainter objects in the presence of a bright one is also reduced. The continuous presence of relatively faint but widespread diffuse auroral emission and the expected presence of features having a range of brightness was the major factor in the decision to use a multiple-pinhole camera for the PIXIE instrument. Additional factors favoring the pinhole camera were the ability to vary the angular resolution and the ability to "zoom in" on the auroral oval as the satellite's altitude varies in its elliptical orbit.

The PIXIE instrument, shown in Fig. 5, is a dual multiple-pinhole camera. The dual cameras result from the use of two independently adjustable aperture plates, each of which transmits x rays to half of the active detector area. The primary reason for the dual plates is to allow one camera to operate with large pinholes and hence maximum sensitivity while the other has small pinholes and hence improved angular resolution. The dual plates also confer a degree of redundancy on the instrument. In fact, PIXIE would retain 50 to 86% of its effectiveness in the event of a complete failure of one aperture-plate drive. The detector is a position-sensitive proportional counter housed in the domed vessel at the rear in the figure. In reality there are four separate detectors in a layer arrangement in two separate gas chambers. The front two layers are designed to detect low-energy x rays (below 12 keV) and transmit higher energy x rays to the rear chamber. The front chamber is filled with argon (and 10% CO_2) to a pressure of 1 atm and has a 0.01-cm-thick beryllium entrance window. The rear chamber, containing the rear two layers, is filled with xenon (and 10% CO_2) to a pressure of 2 atm, and the two chambers are separated by a beryllium window of thickness 0.2 cm.

Each layer of the PIXIE detector has a central anode plane with cathode planes above and below. The wires in one cathode plane are parallel to the anode wires, and those in the second cathode plane are perpendicular to the anode. The charge collected on the anode is a measure of the x-ray energy, and the cathodes each provide position information in one dimension. PIXIE uses graded-density cathodes to provide the position information. In the basic graded-density cathode scheme,[15] signals are taken from two interleaved sets of wires

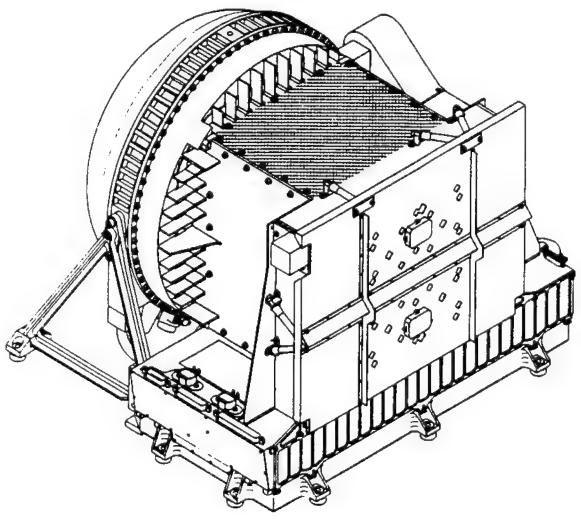

Fig. 5 The PIXIE instrument.

A and B. The density of A wires linearly increases and the density of B wires linearly decreases from one end of the cathode to the other. The grading is arranged so that the ratio of charges $q_B/(q_A + q_B)$ induced on the wires by an avalanche at the anode is linearly related to the position of the avalanche. PIXIE uses a refinement of this idea[16] in which the cathode is subdivided into two identical halves that are mirror images of one another. The signal wire sets A and B (which are no longer interleaved with one another) are both interleaved with a third set of graded-density wires that serves to couple them. The density grading is arranged so that the charge ratio $q_B/(q_A + q_B)$ is again nearly linearly related to the position of the anode avalanche. A programmable ROM look-up table is used to remove small nonlinearities in the relationship between the charge ratio and the position. This scheme allows the position of each x-ray interaction to be determined to an accuracy of 2 mm, anywhere within the active volume of the detector. The third dimension, depth, is determined to an accuracy of ± 5.5 mm by identifying the anode that records the energy signal.

Figure 6 illustrates the operation of the dual-aperture system. We are looking through the single fixed aperture plate to the two movable plates. The blank pinholes are in the fixed plate, and the shaded ones are in the moving plates. X rays are transmitted where pinholes on the fixed and moving plates overlap. All of the motion system is contained within the box formed by the fixed aperture plate on the front, the four sides of the collimator, and the detector window-support structure in the rear. The movable plates move in a direction parallel to their long dimension. Each plate's motion is accomplished by a lead screw that is driven by a stepper motor, with the total travel of each plate, 5.7 cm, accomplished in 11,300 steps. The plate position is specified as a number of steps from the opening of a limit switch (Microswitch 1HM19) at either end of travel. Laboratory tests have shown that the opening position of these switches is repeatable within a standard deviation of approximately 2 μm. Although experience with the SOLEX instrument on the U.S. Department of Defense P78-1 satellite[17] indicates that the switches are very reliable and robust, we have used a redundant pair of switches at each end of travel for each plate for a total of eight switches in all.

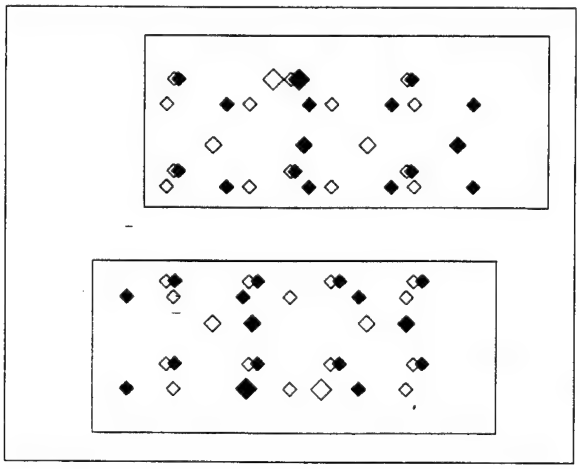

Fig. 6 The PIXIE aperture plates as viewed from the front, with the movable plates viewed through the fixed outer plate. The pinholes in the two movable plates are shaded; those in the fixed plate are unshaded.

Each aperture plate has four sets of pinholes for use at different phases of the satellite orbit. In Fig. 6, the lower plate is positioned to open the set of eight pinholes that are used near apogee, when the maximum number of nonoverlapping images can be formed on the detector plane. (This plate is the high-resolution plate, with the pinholes only slightly opened.) The upper plate is positioned to open the set of six pinholes that are used at intermediate altitudes. (This plate is the high-sensitivity plate.) Each plate has a pair of holes, the slightly enlarged ones near the center of the plates, that are used at lower altitudes, and a single hole, the large one at the outer edge, for observations of the south polar cap from near perigee. The PIXIE high-voltage power supplies are turned off and no observations are made when the satellite is in the Earth's radiation belts, between the low-altitude and perigee observing periods. Not shown in the figure are the four radioactive sources, two for each camera, that irradiate the detector when the movable plates are in a specified calibration position. Two of the sources are Fe^{55} and emit 5.9-keV x rays that are detected primarily in the front chamber, and the other two are Cd^{109} and emit 22-keV x rays that are primarily detected in the rear chamber. Since a single motor step corresponds to 5 μm of motion, the plate position, and therefore the pinhole size, is essentially continuously adjustable.

Both the instrument sensitivity and the spatial resolution of the PIXIE cameras depend on the size of the pinholes. Since both the area and the solid angle of a resolution element are proportional to the pinhole area, the dependence of the signal counting rate on the pinhole dimension d may be as high as d^4. The dependence is usually somewhat weaker because from high altitudes an auroral x-ray emitting structure rarely fills an entire resolution element. The maximum pinhole dimensions (side of the square holes) are 0.47, 0.47, 0.57, and 0.70 cm for the high-altitude, mid-altitude, low-altitude, and perigee sets, respectively. The distance from the aperture plates to the front detector is 21 cm. Because the signal is very sensitive to the pinhole size, the latter will not be reduced below the detector spatial resolution, which is slightly less than 0.2 cm. Therefore, the best available spatial resolution is 9.5 mrad, which corresponds to 485 km when the satellite is at apogee and reduces to 270 km just above the trapped-radiation belts.

The high-altitude auroral x-ray fluxes and the PIXIE telemetry allotment are such as to allow 24 bits of position and energy information to be separately telemetered for each validated x ray detected. The position coordinate determined by each graded density cathode is encoded into 8 bits of data, yielding an oversampling compared to the position resolution by a factor of approximately 3. Two bits provide the depth information by identifying the anode on which the avalanche occurred, and the six remaining bits provide each detector with 64 energy channels over the ranges 2 to 12 keV and 8 to 60 keV for the argon- and xenon-filled chambers, respectively. Telemetering all of these data for each event allows all image reconstruction to occur on the ground and also allows *post facto* control of the exposure times. A typical time period for accumulation of an image will be approximately 5 min, but the fainter and more stable diffuse aurora

can be imaged for as long as half an hour when the satellite is near apogee. Except when the satellite is near perigee, most auroral features will not be resolved by PIXIE. Nevertheless, the global scientific objectives discussed in Sec. 2 can be achieved with the available resolution.

4 The MAXIE Instrument

The Magnetospheric Atmospheric X-ray Imaging Experiment (MAXIE) was developed by Lockheed Palo Alto Research Laboratory, The Aerospace Corporation, and the University of Bergen, Norway, for flight aboard the NOAA-I satellite as a U.S. Air Force Space Test Program payload of opportunity. NOAA-I was launched into a Sun-synchronous (800-km altitude) polar orbit on August 8, 1993. MAXIE is designed to map the intensities and energy spectra of auroral x rays.

Because MAXIE will be flown in a low-Earth orbit, different considerations from those that applied to PIXIE governed its design. While global imaging is impossible from low orbit, MAXIE enjoys a number of advantages because of its low altitude: better spatial resolution, better time resolution, and higher sensitivity. Neither a 2-D pinhole camera nor a coded aperture is suitable for auroral imaging from a low-altitude satellite because of high counting rates and rapid relative motion between the detector and the source. MAXIE's generous telemetry allowance of 11.2 kbit s^{-1} is inadequate to cope with these complications. The system of scanning detectors that was chosen for MAXIE will enable the instrument to obtain as many as 70 images of an auroral feature during the approximately 6 min of each 101-min orbit that it can be observed. Previous x-ray imagers, which were not equipped with movable detector arrays, were able to make only a single image during each orbit. MAXIE is the logical next step in our program of auroral x-ray imaging from low-Earth orbit.

Figure 7 shows the MAXIE instrument, which is mounted on the earthward side of the NOAA-I vehicle. The two large detector heads, shown at the outward extremes of their angular ranges, scan through a range of 87 deg along the satellite track, but with opposite rotation senses to minimize the uncompensated angular momentum imparted to the vehicle.

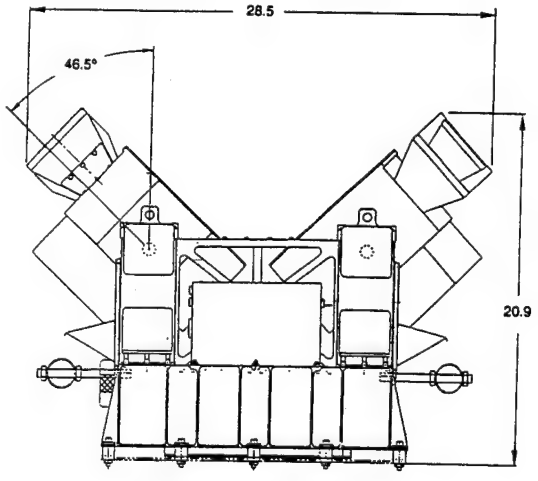

Fig. 7 The MAXIE instrument.

Each scanning head contains eight detector modules, which are quasi-linearly arranged in the cross-track direction (normal to the satellite's orbit plane). The fields of view are such that one head views to the right of the satellite track and the other to the left, with overlap to the extent that the region directly below the satellite is viewed by one detector in each head [see Fig. 3(c)]. MAXIE is, in effect, a scanning pinhole camera, since the detectors in each head look out through a common aperture, a large "pinhole." Each detector module has an area of 5.0 cm^2 and an angular resolution of approximately 7 deg. The angular resolution corresponds to a pixel dimension of 85 km for a detector viewing directly toward nadir. A magnetic field is impressed across the aperture to sweep away electrons that would otherwise impact the detectors and raise backgrounds in the auroral regions to an unacceptable level.

MAXIE uses lithium-drifted silicon [Si(Li)] detectors manufactured at Lawrence Berkeley Laboratory. Each of the 16 detector modules has two 5.0-cm^2-$\times$0.5-cm-thick detectors arranged one in back of the other. The front detector is the primary sensor; the back detector is used both for an anticoincidence veto and for detection of x rays having high enough energy that they have a significant probability of passing through the front detector. Low-energy events in the rear detector are electronically rejected. Si(Li) detectors must be cooled well below room temperature to minimize noise, which affects both the energy resolution and the threshold energy at which the detector is useful. The beam on which the MAXIE detector modules are mounted is cooled by thermoelectric coolers. Analysis predicts an on-orbit beam temperature of -100°C. In thermal-vacuum tests simulating the space environment, we have achieved temperatures of -60°C and energy resolution of 2.4 keV full width at half maximum; this permits us to set the energy threshold at 6 keV. The data are read out in 16 energy channels between threshold and the upper energy limit of approximately 60 keV.

MAXIE's primary contribution to auroral science is the ability to obtain repeated images of dynamic structures in a number of spectral ranges; that is, it can produce "movies" of the spectra of auroral structures. This is made possible by MAXIE's detector-scanning capability. The rotation mechanism has five selectable speeds that yield one-way scan periods, and hence imaging time resolutions of 5, 10, 20, 40, and 100 s. MAXIE will have sufficient sensitivity to allow the brightest features, such as those represented by spectra 3 and 4 in Fig. 1, to be imaged in several energy bands during a single scan at the highest rate. During geomagnetically quiet periods, the slower scan rates are more appropriate.

Precise control and knowledge of the detector-head scan angles is extremely important to the success of MAXIE's mission. While the instrument can and will be operated with the heads fixed, making MAXIE very similar to the Atmospheric X-Ray Imaging Spectrometer[18] aboard NASA's Upper Atmosphere Research Satellite, most of MAXIE's new science will be derived from the ability to make many successive images of the same region. Figure 3(c) is a simplified picture of the instantaneous fields of view of the MAXIE detectors, which are distorted because the instrument views a spherical x-ray emitting layer from above. The MAXIE detector data-accumulation period is 0.25 s, during which time the detector heads scan through an angle between 0.22 and 4.35 deg, and the satellite moves by approximately 2 km

(which is negligible compared to MAXIE's spatial resolution). With these complications, analysis of the MAXIE image data becomes a formidable problem. This complexity is mitigated to a great degree by the imposition of a synchrony between the image-data readout and the detector-head scans. Thus, the image data are read out to telemetry at the same phases of every scan. This mitigation depends on precise control of the scans.

Each of the two detector heads is driven by a six-pole permanent-magnet brushless dc motor with a 100:1 gear-reduction harmonic drive. The harmonic drive has practically no backlash and is very stiff on the output side, which is essential for precise servo control of the detector-head scan angles. Because the MAXIE detectors are very sensitive to acoustic noise, the motors are located at the bases of the stanchions that support the heads, and they drive the heads by means of pulleys with kapton belts. The belts are clamped to the pulleys at both ends to prevent slippage and to achieve a 1:1 correspondence between the motor angle that is monitored by the motion-control system and the scan angle of the detector housing. The motor angles are measured by optical encoders and transferred in 3 bytes (24 bits) every 2 ms to the microprocessor that controls the scan angles. Twelve of the 24 bits are used by the processor. Optical encoder bits 6 to 13 (of 24) are read out to telemetry every quarter second, with bits 14 to 17 read out every second (bit 6 is the least significant of the 12 bits that are used for control). In addition, potentiometers attached to each of the detector-housing rotation shafts provide an absolute scan-angle measurement that is available in the housekeeping telemetry regardless of whether the motion-control system is turned on or off. These last data are also read out to the main telemetry stream on 1-s intervals.

Just as with PIXIE, the MAXIE detectors must be turned off when the satellite is in the radiation belts. This has a minor effect on the primary auroral science for which the instrument is designed, since the radiation belts lie at lower latitude than the polar regions. In addition, past low-altitude nadir-viewing auroral x-ray instruments have experienced difficulties with high backgrounds when passing directly over a region of bright auroral emission. These difficulties come about because the magnetic field lines around which the primary auroral electrons spiral down into the atmosphere are nearly vertical in the polar regions. MAXIE's in-track detector-head scan, with the ability to look both ahead and behind, will be invaluable in overcoming this problem.*

5 Summary

In the Earth's polar regions, the dominant ionizing agent for the E region of the Earth's ionosphere (altitude of approximately 100 km) is the precipitation of energetic charged particles associated with auroral phenomena. The ionization that is formed controls ionospheric conductivity and thus is an important factor in the global atmospheric electric circuit. Precipitating electrons lose their energy primarily by colliding with and ionizing or exciting atmospheric species. Relaxation of these excited species results in the well known and often spectacular visible auroral displays. Electrons lose a very small amount of their energy by the emission of bremsstrahlung x rays in these same collisions. Spatially resolved bremsstrahlung x-ray spectra allow the investigator to obtain, in a relatively straightforward manner, important physical information on the precipitating electron spectrum, the energy transfer from the magnetosphere to the ionosphere by energetic electrons, and height profiles of atmospheric conductivity in the polar regions.

Satellite-borne auroral x-ray detectors have been available for approximately the past two decades. The earliest instruments simply stared downward and obtained spectra of the subsatellite regions. Later, scanning detectors allowed images to be built up during a satellite pass over the auroral regions. These detectors were limited in that only a single image could be obtained per orbit, so temporal coverage was poor and it was impossible to separate temporal from spatial variations in the x-ray source region. Linear arrays of fixed detectors offered an improvement in that simultaneous observation of a 1-D pixel array was possible. This paper has discussed two new x-ray imagers, MAXIE and PIXIE, that will provide, in the next few years, multiple 2-D images during a single satellite orbit. Because these instruments will fly in very different orbits, their imaging techniques differ markedly from one another.

If we were to imagine an ideal operational auroral x-ray imager, it might have the following attributes: time resolution of a few seconds; spatial resolution on the order of 10 km; global coverage (images of an entire polar cap); and the ability to recover auroral electron spectra from the measured x-ray spectra. The last attribute requires essentially two things: moderate spectral resolution and high sensitivity. Current technology and satellite resources do not permit us to achieve the ideal detector; in particular, we cannot envision achieving the combination of 10-km spatial resolution and global coverage in the x-ray region any time in the foreseeable future. The MAXIE instrument will be able to provide the desired time resolution, sensitivity, and spectral resolution, but its spatial resolution still falls short of ideal, and global imaging cannot be achieved from low-Earth orbit. The PIXIE instrument's strong point is its ability to provide global images, but with low spatial resolution. In this connection it is important to realize that PIXIE is part of a complement of three instruments that together will provide multispectral global auroral images. PIXIE's contribution will be spectral images that cover all local times and allow for straightforward determination of the properties of the polar ionosphere. PIXIE and MAXIE will thus open up new opportunities for the application of x-ray images to the study of auroral phenomena. The future holds the possibility for continued evolutionary progress in this field, but to achieve this progress it will be necessary to bring significantly greater spacecraft resources to bear.

Acknowledgments

This work was supported by the U.S. Air Force Space Systems Division under Contract F04701-88-C-0089, the National Aeronautics and Space Administration under Contract NAS5-30369 at The Aerospace Corporation and at Lockheed Palo Alto Research Laboratory by NASA Contract NAS5-30372, the Office of Naval Research under Contract N00014-87-C-0050, and the Lockheed Independent Research Program. The authors wish to thank numerous colleagues at The

* On orbit, the MAXIE instrument performed as designed and expected, but communication with the satellite was lost a few days after launch.

Aerospace Corporation, Lockheed Palo Alto Research Laboratory, the University of Bergen, and the University of Maryland, without whose invaluable contributions this program of auroral x-ray research would not be possible.

References

1. P. F. Mizera, J. G. Luhmann, W. A. Kolasinski, and J. B. Blake, "Correlated observations of auroral arcs, electrons, and X rays from a DMSP satellite," *J. Geophys. Res.* **83,** 5573–5578 (1978).
2. D. Schwartz and H. Gursky, "The cosmic X-ray background," Chap. 10 in *X-ray Astronomy*, R. Giacconi, H. Gursky, Eds., pp. 359–388, D. Reidel, Dordrecht, Holland (1974).
3. W. L. Imhof, G. H. Nakano, and J. B. Reagan, "High-resolution measurements of atmospheric gamma rays from a satellite," *J. Geophys. Res.* **81,** 2835–2843 (1976).
4. D. L. McKenzie, H. R. Rugge, and P. A. Charles, "Soft X-rays from the sunlit earth's atmosphere," *J. Atmos. Terr. Phys.* **44,** 499–508 (1982).
5. T. J. Rosenberg, D. L. Detrick, P. F. Mizera, D. J. Gorney, F. T. Berkey, R. H. Eather, and L. J. Lanzerotti, "Coordinated ground and space measurements of an auroral surge over South Pole," *J. Geophys. Res.* **92,** 11,123–11,132 (1987).
6. R. R. Vondrak, R. M. Robinson, P. F. Mizera, and D. J. Gorney, "X-ray spectrophotometric remote sensing of auroral ionization," *Radio Sci.* **23,** 537–544 (1988).
7. P. F. Mizera, D. J. Gorney, and J. L. Roeder, "Auroral X-ray images from DMSP-F6," *Geophys. Res. Lett.* **11,** 255–258 (1984).
8. W. L. Imhof, J. R. Kilner, G. H. Nakano, and J. B. Reagan, "Satellite X-ray mappings of sporadic auroral zone electron precipitation events in the local dusk sector," *J. Geophys. Res.* **85,** 3347–3359 (1980).
9. W. L. Imhof, H. D. Voss, D. Datlowe, and J. Mobilia, "Bremsstrahlung x-ray images of isolated electron patches at high latitude," *J. Geophys. Res.* **90,** 6515–6524 (1985).
10. D. J. Gorney, P. F. Mizera, and J. L. Roeder, "A maximum entropy technique for deconvolution of atmospheric bremsstrahlung spectra," Report TR-86(6940-06)-6, The Aerospace Corporation (1986).
11. R. H. Dicke, "Scatter-hole cameras for X-rays and gamma rays," *Astrophys. J. Lett.* **153,** L101–L106 (1968).
12. J. Gunson and B. Polychronopulos, "Optimum design of a coded mask X-ray telescope for rocket applications," *Mon. Not. R. Astron. Soc.* **177,** 485–497 (1976).
13. E. E. Fenimore and T. M. Cannon, "Coded aperture imaging with uniformly redundant arrays," *Appl. Opt.* **17,** 337–347 (1978).
14. R. J. Proctor, G. K. Skinner, and A. P. Willmore, "The design of optimum coded mask X-ray telescopes," *Mon. Not. R. Astron. Soc.* **187,** 633–643 (1979).
15. E. Mathieson, G. C. Smith, and P. G. Gilvin, "The graded-density cathode," *Nucl. Instrum. Methods* **174,** 221–225 (1980).
16. P. G. Gilvin, E. Mathieson, and G. C. Smith, "Subdivision of a graded-density cathode," *Nucl. Instrum. Methods,* **185,** 595–597 (1981).
17. P. B. Landecker, D. L. McKenzie, and H. R. Rugge, "CRLS-229 solar x-ray spectrometer/spectroheliograph experiment," *Space Optics—Imaging X-Ray Optics Workshop,* M. Weisskopf, Ed., *Proc. SPIE* **184,** 285–290 (1979).
18. D. L. Chenette, D. W. Datlowe, W. L. Imhof, T. L. Schumaker, and J. D. Tobin, "Global spectroscopy and imaging of atmospheric x-ray bremsstrahlung: instrumentation and initial results from the PEM/AXIS instrument aboard the Upper Atmosphere Research Satellite," *Instrumentation for Planetary and Terrestrial Atmospheric Remote Sensing,* S. Chakrabarti and A. B. Christensen, Eds., *Proc. SPIE* **1745,** 16–25 (1992).

David L. McKenzie received his BS degree in physics from the University of Washington in 1964 and his PhD in physics from the University of California, San Diego, in 1971. Dr. McKenzie joined the Space Physics Laboratory of The Aerospace Corporation in March 1972 as a member of the technical staff and currently holds the position of research scientist in the Space and Environment Technology Center. His research interests include x-ray spectroscopy, solar physics, atmospheric physics, and remote sensing of the Earth's atmosphere. Dr. McKenzie is the author or coauthor of 35 refereed research publications. He is a member of the American Astronomical Society and of Phi Beta Kappa.

David J. Gorney received his BS in physics at the University of Bridgeport, Connecticut, in 1977 and his MS and PhD in atmospheric sciences from the University of California at Los Angeles in 1979 and 1982, respectively. He joined The Aerospace Corporation in 1979 and has held the positions of research scientist, manager, and department director in the Space Sciences Laboratory. Currently, he is principal director of the Office of Research and Program Support in Technology Operations. His scientific activities have included the analysis and theory of auroral energetic particles and fields and the development and application of experimental techniques for remote sensing of the atmosphere, ionosphere, and magnetosphere. He is the author or coauthor of more than 40 refereed scientific publications. Dr. Gorney is a member of the American Geophysical Union, the American Institute of Astronautics and Aeronautics, the American Physical Society, the American Meteorological Society, and Sigma Pi Sigma.

William L. Imhof received his BA, MA, and PhD degrees in physics from the University of California, Berkeley, in 1951, 1953, and 1956, respectively. He has been employed at the Lockheed Palo Alto Research Laboratory since 1956 and has held various research and group leader positions. His scientific activities have involved studies of the Earth's radiation belts, including the sources and loss mechanisms for trapped particles. He has participated in the development of particle detectors and x-ray imagers. He is author of more than 100 refereed scientific publications. He is a member of the American Geophysical Union, the American Astronomical Society, the American Physical Society, Phi Beta Kappa, and Sigma Xi.

11/22/95

MAXIE : A Remote Sensing Satellite Experiment for Rapid Imaging of Auroral X-rays

H. D. Voss*, W. L. Imhof, V. L. Chinn, M. Hilsenrath,
D. O. Murray, J. Mobilia, D. W. Datlowe, R. R. Vondrak**,
Lockheed Palo Alto Research Laboratory
D. L. McKenzie, C. J. Rice, D. Roux, R. Young
The Aerospace Corporation
K. Broenstad, J. Stadsnes, A. O. Solberg, A. Myskja+
University of Bergen, Norway

Abstract

The Magnetospheric Atmospheric X-ray Imaging Experiment (MAXIE), the ONR 401 experiment , is the first in a new class of satellite-borne remote sensing instruments. The primary innovation is the ability to obtain rapid, sequential, images with high sensitivity of the earth's X-ray aurora from a low altitude polar orbiting satellite. These images can be used to identify dynamic temporal variations in the three-dimensional (energy and position) distribution of electron precipitation into the atmosphere. MAXIE mechanically scans using an array of 16 cooled silicon telescopes to acquire a 256 pixel image of the earth's atmosphere, at selected periods such as once every five seconds, over the X-ray energy range of 6 to 120 keV. Each image covers a cross-track horizon-to-horizon distance of 6100 km (area of 20 million km^2) with a spatial resolution of 125 km in the nadir pixels. Up to 150 successive images are made during each auroral oval pass. MAXIE was launched on the TIROS NOAA-13 satellite on 9 August 1993. The experiment performed well during its turn-on sequence; however, the spacecraft bus failed on 21 August 1993. New spacebased technologies successfully used in MAXIE were mixed-mode ASIC microcircuits, a zero torque scanning system with associated viscoelastic damping, a paraffin stow

release mechanism, a parallel integrating PHA processor, a low noise Si(Li) sensor telescope, and an advanced thermal cooling system. MAXIE's on-orbit operation, control of penetrating particle backgrounds, and scientific data indicated good overall performance.

* Now at Taylor University, 500 W. Reade Avenue, Upland IN 46989, IEEE 3490018
** Now at NASA Goddard Space Flight Center, Code 690, Greenbelt, MD 20771
+ Now at NERA, Kokstadveieu 23, N-5061 Kokstad, Norway

I. Introduction

The primary external sources of energy input into the upper atmosphere are solar ultraviolet (UV) radiation, joule heating by ionospheric electrical currents, and energetic particle precipitation. At high latitudes energetic electrons are observed to provide a significant energy input into the upper atmosphere that is quite variable in both time and position. For investigations of atmospheric effects, as well as studies of magnetospheric phenomena, it is important to provide adequate measurements of these inputs. In situ electron spectrometers provide detailed spatial, temporal, and energy information, but only at the point of observation. To obtain measurements of large scale events, remote sensing techniques must be employed. Optical, UV, and bremsstrahlung X-ray photons are all produced by energetic particles hitting the atmosphere. Bremsstrahlung X-rays are generated by more energetic electrons ($E > 5$ keV), whereas optical and UV emissions are associated primarily with lower energy electrons. A unique advantage of X-ray remote sensing is that both day and night coverage is obtained. The bremsstrahlung interaction process and the corrections for albedo, absorption, and background are all well

understood. Using mathematical techniques, the characteristics of the electron population can be calculated from the X-ray measurements using multiparameter fits [1],[2].

Satellite X-ray imaging techniques have recently been summarized by Imhof et al. (1994) [3] and McKenzie et al. (1994) [4]. The first satellite measurements of bremsstrahlung X-rays produced in the atmosphere by precipitating electrons were performed in 1972 from a spinning platform [5]. The X-ray spectrometer was designed with a wide angle collimation and therefore only broad spatial mappings were obtained from a single spectrometer. The spatial resolution was improved in 1979 with a six sensor unit spectrometer that was also on a spinning satellite [6]. A cross-track scanning sensor on the DMSP-F6 satellite produced a single raster scan X-ray image every orbit [7],[8]. Other X-ray imaging experiments produced images using an array of sensor elements and the construction of a 2-D image through a push broom method [9],[10],[11]. Push broom or cross-track line scans allow only one image to be obtained every orbit; a major disadvantage is that the region of interest is only observed for a small period of time.

MAXIE (Magnetospheric Atmospheric X-ray Imaging Experiment) was designed to overcome limitations of previous magnetospheric X-ray imaging experiments. MAXIE represents the first in a new class of satellite two-dimensional atmospheric X-ray imagers. The innovative capability of MAXIE is the ability to obtain rapid sequential images with a large geometrical factor. The MAXIE instrument is a joint effort between Lockheed, The Aerospace Corporation, and the University of Bergen, Norway. MAXIE, the ONR (Office of Naval Research) 401 experiment on the NOAA-13 spacecraft, was launched into an 800 km sun-synchronous polar orbit on 9 August 1993. After a brief period of operation the satellite failed due to an electrical power short on 21 August 1993. Several orbits of data were obtained during the MAXIE turn-on process.

The purpose of this paper is to present the MAXIE instrument design and calibration. On-orbit data, although brief, allows for an assessment of the new technologies pioneered in MAXIE and of the sensor performance with respect to penetrating background particles. Because the MAXIE five second sequential images are the first of a new type of X-ray data some considerations are discussed regarding data presentation for future missions that rapidly image from a moving satellite.

II. Science and Technical Objectives

Design of the MAXIE instrument was guided by several important considerations. In order to measure the spatial and temporal characteristics of electron precipitation it was desirable to perform X-ray measurements with a multisensor instrument on a low-altitude satellite. Because the electron-induced X-ray flux is relatively weak (about 10^{-5} of the typical precipitating auroral electron flux), the instrument must feature high sensitivity with good background rejection. The spatial, spectral, and temporal characteristics of the X-ray emissions are obtained by repeated observations of a given region in space as illustrated in Figure 1; a mechanical scanning spectrometer accomplished this. Mechanical scanning of a one-dimensional sensor array was a compromise based on the limiting requirement of having a 16 by 16 pixel image (256 pixels), instrument cost, and mass requirements allowing for a limited number of sensors (sixteen 5.0-cm^2 telescopes). With such a device, the atmosphere was observed continuously, in contrast with the lower duty cycle (typically <25%) achievable from a spinning satellite.

Limb to limb scans in a direction parallel to the satellite's orbit plane were obtained as fast as once every 5 seconds. Adequate spatial resolution (~100 km at nadir)

was obtained with collimation that was sufficiently wide to provide a reasonable sensitivity for detection of bremsstrahlung X-rays from the atmosphere and yet was adequately narrow for mapping purposes. A suitable energy range of detection (6 to 120 keV) was achieved with cooled silicon detectors.

An outline of the MAXIE total field-of-view projected from a low altitude polar orbit on the aurora during a modeled auroral substorm event is shown in Figure 2. The substorm features in the model are described by Miller and Vondrak (1985) [12]. As the polar orbiting satellite moves across the auroral oval, MAXIE observes approximately one half of the auroral oval with multiple images per pass. Previous X-ray imagers have acquired only one image per satellite pass. MAXIE was designed to obtain up to 60 images of an individual auroral form at a specific geographic location during 5 minutes of satellite overpass. By acquiring repeated sequential images (movies) of the atmosphere, the experiment provides the opportunity to study auroral dynamics on a fast time scale.

The spacecraft resources available for the instrument were a power of 38 W, inclusive of thermoelectric cooling, and a mass of 47 kg. The telemetry rate of 11.2 kbits s^{-1} required on-board data compression. Furthermore, the instrument requirements for the NOAA-13 spacecraft demanded a net uncompensated angular momentum of $< 2.9 \times 10^{-6}$ kg m^2/s and EMI requirements below those called out in MIL-STD-461.

III. INSTRUMENT DESCRIPTION

Design overview and measurement capabilities

The MAXIE instrument consists of two identical counter-rotating pinhole cameras. Figure 3 is a cross-sectional view of the instrument. The eight telescopes in

each head view through a common aperture, a large "pinhole". The camera approach has several advantages over eight individual telescopes with collimators: lower weight and size, greater local radiation shielding, ease of cooling the sensor array, a single sweeping magnet, and a single collimator and aperture window. The housing and external collimators were made of aluminum to provide structure with a low atomic-number (Z) material. The low Z is required to minimize the production of local bremsstrahlung X-rays by penetrating electrons. The broom magnet has a maximum internal field of 0.1 tesla (1.0 kG) in the center of the gap to bend potentially contaminating electrons away from the aperture. The two internal collimators are made of a high Z material (lead) to absorb local bremsstrahlung and help define the field of view edges.

The individual sensor modules or telescopes are each housed in a cylinder of tungsten for added passive shielding and all are positioned to view the aperture window. The telescopes are angled in such a way that the nadir viewing sensors are spaced farther away from each other and have shorter focal lengths than the limb viewing sensors, as given in Table 1 and plotted in Figure 4. The reason for this is to better approximate equal viewing regions on the sphere of the earth's auroral emitting region (at about 100 km altitude). Some region of overlap in spatial coverage at nadir was desired to separate time-space ambiguities when the heads were not scanning.

The focal "plane", that includes the eight telescopes (U-beam structure), is thermally and electrically isolated from the housing. The structure is cooled below -60°C by a 4-stage thermoelectric cooler. Thermal isolation is achieved by using four thin fiberglass U-beam mounts to the housing and a multilayer thermal blanket around the focal plane. The housings themselves are cooled passively to about -10°C to insure that the thermoelectric coolers have a cold operating base.

Figure 5 shows the MAXIE instrument, which is mounted on the earthward side of the NOAA-13 vehicle. The two large heads, shown at the outward extremes of their angular ranges, scan through a range of 87 degrees along the satellite track, but with opposite rotation senses to minimize the uncompensated angular momentum imparted to the vehicle. The low noise preamplifier electronics are located in the rectangular box on the housing. Vertical stanchions support the sensor heads at bearings and are made of stainless steel to add the necessary structural strength while maintaining thermal isolation from the baseplate and electronics boxes. The baseplate is cooled with a nadir viewing radiator shelf and is thermally isolated from the spacecraft with fiberglass standoffs. The main digital electronics box, high voltage bias supply box, and motion control box are mounted to the baseplate.

High reliability was accomplished by using two independent instrument halves: two sensor heads, two high voltage power supplies, two microprocessors, and two low voltage power supplies. Half of the instrument could be operated while the other half was shut down. This design philosophy provided fault tolerance and the ability to diagnose and reconfigure the instrument. The instrument is microprocessor controlled with a dedicated microprocessor for the motion control system. Pulse height and anticoincidence analysis from each of the silicon sensors is obtained with custom built application specific integrated circuits (ASICs). The completed instrument photo is given in Figure 6 and instrument specifications are given in Table 2.

Sensor Operation

MAXIE uses lithium-drifted silicon [Si(Li)] detectors manufactured at the Lawrence Berkeley Laboratory. Each of the sixteen detector modules has two 5.0 cm^2 x 0.5 cm thick detectors arranged one in back of the other, as shown in Figure 7. The front

detector (Si 1) is the primary sensor; the back detector (Si 2) is used both for an anticoincidence veto and for detection of X-rays having high enough energy that they have a significant probability of passing through the 5 mm thick front detector. The efficiency curves for the Si 1 and Si 2 detectors are given in Figure 8.

Si(Li) detectors must be cooled well below room temperature in order to minimize noise, which affects both the energy resolution and the threshold energy at which the detector is useful [13]. The leakage current and full-width-at-half-maximum (FWHM) noise are shown as functions of temperature in Figure 9. For operation, the sensors must be cooled to <-60 °C. In thermal-vacuum tests simulating the space environment at temperatures of -60 °C an energy resolution of 2.4 keV FWHM was obtained. This permits an energy threshold of 6 keV.

Low-energy events in the rear detector are electronically rejected. A detailed sensor electronics schematic is shown in Figure 10. The data are read out in 16 energy channels between the threshold and the upper energy limit of approximately 60 keV for the front Si 1 detector and in four energy ranges between 20 and 120 keV for the rear Si 2 detector.

System Electronics

A block diagram of one half-section of the electronics is shown in Figure 11. The signals from eight detector modules are amplified. The peak pulse output voltage is proportional to the incident X-ray energy. For Si 1 the maximum energy was 60 keV and for Si 2 the maximum energy was 120 keV. A unique custom microcircuit was developed [14] to convert the analog pulse height and/or area to an 8-bit digital byte. The low power CMOS microcircuit was called an energy processor since it used a 256 channel flash converter operating with a throughput of 5 MHz to analyze each pulse for pile-up, peak

energy, integral pulse energy, threshold level, and coincidence status. The integral summing of area under the pulse greatly improved the differential linearity of the pulse height analysis.

After analysis by the energy processor the counts were accumulated in two ways. All the counts above the programmable threshold were accumulated in a scaler microcircuit. This was also a custom analog/digital microcircuit that contained eight 17 bit counters with interface logic. The 256 level byte of pulse height information from the energy processor was tri-stated to the address bus of a look-up table to perform a log type energy compression to 16 channels. This was required because the telemetry bandwidth was limited and the bremsstrahlung spectra typically have a power-law form. After the energy compression the corresponding count was accumulated in a 1k by 16 bit RAM. Every 0.5 seconds the scaler counter was read out and reset and every 0.25 seconds the RAM spectra were read out and zeroed.

The NSC800 microprocessor system was used to interface with the spacecraft command and telemetry, to read and compress the accumulated X-ray and background count rates, and to control the instrument internal calibration pulser, high voltage level, and general health and safety.

Motion Control System

The motion control system was developed by the University of Bergen [15]. The scanning of the two sensor housings A and B, containing the collimated detector arrays, is done by the motion control system. The system is built around a common microprocessor (NSC800) controlling two separate brushless DC-motor/gear systems, one for each housing. A block diagram of the motion control system is shown in Figure

12. The MAXIE dual heads were rotated about their centers of mass to minimize torques to the spacecraft.

The motion control was designed as a closed loop servo where the movement of the motors is slaved to a numeric scan angle profile stored as a fixed number table in the microprocessor system's control ROM. This number table gives the rounded triangular angle profile as shown in Figure 13. The motion is synchronized (slaved) to the telemetry in such a way that there is always a one-to-one correspondence between the scan angle and the data accumulation period of the X-ray spectra, which are telemetered every 1/4 second. By slaving the scan to a numeric table, there are no switches and end-stops to be touched that could disturb the spacecraft. An end-switch touch is only used for a one time angle calibration and only with a very slow sweep motion.

Motor control is obtained by checking the motor angle (position) every 20 ms by reading the 4000 step per revolution incremental angular encoder fixed to the motor shaft. Based on these values and the scan angle profile data, updated motor control data are computed and given to the motor as pulse width modulated current pulses at the rate of 9689 pulses/second, thus resulting in a very smooth and accurate motion over a great range of torque loads. For a full scan angle of 87 degrees, the motor will make ~25 revolutions, and a harmonic drive gear system with a 100:1 reduction was used for making the proper scan angle and giving sufficient torque. The harmonic drive, with its near-zero backlash, has a very high output torque capacity and is suitable for controlling large moments of inertia. This motion control concept resulted in accurate, synchronous, and opposite-spin-compensated motion of the sensor housings with a minimum of net angular momentum transferred to the spacecraft. The integrated gear/motor/optical encoder unit is shown in Figure 14 with a cross-sectional view of pulleys, kapton belt, mechanical end stops, and end microswitch assembly.

To avoid having mechanical vibrations originating in the motor/gear system propagate and generate microphonics in the detectors, some mechanical filtering was built into the system. A viscoelastic damping material with a mass plate was glued to the motor/gear/mounting plate for damping the local vibrations generated around the motor. To further isolate the mechanical vibrations, the motion at the output of the gears was transferred to the housings by a pulley and kapton belt system, thus utilizing the filtering effect of the low kapton belt mass/length and elasticity relations.

Operational Modes

The control system program was designed to operate for different scan modes which could be changed by an 8-bit mode code given to the control through the spacecraft command system [16]. The modes of scanning are listed in Table 3. Modes were also made for stop at home, at nadir or at stow position. Some examples are shown in Figure 13. The program had options for down-loading data and program sequences, thus enabling a fine tuning of the control parameters with the system in its final configuration. The program also interacted with a built-in watchdog that would automatically restart the system if program execution stopped for some reason. The only restriction on the watchdog restarting the system was that the 8-bit mode command code register had to be undisturbed.

The different sweep times, i.e. the time for a sweep in one direction or the time for a sweep back again, were designed to be 5, 10, 20, 40, or 200 seconds, thus enabling generation of images with this same time resolution. To save the mechanism from unnecessary wear, an option was included that stopped the scanning and parked the housings in the nadir position for orbit latitudes lower than +/- 45 degrees. A listing of the various operational modes of the instrument is given in Table 3.

During launch the heads were held in place using a paraffin actuator, Starsys Research 1H-5055 HO, based stow release mechanism (see figure 12). When power is applied to the built-in redundant heater filaments, the paraffin melts and expands. The thermal expansion forces the piston to move linearly out over a working distance of 1.27cm with a force > 10 kg. The paraffin expansion is stopped by an end switch that shuts off the heater power. The paraffin actuator system is nondestructive and can be recycled/tested over and over again. To make the mechanism an only-one-time operation device, lock springs were built-in to prevent the locking pins from sliding back. In orbit the stow release mechanism worked as designed.

Figure 15 shows scanning data for orbit 158. The two upper panels show the position of the detector housings (POSA and POSB) related to home (h), nadir (n) and turn (t). These position data are based on the 12 bit numbers that are used in the microprocessor algorithm for controlling the motors. The two lower panels (ABSA and ABSB) are analog to digital converted angle data based on the analog angle potentiometer encoders that were mounted directly to the housing rotational shafts. The figure shows scanning with a 40 second sweep time followed by a ground issued STOP SCANNING. This command was followed by a GO TO NADIR which was sent at about 14:49 UT.

IV. Calibration

The instrument main sensor calibration was accomplished using radioactive sources. A high resolution Pulse Height Analyzer (PHA) was connected externally to the amplifier output and used to compare with the instrument PHA and processors. An internal calibration pulser was used to cross-calibrate amplifiers over various energies. The instrument PHA output for a single telescope using an Am-241 source is shown in

Figure 16. The 13.9 to 20.8 keV L-shell source lines are predominantly stopped in the Si 1 detector and are very weak in the Si 2 detector while the 59.54 keV gamma is about the same in Si 1 and Si 2, in agreement with the efficiency curve shown in Figure 8. The 256 bins of pulse height data from the energy processor were log compressed into 16 channels for telemetry transmission (Figure 17). The bremsstrahlung spectrum typically increases strongly with decreasing energy (e.g. an *e*-folding energy of about 4 keV).

The angular response curve for a typical pixel near nadir is shown in Figure 18. The full-width-at-half-maximum (FWHM) is about 10 degrees near nadir and 7 degrees near the limb. For NOAA-13 at 800 km altitude and assuming the X-ray production layer at ~100 km, the region covered is about 125 km at nadir. As the instrument scans, the angular response distributions are projected onto the spherical earth to obtain the atmospheric source location.

V. Data Projection and Presentation Formats

The projection of the MAXIE sensor on the Earth at various locations along the satellite trajectory when nadir pointing is illustrated in Figure 19a. The projection of a moving and scanning sensor on the earth when viewing from limb to limb is complicated as illustrated in Figure 19b which shows the area viewed during a single scan.

Precise control and knowledge of the detector-head scan angles are fundamental. While the instrument could operate with the heads fixed, making MAXIE very similar to the Atmospheric X-ray Imaging Spectrometer aboard NASA's Upper Atmosphere Research Satellite [11], most of MAXIE's new science capability derives from the ability to make many successive images of the same region. The MAXIE detector data-accumulation period was 1/4 second, during which time the detector heads scanned

through an angle between 0.11° and 4.35°, depending on scan mode, while the satellite moved approximately 2 km (negligible when compared with MAXIE's spatial resolution). Because of these motions, the analysis of the MAXIE image data becomes a complicated task. This complexity is mitigated to a great degree by the imposition of a synchrony between the image-data read-out and the detector-head scans. Thus the image data were read out to telemetry at the same phases of every scan. The scan angles were read out by two methods: (1) with high accuracy as the actual position numbers used by the microprocessor control algorithm; and (2) with lower accuracy as an analog voltage from a voltage divider potentiometer attached to each housing shaft.

VI. Expected Count Rates

The differential bremsstrahlung spectrum in the auroral region is generally characterized as a power law, $dJ/dE = J_o(1\ keV)\ E^{-2}$, with a power law of exponent -2 and a 1 keV flux constant, J_o, of 3000 $cm^{-2}\ s^{-1}\ sr^{-1}$ for a weak auroral feature and about $6x10^4$ $cm^{-2}\ s^{-1}\ keV^{-1}\ sr^{-1}$ for a strong feature [12]. A strong feature is typical of a westward traveling surge while a bright auroral arc has a flux constant of about 10^4 $cm^{-2}\ s^{-1}\ keV^{-1}\ sr^{-1}$.

When integrated, assuming the detector efficiency is constant, the count rate per pixel is given by $CR(E) = J_o\ GF\ DE/E\ e\ E^{-1}$, where GF is the geometric factor (about 0.04 cm^2 sr), DE/E is the energy bandwidth (about 0.2) and e is the efficiency of collection (about 0.5 between 4 and 40 keV). Using these approximate numbers the MAXIE count rate per second per keV varies between $12E^{-1}$ and $240\ E^{-1}$ for a weak and strong auroral event, respectively. The total count rate per second between 6 and 60 keV would be about 20 and 400 for the weak and strong events, respectively. Since a given

emission region at 100 km altitude is viewed for about 12 seconds from a satellite at 800 km, the total counts for a single event would be approximately ten times the instantaneous counting rates. The total counts per pixel during a pass would then range from about 200 to 4000 counts.

VII. On-orbit Data

Only one orbit of data was obtained with the MAXIE instrument scanning just before the spacecraft demise. The data for one of the pixels (Housing B pixel 5) during this orbit are shown in Figure 20. The pass starts over the northern polar cap, proceeds to the low cosmic ray backgrounds at the magnetic equator, then to the southern polar cap with the two conspicuous auroral oval horns, then to the high background environment of the South Atlantic Magnetic Anomaly (SAMA), back over the northern polar cap with its auroral oval horns, and finally ending in the low background near the magnetic equator. The superimposed count rate spikes, particularly over the SAMA region, are due to the scan motion permitting locally trapped energetic particles to penetrate into the sensor enclosure. The penetrating background count rate, without anticoincidence, is about ten counts/s over the polar cap and about two counts/s near the equator for the 800 km orbit. For a weak auroral event the count rate without integration and anticoincidence rejection would be well above the noise over the polar cap. Unfortunately, at this time the magnetic and auroral activity was low, and no strong X-ray auroral forms were observed. The scan motion is particularly useful at identifying auroral forms over the polar cap where the background is relatively constant so that the scanning modulation can be readily subtracted from the slowly varying background.

VIII. Conclusion

The development of the MAXIE satellite X-ray imager is a great advance in the evolution of satellite remote sensors of atmospheric X-rays. The MAXIE instrument design provides the sensitivity, time resolution, spectral resolution, and background rejection needed for the imaging of the dynamic aurora. The spatial resolution is greatly superior to previous designs and is adequate for detailed images. New satellite instrument technologies in MAXIE were proven, such as ASIC microcircuits, a "zero" torque scanning system, a paraffin stow release mechanism, a parallel integrating PHA processor microcircuit, a low-noise sensor telescope, a mechanical scanning system that effectively suppresses microphonics with viscoelastic damping, and an advanced thermal cooling system. Instrument on-orbit operation, penetrating particle backgrounds and science data validate satisfactory overall performance.

Acknowledgments

This work was supported at Lockheed by the Office of Naval Research (ONR) under contract N00014-87-C-0050, by the National Aeronautics and Space Administration under contract NAS5-30372, and by the Lockheed Independent Research Program. At Aerospace, this work was supported by the US Air Force Space and Missile Systems Center under contract F04701-88-C-0089. At the University of Bergen this work was supported by the Norwegian Research Council. We thank Mr. R. G. Joiner at ONR for his program direction. We wish to thank numerous colleagues at the Lockheed Martin Palo Alto Research Laboratory, The Aerospace Corporation, and the University of Bergen without whose invaluable contributions, the completion of this instrument

would not have been possible. In particular, at Lockheed we thank Mr. Kevin Appert for flight software development, Mr. Bernie Gordon and Mr. Ralph Lindsey for mechanical design, Ms. Brenda Costanzo for thermal design, Mr. Gary Heyman for GSE software development, Ms. Marion Bumula and Mr. Ken Strickler for their role in the hardware development, and Drs. J. B. Reagan, L. F. Chase, T. R. Fisher, and M. Walt for their various programmatic contributions. At The Aerospace Corporation we thank Mr. Jon Osborn for his design of the GSE hardware. At the University of Bergen we thank Mr. Ragnar Aas and Aadne Sandoey for their efforts in the data analysis software development and processing. We thank Mr. Per Sundail at Prototech for his efforts on the design and development of the motor/gear system. We would also like to thank Mr. John Valentine at Lockheed Martin Astro for his support in the instrument accommodation on to the NOAA 13 satellite.

References

[1] Vondrak, R. R., R. M. Robinson, P. F. Mizera, and D. J. Gorney, "X-ray spectrophotometric remote sensing of auroral ionization", *Radio Sci.*, 23, 537-544, 1988

[2] Robinson, R. M. and R. R Vondrak, "Validation of Techniques for Spaceborne Remote Sensing of Auroral Precipitation and its Ionospheric Effects", *Sp. Sci. Rev.*, 69, 331-407, 1994

[3] Imhof, W. L., H. D. Voss, and D. W. Datlowe, "Imaging of X rays for Magnetospheric Investigations", *Optical Engineering*, 33, 383-390, 1994

[4] McKenzie, D. L., D. J. Gorney and W. L. Imhof, "Auroral X-ray Imaging from High- and Low-Earth Orbit", *Optical Engineering*, 33, 414-422, 1994

[5] Imhof, W. L., G. H. Nakano, R. G. Johnson, and J. B. Reagan, "Satellite Observations of Bremsstrahlung From Widespread Energetic Electron Precipitation Events", *J. Geophys. Res.*, 79, 565-574, 1974

[6] Imhof, W. L., J. R. Kilner, G. H. Nakano, and J. B. Reagan, "Satellite X Ray Mappings of Sporadic Auroral Zone Electron Precipitation Events in the Local Dusk Sector", *J. Geophys. Res.*, 85, 3317-3359, 1980

[7] Mizera, P. F., J. G. Luhmann, W. A. Kolasinski, and J. B. Blake,"Correlated observations of auroral arcs, electrons, and X rays from a DMSP satellite", *J. Geophys. Res.*, 83, 5573-5578, 1978

[8] Mizera, P. F., D. J. Gorney, and J. L. Roeder,"Auroral X-ray Images from DMSP-F6", *Geophys. Res. Letters*, 11, 255-258, 1984

[9] Imhof, W. L., H. D. Voss, D. W. Datlowe, and J. Mobilia, "Bremsstrahlung X Ray Images of Isolated Electron Patches at High Latitudes", *J. Geophys. Res.*, 90, 6515-6524, 1985

[10] Calvert, W., H. D. Voss, and T. C. Sanders,"A Satellite Imager for Atmospheric X Rays", *IEEE Trans. Nucl. Sci.*, NS-32, 112, 1985

[11] Winningham, J. D., J. R. Sharber, R. A. Frahm, J. L. Burch, N. Eaker, R. K. Black, V. A. Blevins, J. P. Andrews, J. Rudzki, M. J. Sablik, D. L. Chenette, D. W. Datlowe, E. E. Gaines, W. I. Imhof, R. W. Nightingale, J. B. Reagan, R. M. Robinson, T. L. Schumaker, R. R. Vondrak, H. D. Voss, P. F. Bythrow, B. J. Anderson, T. A. Patemra, L. J. Zanetti, D. B. Holland, M. H. Rees, D. Lummerzheim, G. C. Reid, R. G. Robel, C. R. Clauer, and P. M. Banks, "The UARS Particle Environment Monitor", *J. Geophys. Res.*, 98, 10649-10666, 1993

[12] Miller, K. L. and R. R. Vondrak, "A High-Latitude Phenomenological Model of Auroral Precipitation and Ionospheric Effects", *Radio Science*, 20, 431-438, 1985

[13] Voss, H. D., J. B. Reagan, W. L. Imhof, D. O. Murray, D. A. Simpson, D. P. Cauffman and J. C. Bakke, "Low Temperature Characteristics of Solid State Detectors for Energetic X Ray, Ion and Electron Spectrometers", *IEEE Trans. Nucl. Sci., NS-29,* 173, 1982

[14] Hilsenrath, F., H. D. Voss, and J. C. Bakke, "A Single Chip Pulse Processor for Nuclear Spectroscopy", *IEEE Trans. Nucl. Sci.*, NS-32, 145, 1985

[15] Broenstad, K and A. O. Solberg, MAXIE Motion Control System Handbook, Univ. of Bergen, Physics Dept., Sci./Tech. Rep. 1991-26 (1989-209), ISSN 0803-2696, 1-189, 1991

[16] Myskja, A. F., Microprocessor-based Motion Control System for the MAXIE Scanning X-ray Imager, Thesis for the Cand. Scient Degree in Physics, Dept. of Physics, Univ. of Bergen, 1989

Table 1 Telescope location relative to the aperture coordinates

Pixel #	Focal Length	Side view angle	End view angle
	(cm)	(Deg)	(Deg)
1	17.9	-7	2.4
2	17.8	7	5.3
3	17.9	18	7.4
4	18.0	28	7.3
5	18.3	36.5	7.2
6	18.6	45	7.1
7	19.2	52	6.8
8	19.63	60	6.7

Table 2 MAXIE instrument specifications

Imaging Principle	Two counter-rotating pinhole cameras with 16 instantaneous look directions
Detectors	5 mm thick by 5.00 cm^2 area Si(Li) detectors
Telescopes	Two back to back Si(Li) detectors, Si 1 Front and Si 2 Rear
Number of Telescopes	16
Number of Image Pixels	256
Detector Temperature	<-60° C design, operating range <0° C
Detector Coupling	AC coupling with bias resistor tied to signal ground
Detector Resolution	1.8 to 2.5 keV FWHM at -60 degrees C
Energy Range Front (Si 1)	6 to 60 keV in 16 log spaced channels
Energy Range Back (Si 2)	20 to 120 keV in 4 log spaced channels
Background Rejection	Passive Shielding, active anticoincidence, broom magnet
Cross-track Field-of-view	Limb to limb, ±62° from nadir (East-West view)
Scan Angular Range	±43.5° from nadir (North-South view)
Sweep Times	5, 10, 20, 40, 200 second
Angular Resolution	0.1° digital encoder
Telescope FOV	Varies between 6° and 12°
Instrument Power	38 W
Thermoelectric Coolers	10 W
Mass	47 kg
Telemetry rate	11.2 kbit/s
Spacecraft	TIROS I, NOAA 13, launched 9 August 1993
Orbit	800 km altitude, 93.6° inclination

Table 3 Instrument operation modes

SCAN MODES	SCAN MODE OPERATIONS
M C Sleep	Stops heads at fully opened position (A +43.5°, B -43.5°)
HOME A or B	Moves Heads to fully opened position (A +43.5°, B -43.5°)
NADIR A or B, A and B	Moves heads to nadir view direction (0°)
SWEEP RATE A or B, A and B	Select sweep periods of 5, 10, 20, 40, 200 seconds
STOW A or B	Moves heads to stow position (A -27.5°, B +27.5)
DATA MODES	DATA MODE OPERATION
SCIENCE	Normal data collection
RING	Microprocessor counting
ENGINEERING	Fast dump of flight software and status
CALIBRATION	Normal data collection with cal pulser on each sensor

List of figures

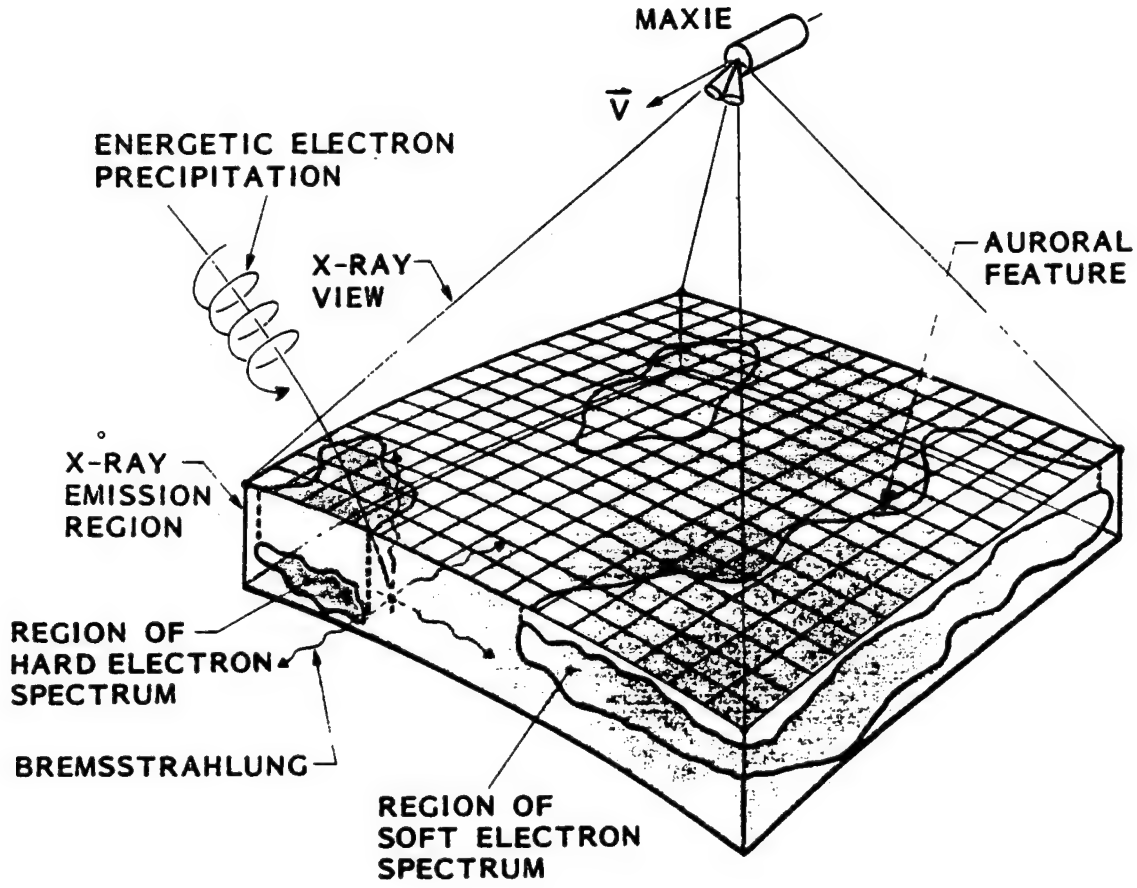
MAXIE
$\vec{V}$
ENERGETIC ELECTRON
PRECIPITATION
X-RAY
VIEW
AURORAL
FEATURE
X-RAY
EMISSION
REGION
REGION OF
HARD ELECTRON
SPECTRUM
BREMSSTRAHLUNG
REGION OF
SOFT ELECTRON
SPECTRUM

Figure 1

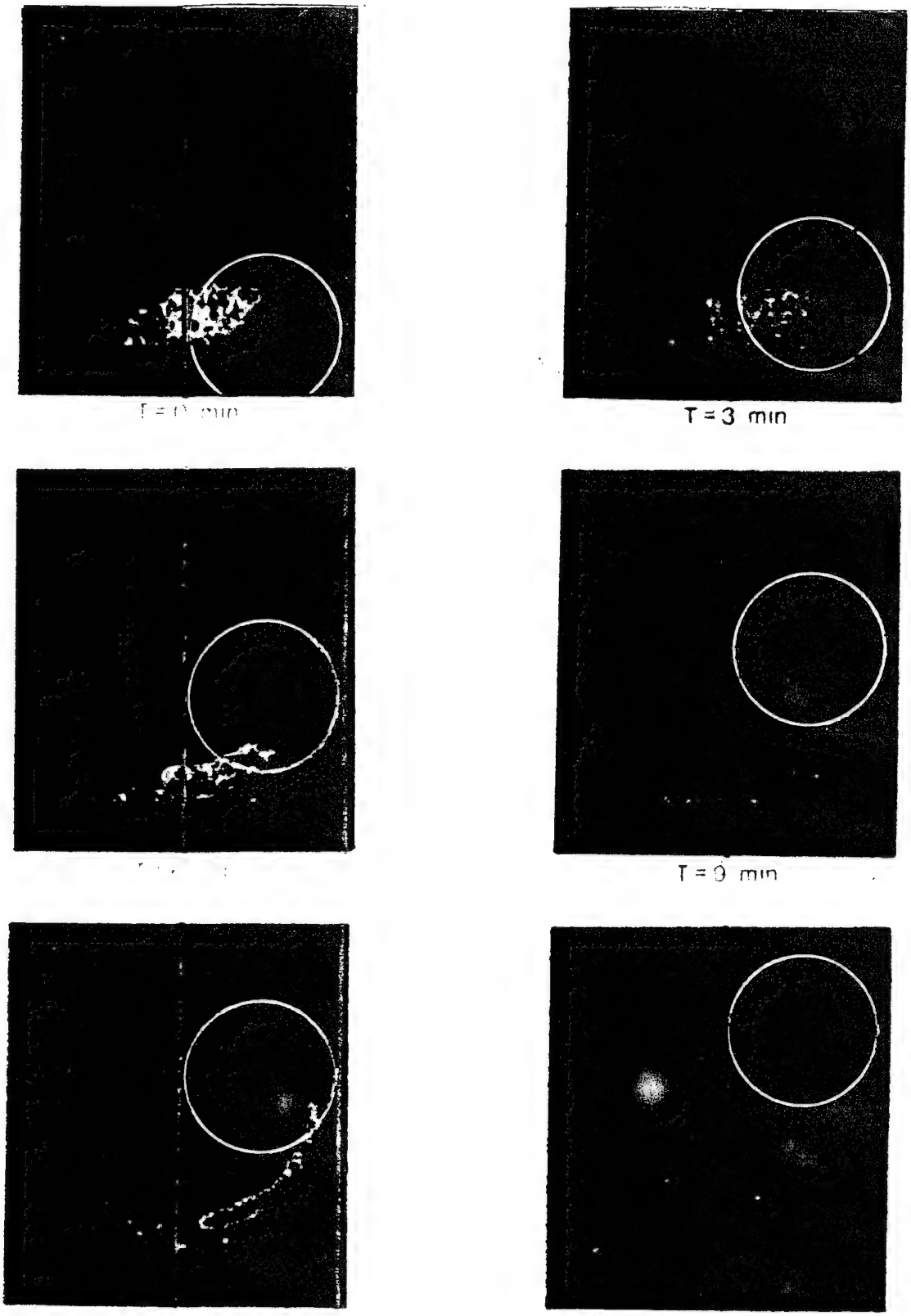

Figure 2

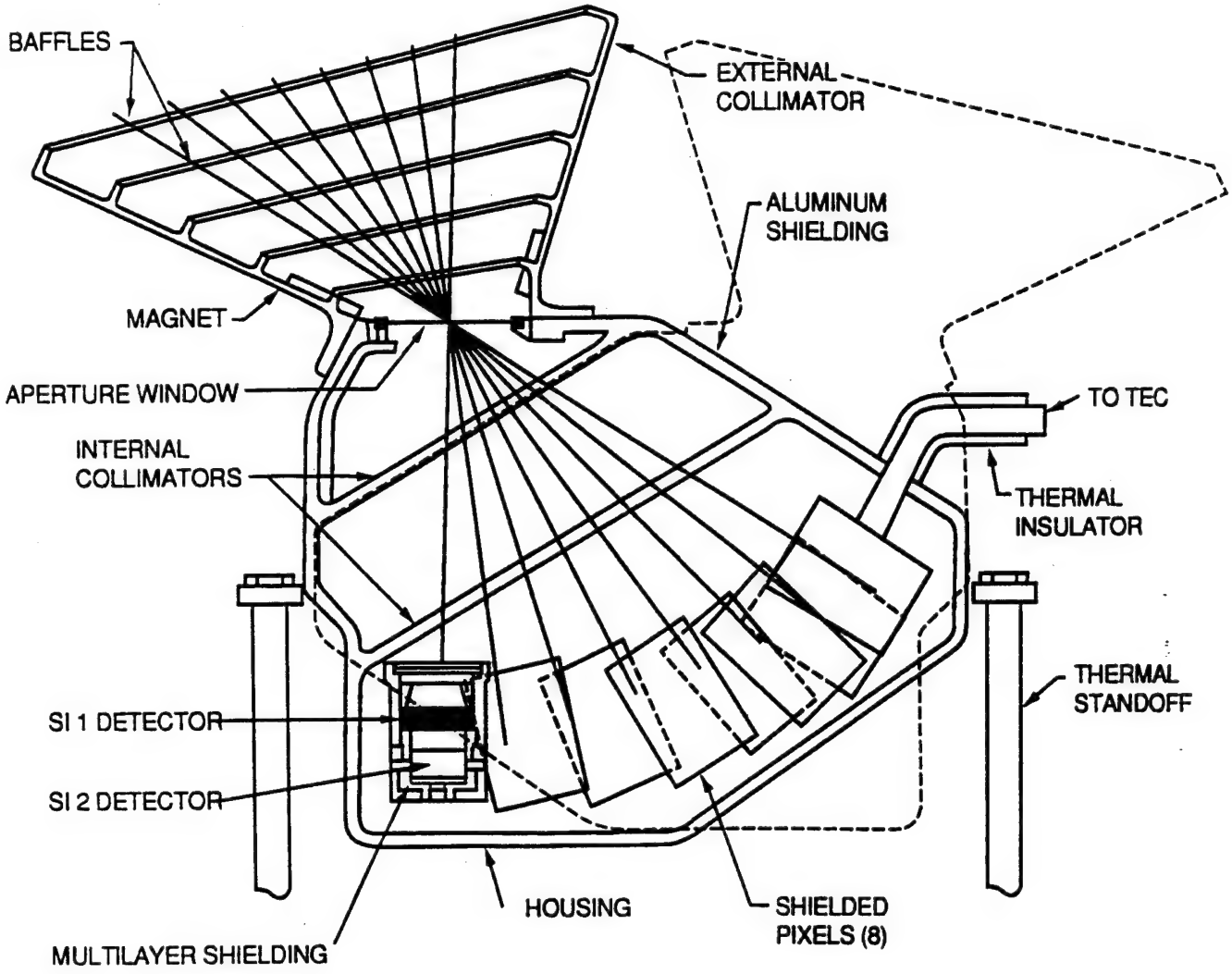
BAFFLES
EXTERNAL COLLIMATOR
ALUMINUM SHIELDING
MAGNET
APERTURE WINDOW
TO TEC
INTERNAL COLLIMATORS
THERMAL INSULATOR
THERMAL STANDOFF
SI 1 DETECTOR
SI 2 DETECTOR
HOUSING
SHIELDED PIXELS (8)
MULTILAYER SHIELDING

Figure 3

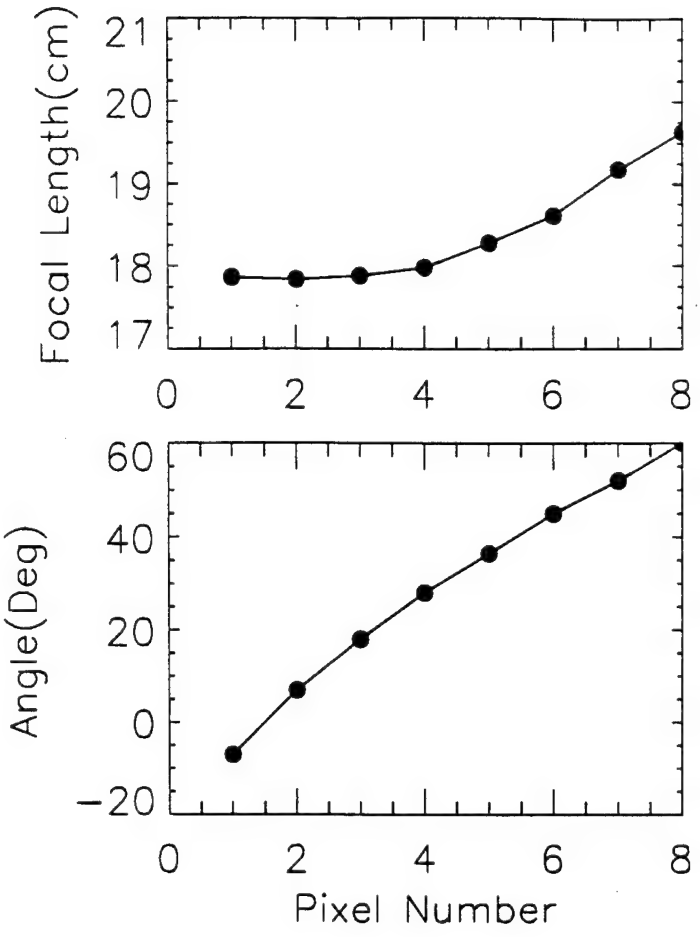
Focal Length(cm)
21
20
19
18
17
0
2
4
6
8
Angle(Deg)
60
40
20
0
−20
0
2
4
6
8
Pixel Number

Figure 4

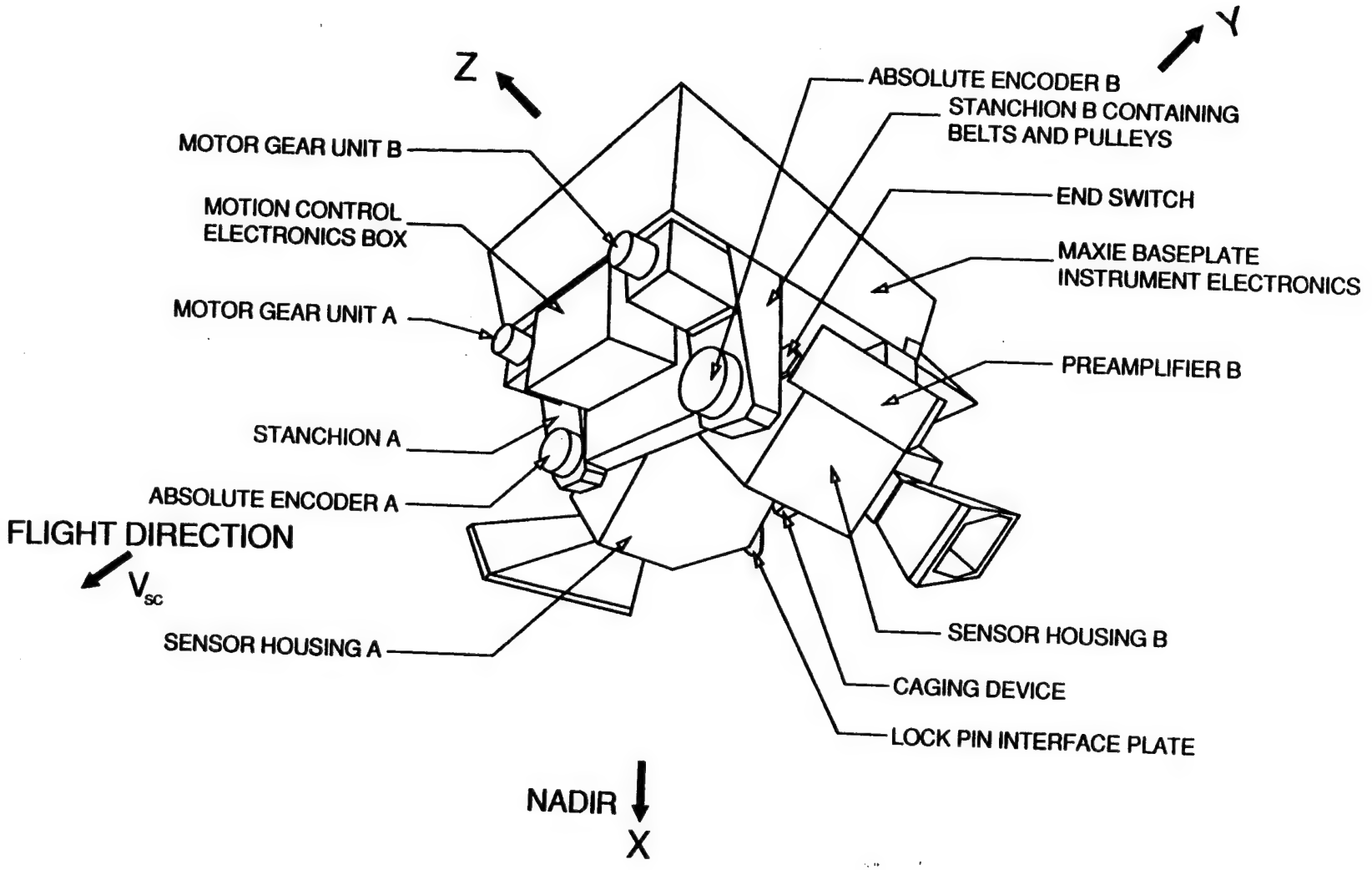
Z
Y
ABSOLUTE ENCODER B
STANCHION B CONTAINING
BELTS AND PULLEYS
MOTOR GEAR UNIT B
END SWITCH
MOTION CONTROL
ELECTRONICS BOX
MAXIE BASEPLATE
INSTRUMENT ELECTRONICS
MOTOR GEAR UNIT A
PREAMPLIFIER B
STANCHION A
ABSOLUTE ENCODER A
FLIGHT DIRECTION
V_{sc}
SENSOR HOUSING B
SENSOR HOUSING A
CAGING DEVICE
LOCK PIN INTERFACE PLATE
NADIR
X

Figure 5

Figure 6

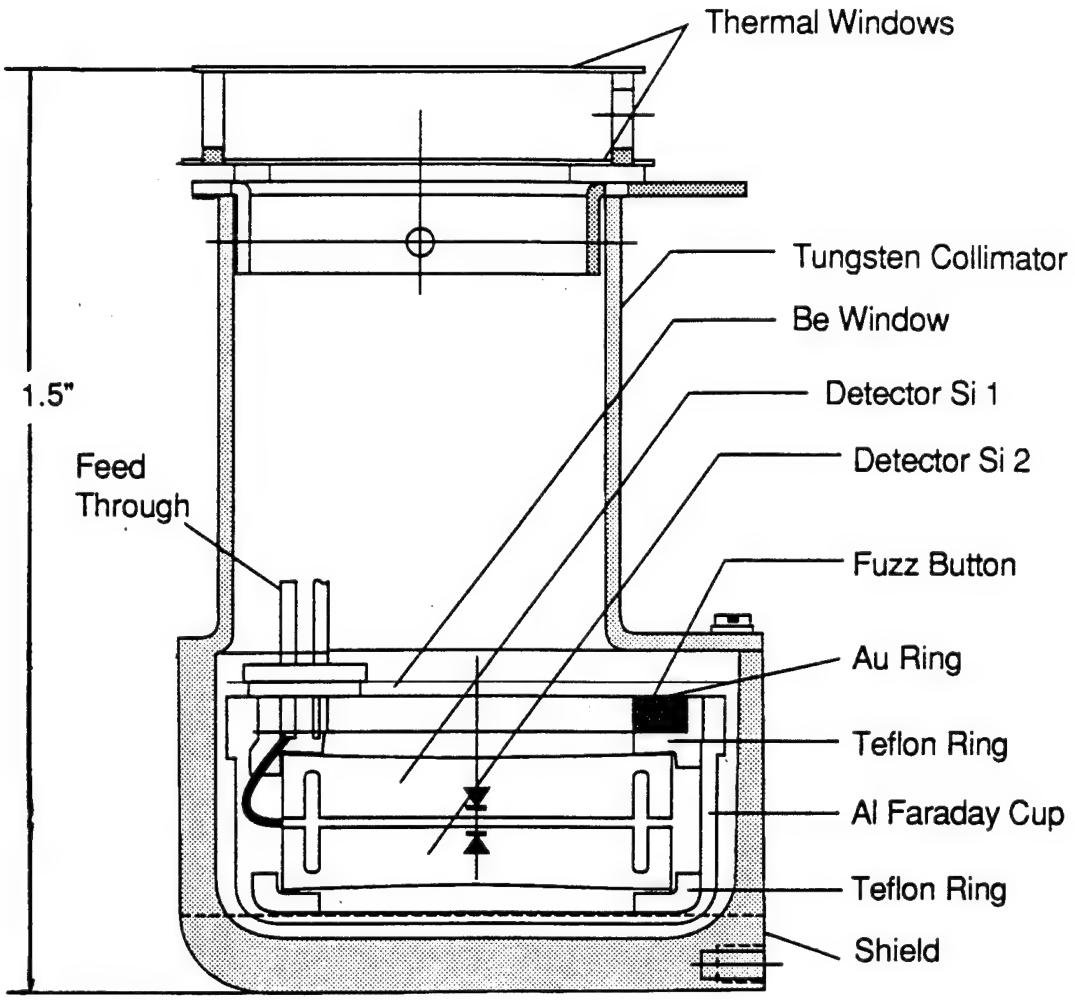
Thermal Windows
Tungsten Collimator
Be Window
Detector Si 1
Detector Si 2
Fuzz Button
Au Ring
Teflon Ring
Al Faraday Cup
Teflon Ring
Shield
1.5"
Feed
Through

Figure 7

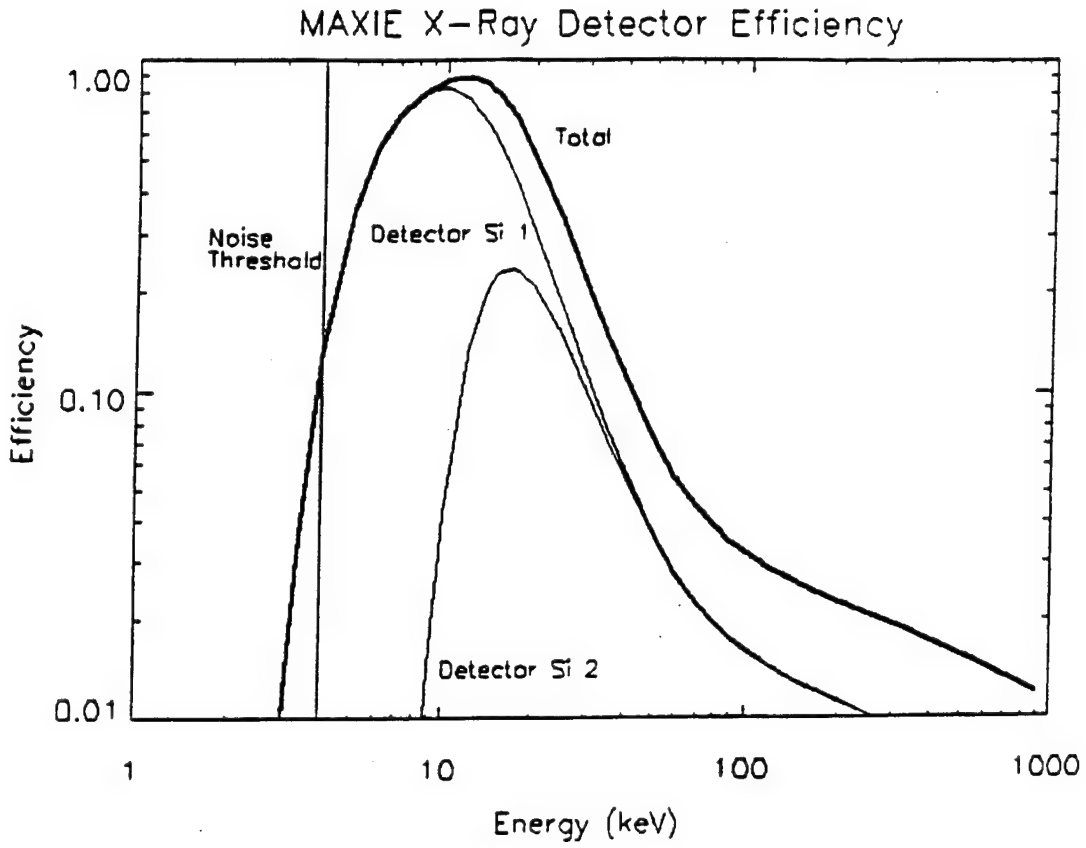
MAXIE X-Ray Detector Efficiency
1.00
0.10
0.01
Efficiency
Noise
Threshold
Total
Detector Si 1
Detector Si 2
1
10
100
1000
Energy (keV)

Figure 8

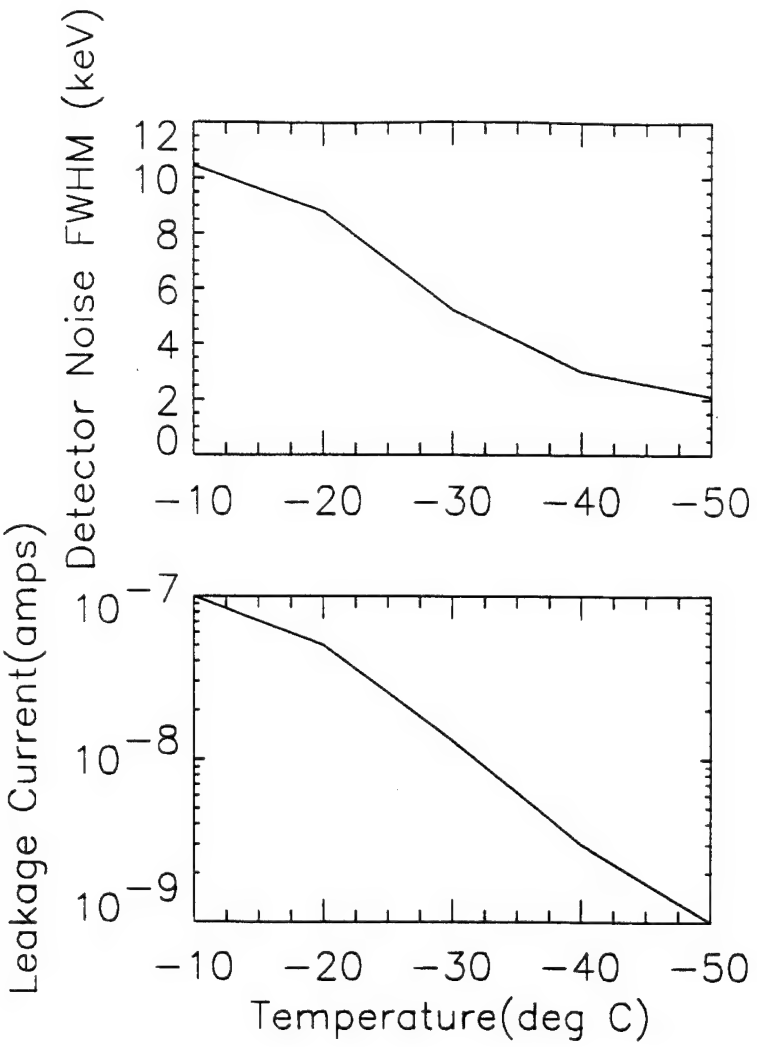
Detector Noise FWHM (keV)
12
10
8
6
4
2
0
−10
−20
−30
−40
−50
Leakage Current(amps)
10^{-7}
10^{-8}
10^{-9}
−10
−20
−30
−40
−50
Temperature(deg C)

Figure 9

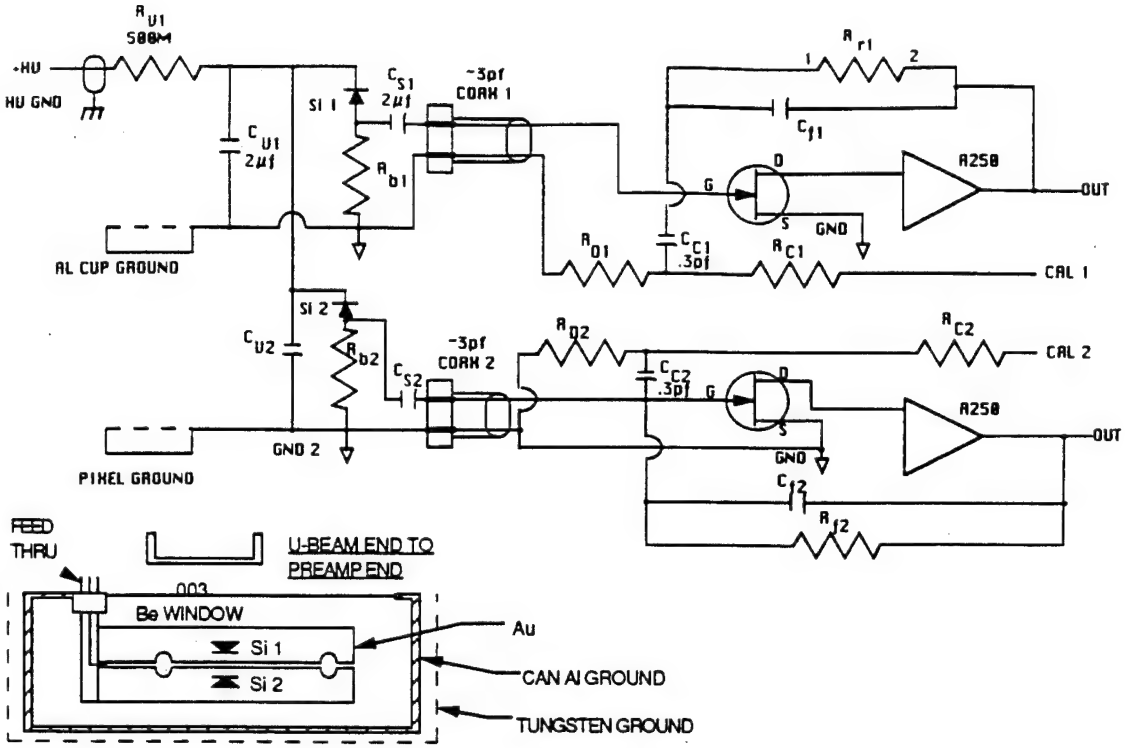
R U1
500M
+HV
HV GND
C U1
2μf
Si 1
C S1
2μf
-3pf
CORK 1
R b1
AL CUP GROUND
R f1
1
2
C f1
D
G
S
GND
A250
OUT
R D1
C C1
.3pf
R C1
CAL 1
Si 2
C U2
R b2
C S2
-3pf
CORK 2
R D2
C C2
.3pf
R C2
CAL 2
GND 2
PIXEL GROUND
C f2
R f2

FEED
THRU
U-BEAM END TO
PREAMP END
.003
Be WINDOW
Si 1
Si 2
Au
CAN Al GROUND
TUNGSTEN GROUND

Figure 18

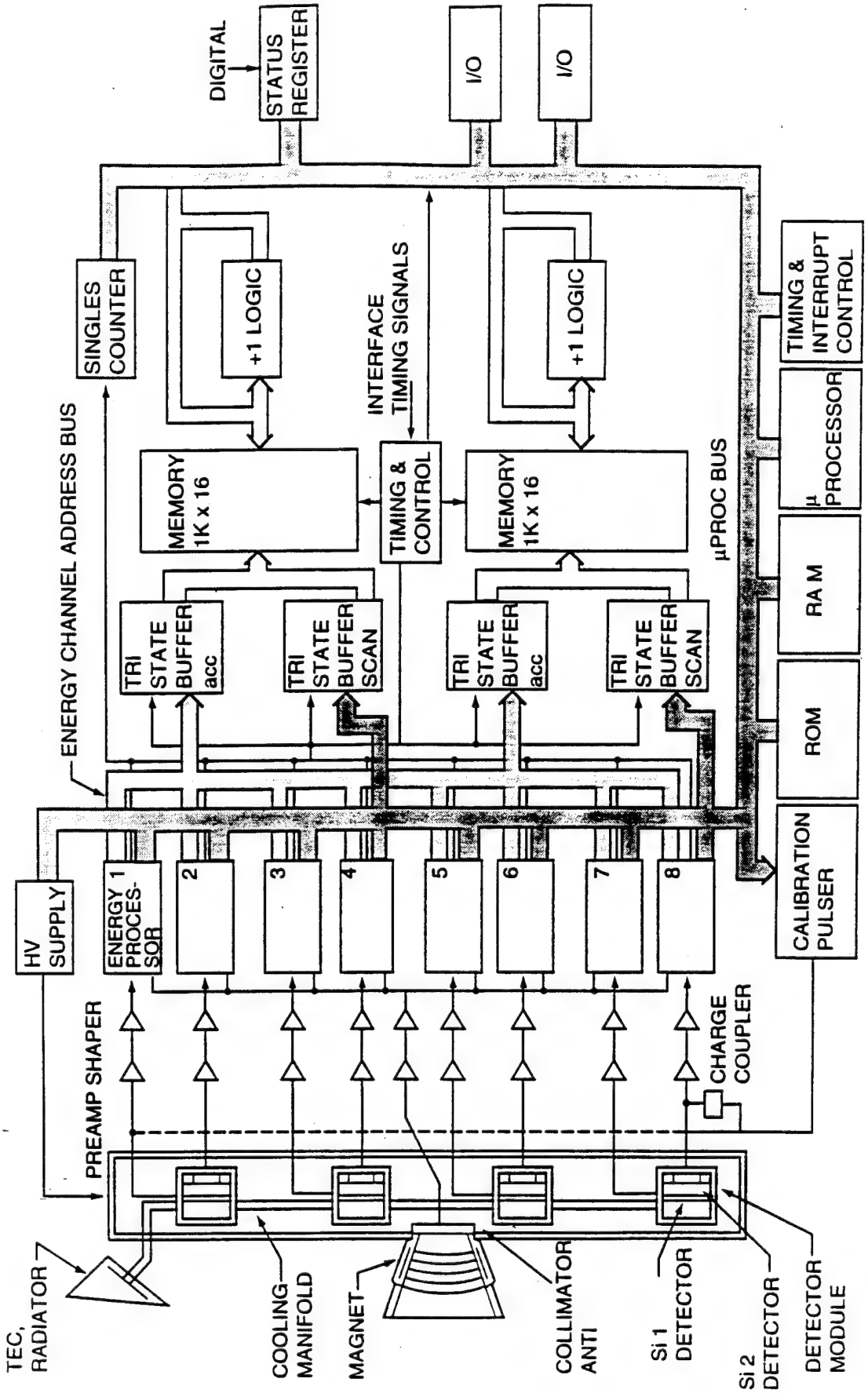
DIGITAL
STATUS REGISTER
I/O
I/O
SINGLES COUNTER
+1 LOGIC
+1 LOGIC
INTERFACE TIMING SIGNALS
TIMING & INTERRUPT CONTROL
ENERGY CHANNEL ADDRESS BUS
MEMORY 1K x 16
TIMING & CONTROL
MEMORY 1K x 16
μ PROCESSOR
μPROC BUS
TRI STATE BUFFER acc
TRI STATE BUFFER SCAN
TRI STATE BUFFER acc
TRI STATE BUFFER SCAN
RA M
ROM
HV SUPPLY
ENERGY 1 PROCES-SOR
2
3
4
5
6
7
8
CALIBRATION PULSER
PREAMP SHAPER
CHARGE COUPLER
TEC, RADIATOR
COOLING MANIFOLD
MAGNET
COLLIMATOR ANTI
Si 1 DETECTOR
Si 2 DETECTOR
DETECTOR MODULE

Figure 11

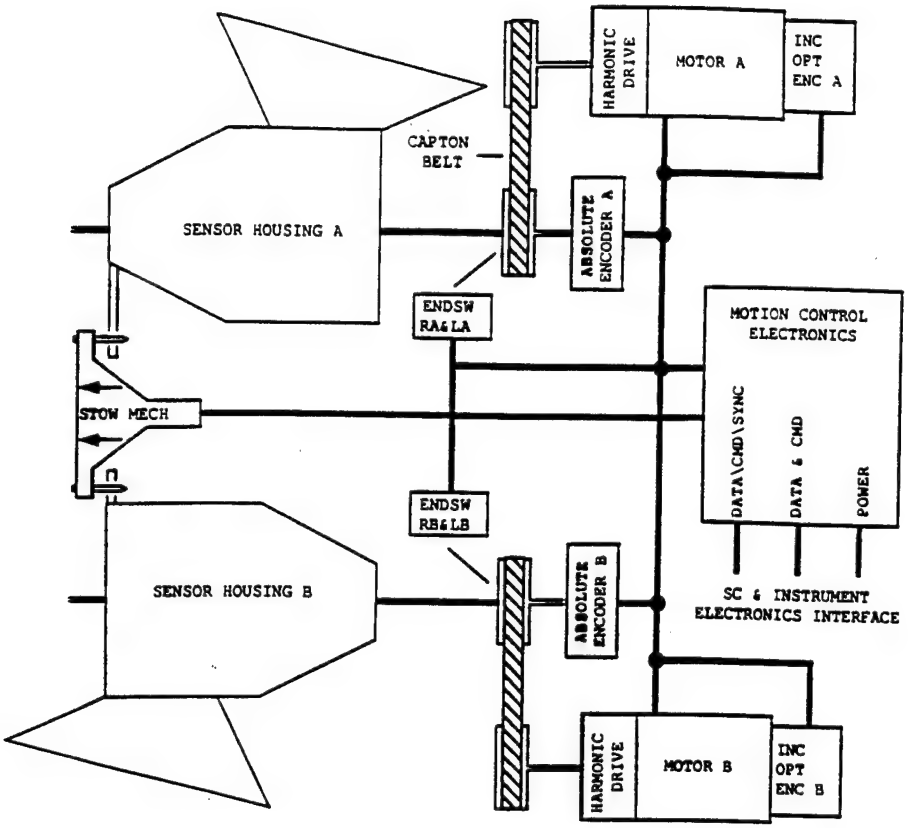
HARMONIC DRIVE
MOTOR A
INC OPT ENC A
CAPTON BELT
SENSOR HOUSING A
ABSOLUTE ENCODER A
ENDSW RA&LA
MOTION CONTROL ELECTRONICS
STOW MECH
DATA\CMD\SYNC
DATA & CMD
POWER
ENDSW RB&LB
SENSOR HOUSING B
ABSOLUTE ENCODER B
SC & INSTRUMENT ELECTRONICS INTERFACE
HARMONIC DRIVE
MOTOR B
INC OPT ENC B

Figure 12

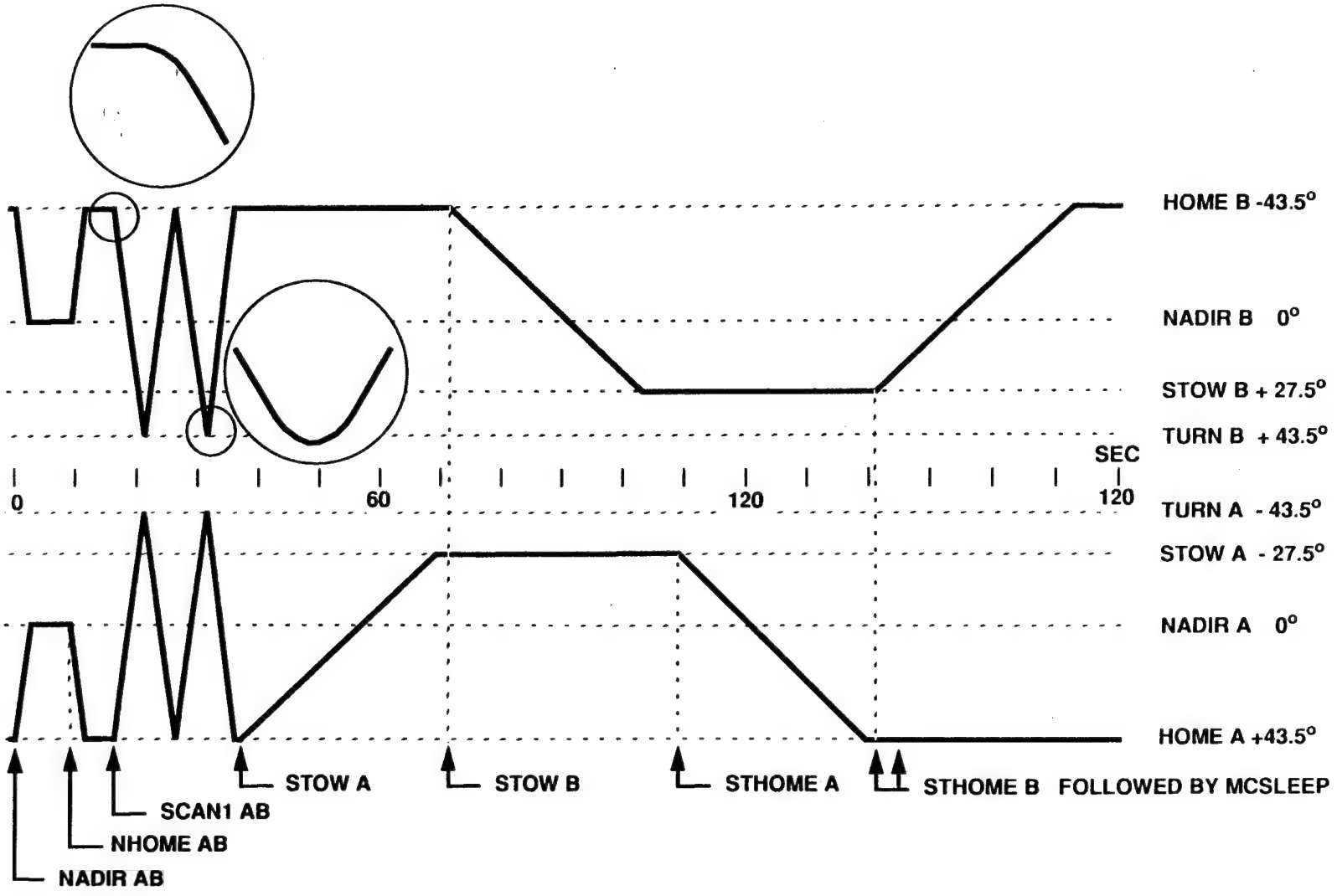
HOME B -43.5°
NADIR B 0°
STOW B + 27.5°
TURN B + 43.5°
SEC
0
60
120
120
TURN A - 43.5°
STOW A - 27.5°
NADIR A 0°
HOME A +43.5°
STOW A
STOW B
STHOME A
STHOME B FOLLOWED BY MCSLEEP
SCAN1 AB
NHOME AB
NADIR AB

Figure 13

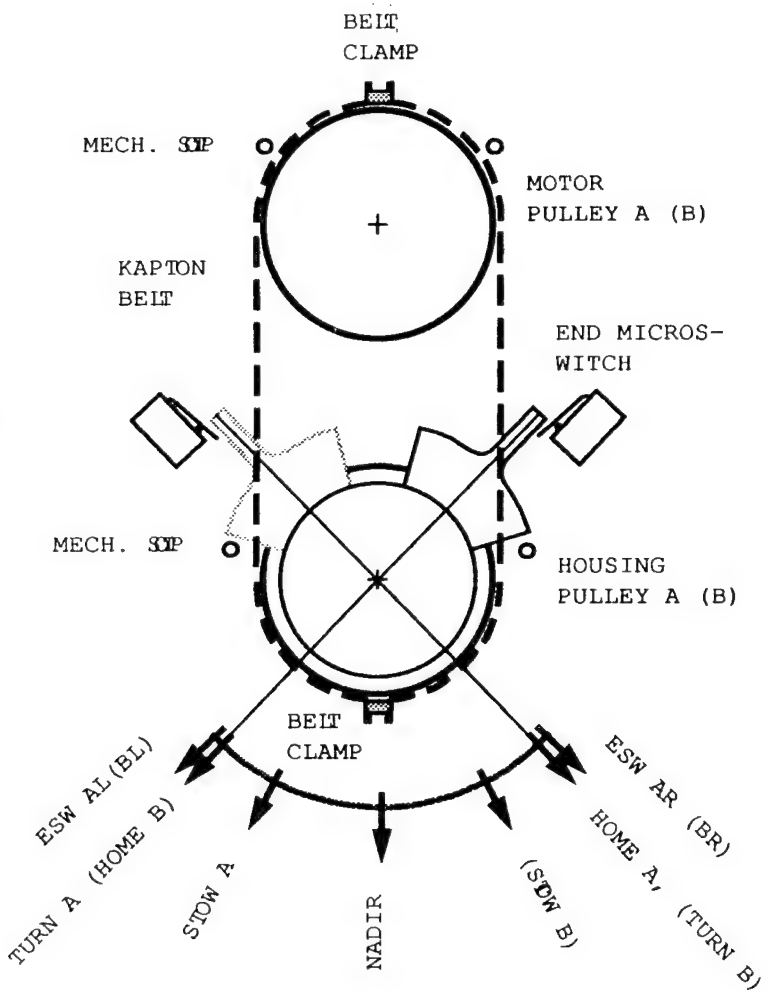
BELT
CLAMP
MECH. STOP
MOTOR
PULLEY A (B)
KAPTON
BELT
END MICROS-
WITCH
MECH. STOP
HOUSING
PULLEY A (B)
BELT
CLAMP
ESW AL(BL)
TURN A (HOME B)
STOW A
NADIR
(STOW B)
HOME A, (TURN B)
ESW AR (BR)

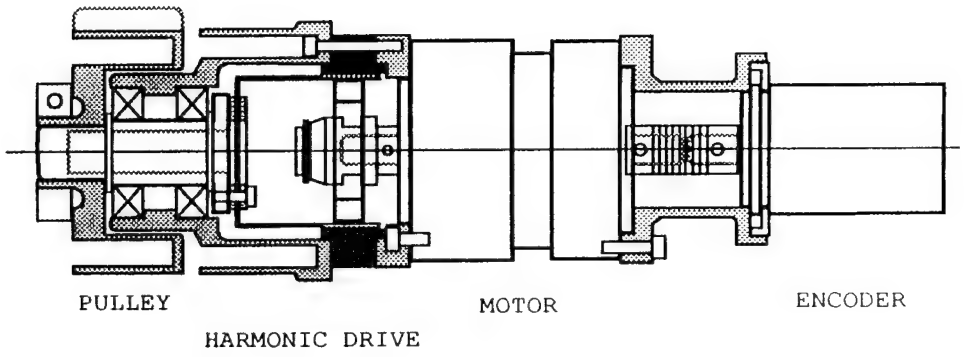
PULLEY
MOTOR
ENCODER
HARMONIC DRIVE

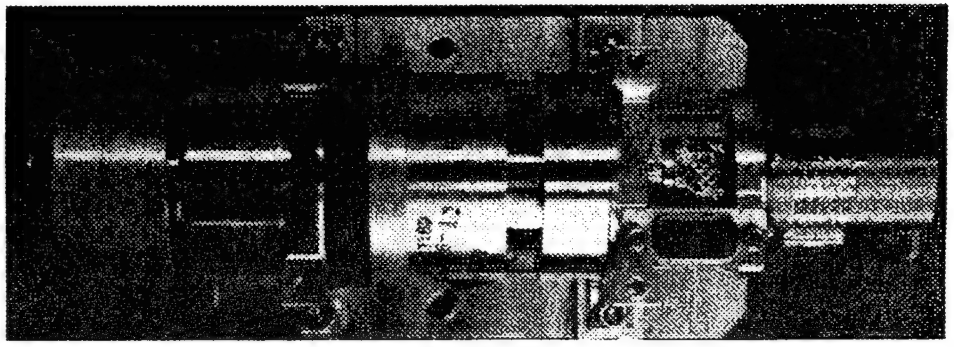

Figure 14

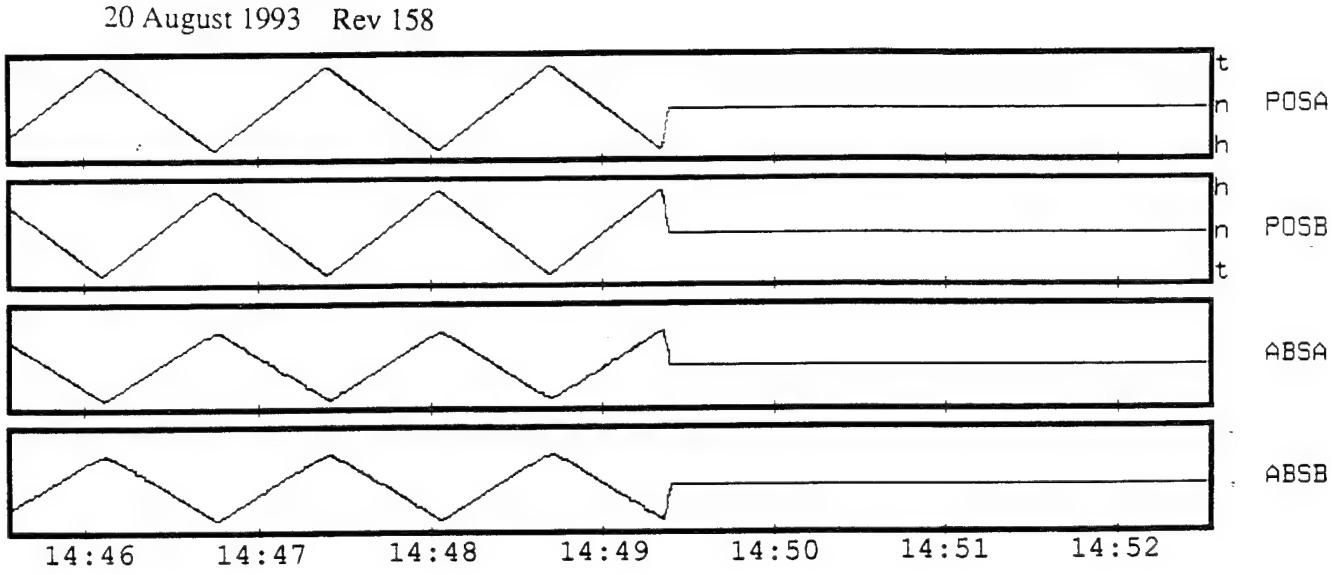
20 August 1993 Rev 158
POSA
POSB
ABSA
ABSB
14:46
14:47
14:48
14:49
14:50
14:51
14:52
Time

Figure 15

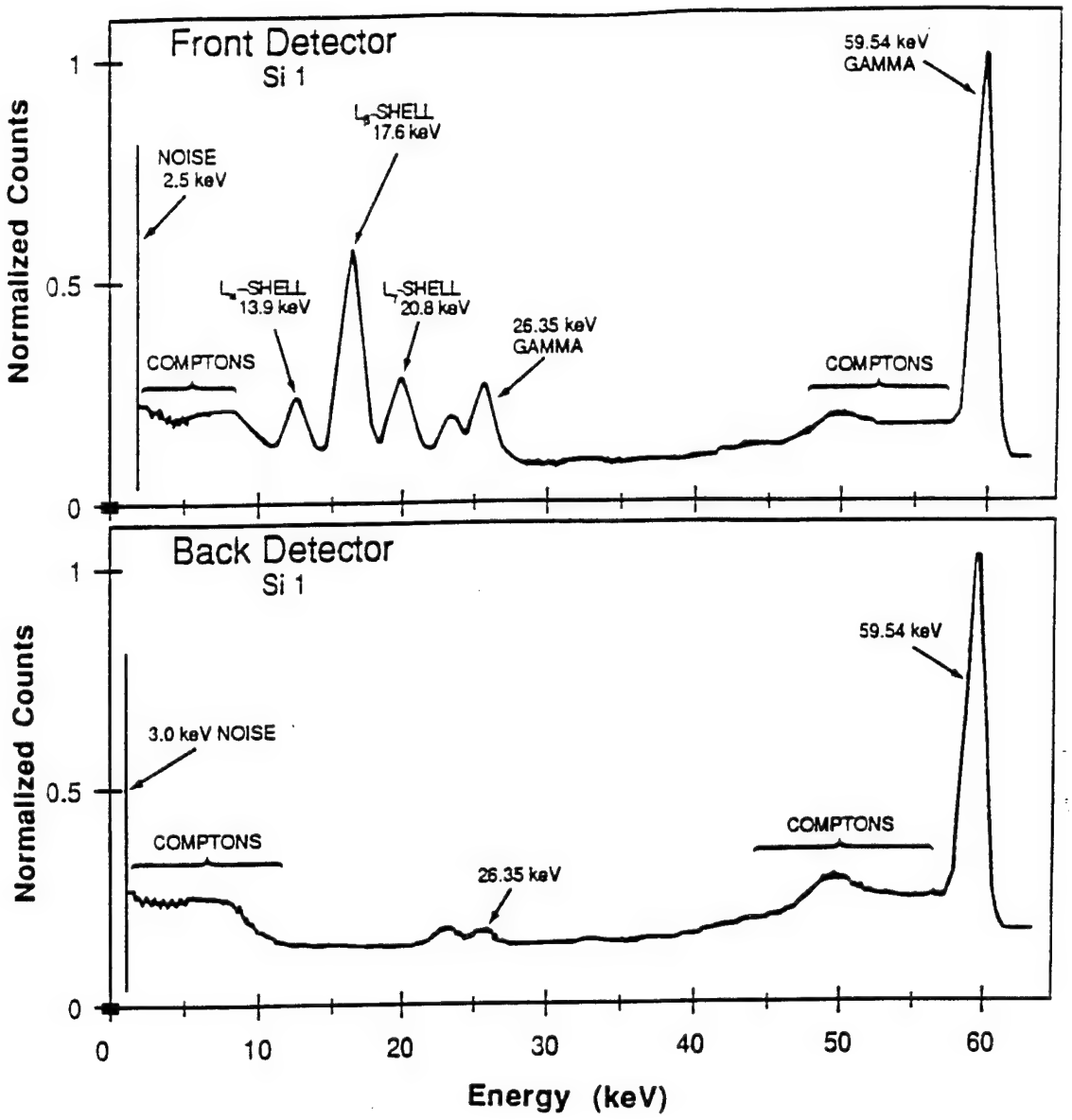
Front Detector
Si 1
59.54 keV
GAMMA
L$_s$-SHELL
17.6 keV
NOISE
2.5 keV
L$_\alpha$-SHELL
13.9 keV
L$_\gamma$-SHELL
20.8 keV
26.35 keV
GAMMA
COMPTONS
COMPTONS
Back Detector
Si 1
59.54 keV
3.0 keV NOISE
COMPTONS
COMPTONS
26.35 keV
Normalized Counts
Normalized Counts
0
0.5
1
0
10
20
30
40
50
60
Energy (keV)

Figure 16

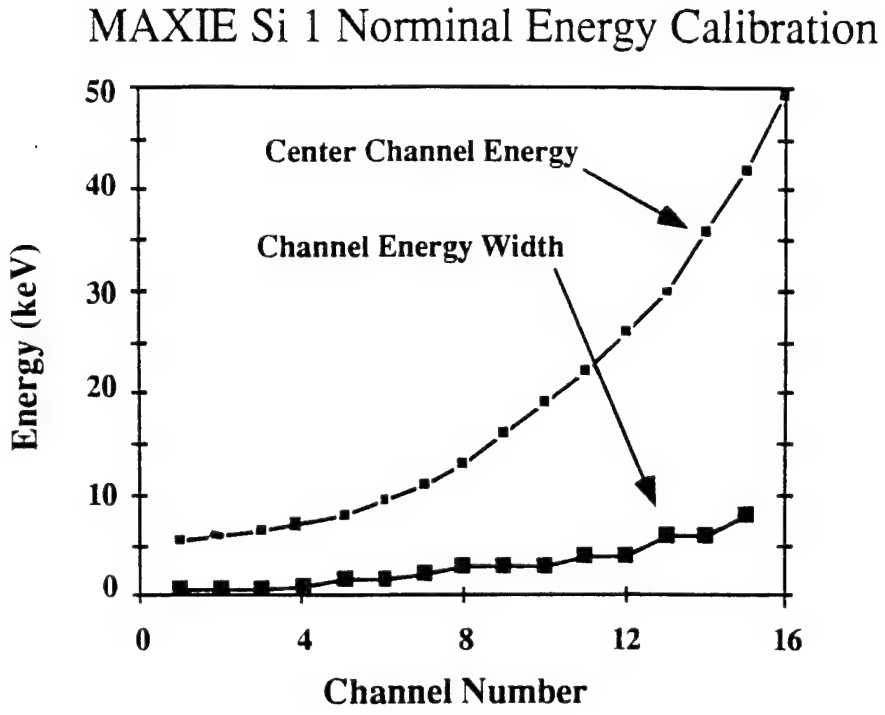
MAXIE Si 1 Norminal Energy Calibration
Energy (keV)
50
40
30
20
10
0
Center Channel Energy
Channel Energy Width
0
4
8
12
16
Channel Number

Figure 17

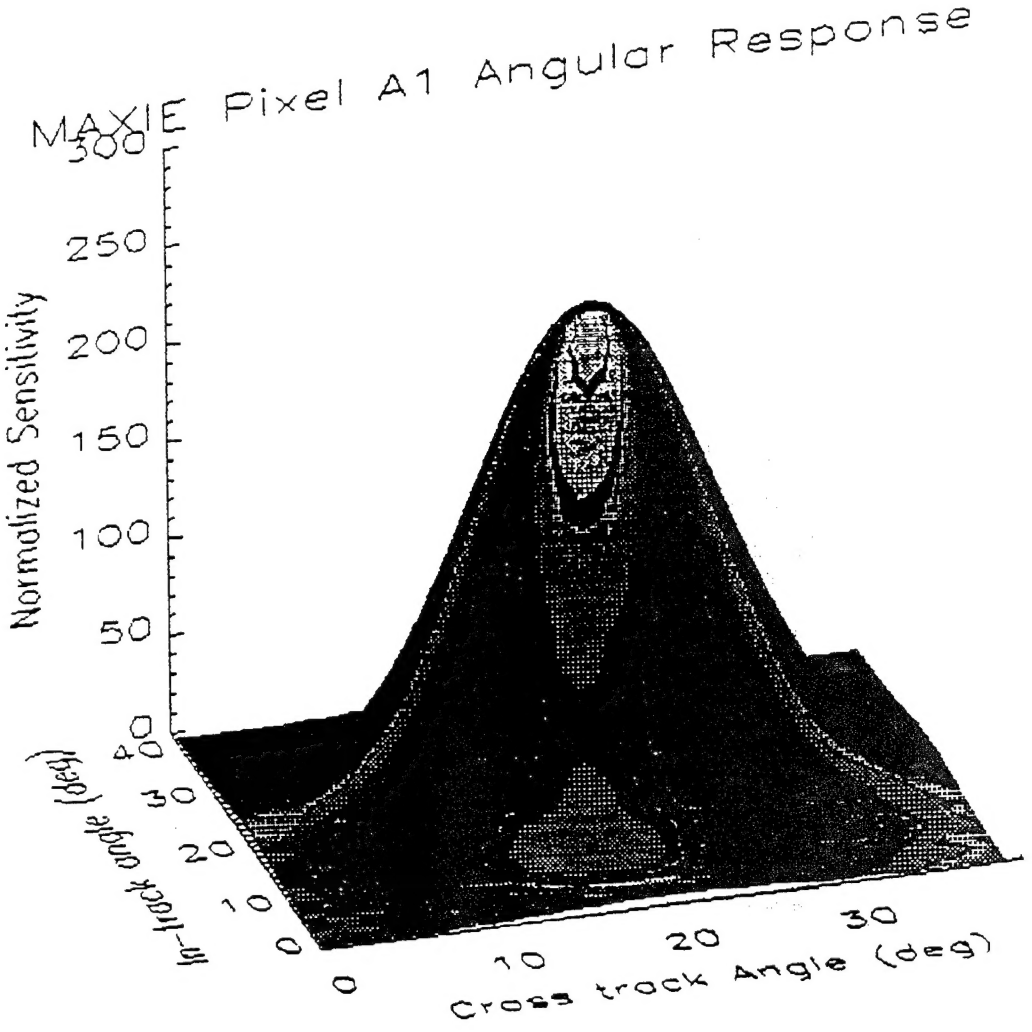
MAXIE Pixel A1 Angular Response
Normalized Sensitivity
300
250
200
150
100
50
0
In-track angle (deg)
40
30
20
10
0
0
10
20
30
Cross track Angle (deg)

Figure 18

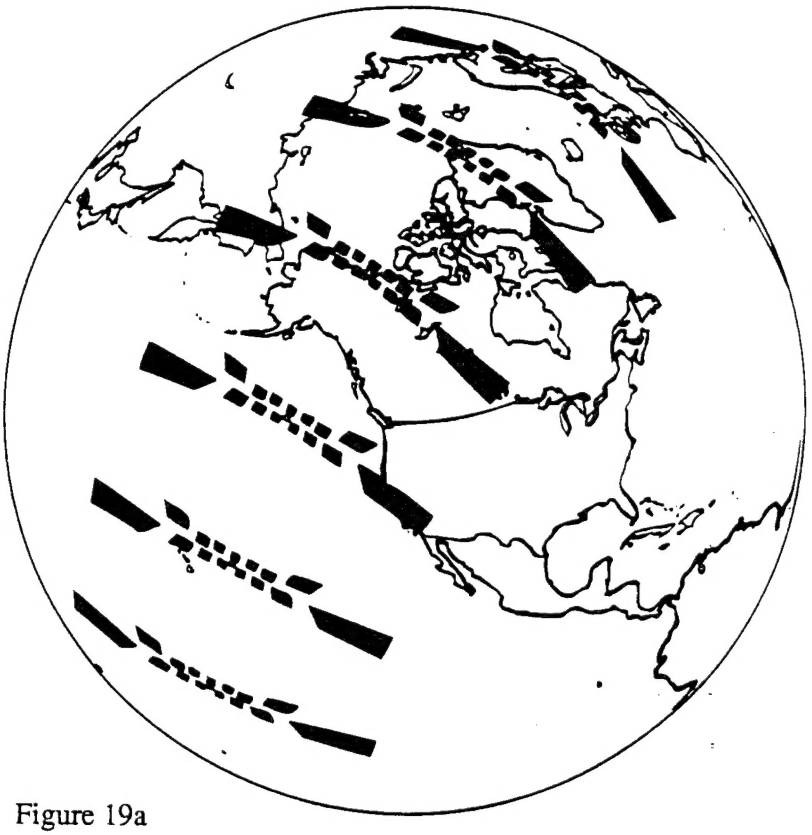

Figure 19a

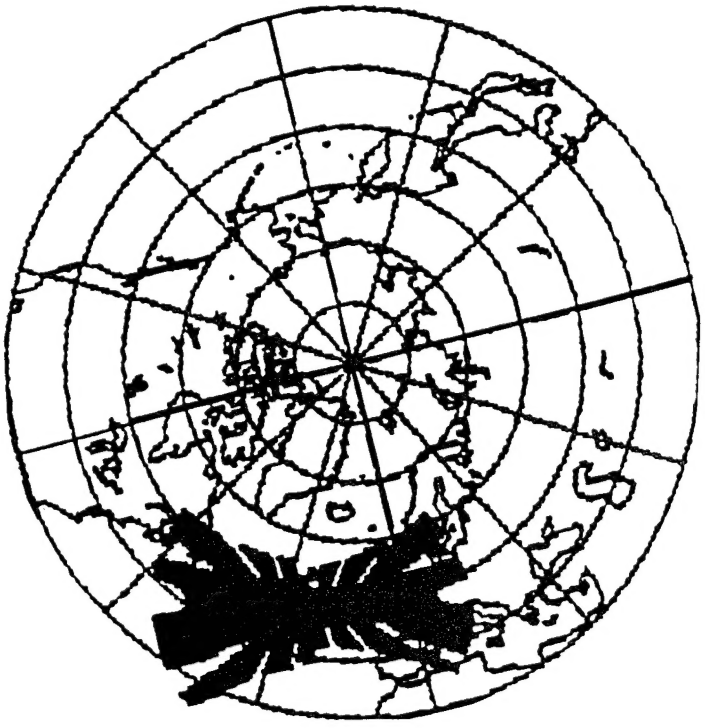

Figure 19b

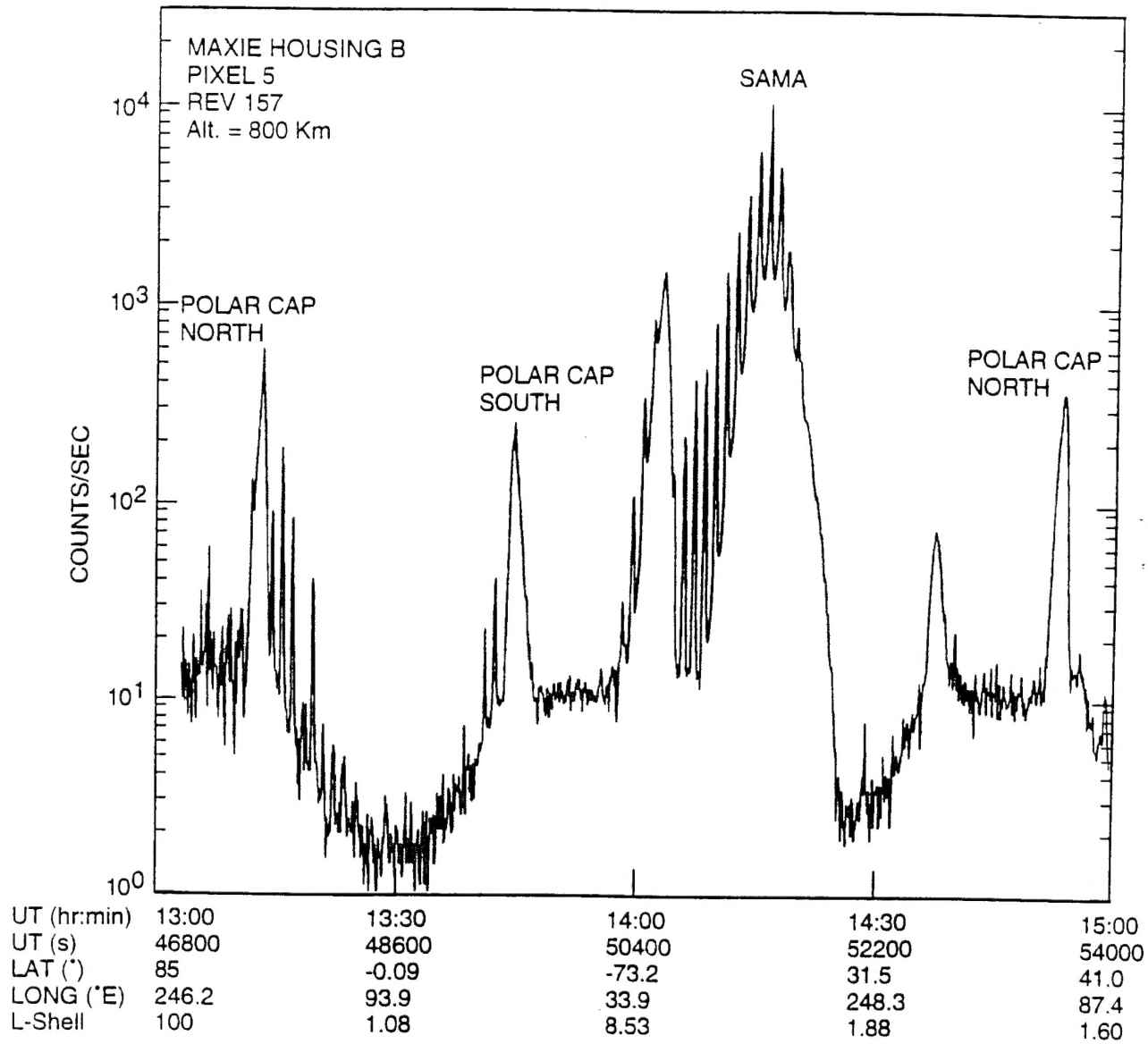

Figure 20

5273/001

SYMBOLS, ABBREVIATIONS, and ACRONYMS

AGU	American Geophysical Union
IEEE	The Institute of Electrical and Electronic Engineers
MAXIE	Magnetospheric Atmospheric X-ray Imaging Experiment.
NASA	National Aeronautics and Space Administration.
NOAA	National Oceanic and Atmospheric Administration.
ONR	Office of Naval Research, the funding agency for the MAXIE effort.
SAMA	South Atlantic Magnetic Anomaly
SOCC	Satellite Operations and Command Center
SPIE	The International Society for Optical Engineering
TIROS	Television InfraRed Observation Satellite